Mathematical description of the ultradian oscillations in the glucose-insulin regulatory system

A C Bridgewater

PhD
December 2018

Mathematical description of the ultradian oscillations in the glucose-insulin regulatory system

Adam Charles Bridgewater

A thesis submitted in partial fulfilment
of the requirements of the
University of Northumbria at Newcastle
for the degree of
Doctor of Philosophy

Mathematics of Complex and Nonlinear
Phenomena research group
Department of Mathematics, Physics and
Electrical Engineering
University of Northumbria at Newcastle
England

December 2018

Dedicated to

This thesis is dedicated to my Grandparents, three of whom are no longer with us.

The support you all showed always made me feel like I could achieve anything.

I love you all.

Abstract

Nonlinear delay-differential equations represent infinite-dimensional systems for which characterising the behaviour of solutions can be technically challenging. Their appearance in many applied fields, such as population biology, is in great part due to their ability to model dynamics with non-instantaneous effects. These phenomena often exhibit behaviour which does not occur in the associated non-delayed counterpart. In particular, it is known that delays can trigger the occurrence of oscillatory behaviour and can, in several cases, bring evidence for mechanisms underlying oscillations in biological systems. Oscillatory dynamics play an important role in the accurate regulation of hormones. Such rhythms in the ultradian regime have been observed in multiple physiological areas such as the HPA-axis, phases of sleep, and the glucose regulatory system.

In this contribution, the effect of diabetic deficiencies on the production of an oscillatory ultradian regime is studied using a deterministic nonlinear model which incorporates two physiological delays. It is shown that insulin resistance impairs the production of oscillations by dampening the ultradian cycles. Four strategies for restoring healthy regulation are explored. The model is thus shown to be suitable for representing the effect of diabetes on the oscillatory regulation and for investigating pathways to reinstating a physiological healthy regime.

Furthermore, a simplified nonlinear polynomial model of the ultradian oscillations in glucose-insulin regulation, at the organ and tissue level, is studied. Particular attention is given to its periodic solutions, arising from a Hopf bifurcation which is induced by delays in pancreatic insulin release, hepatic glycogenesis and a glucose infusion. The model also includes terms accounting for insulin independent and dependent glucose utilisation as well as insulin clearance.

The effect of each of these functions on the amplitude and period of the oscillations is exhibited by performing a Poincaré perturbative analysis of its periodic solutions.

List of publications and presentations

Publications

Some of the material presented in this thesis is based on the research published in the volumes below.

- Bridgewater, A., Huard, B. and Angelova, M. 'Amplitude and frequency variation in nonlinear glucose dynamics with multiple delays via periodic perturbation'.
  - In this contribution, Lindstedt's perturbative method is applied to a simplified model of glucose-insulin regulation (at the organ and tissue level) in order to study quantitatively the effect of physiological parameters on the amplitude and period of the resulting oscillations.
  - Proposed journal: *Journal of Nonlinear Science*.
  - Expected submission: April 2019.
- Bridgewater, A., Huard, B., Stringer, B. and Angelova, M. 'Ultradian rhythms in glucose regulation: A mathematical assessment', *AIP Conference Proceedings* **2090**, pp. 050010-1-050010-9.
- Huard, B., Bridgewater, A. and Angelova, M., 2017. Mathematical investigation of diabetically impaired ultradian oscillations in the glucose-insulin regulation. *Journal of Theoretical Biology* **418**, pp.66-76.

Contributed talks

- Bridgewater, A. 2018. *Perturbation analysis of a delayed model of glucose-insulin regulation with a commensurate delay.* European Conference on Mathematical and Theoretical Biology, 26th July, University of Lisbon.

- Bridgewater, A. 2018. *Application of Lindstedt's method to a delayed model of glucose-insulin regulation.* British Applied Mathematical Colloquium, 26th March, University of St Andrews.

- Bridgewater, A. 2017. *Mathematical investigation of diabetically impaired ultradian oscillations in the glucose-insulin system.* Mathematics and Mathematical Physics Series, 11th October, University of Northumbria at Newcastle.

- Bridgewater, A. 2017. *Mathematical investigation of diabetically impaired ultradian oscillations in the glucose-insulin system.* Engineering & Environment Faculty PGR Conference, 15th June, University of Northumbria at Newcastle.

- Bridgewater, A. 2017. *Mathematical investigation of diabetically impaired ultradian oscillations in the glucose-insulin system.* British Applied Mathematical Colloquium, 12th April, University of Surrey.

Poster presentations

- Bridgewater, A. 2018. *The effect of diabetes on the ultradian rhythms in the glucose-insulin system.* BioDynamics, 12th April, Royal College of Physicians, London.

- Bridgewater, A. 2017. *The effect of diabetes on the ultradian rhythms in the glucose-insulin system.* Diabetes UK conference, 10th March, Manchester Central Convention Complex.

- Bridgewater, A. 2016. *Numerical investigation of the effect of diabetes on the ultradian rhythms in the glucose-insulin system.* BioDynamics, 7th September, University of Exeter.

- Bridgewater, A. 2016. *Numerical investigation of the effect of diabetes on the ultradian rhythms in the glucose-insulin system.* European Conference on Mathematical and Theoretical Biology, 14th July, University of Nottingham.

- Bridgewater, A. 2016. *Numerical investigation of diabetically impaired ultradian rhythms in the glucose-insulin system.* Engineering & Environment Faculty PGR Conference, 20th June, University of Northumbria at Newcastle.

Contents

Abstract **iii**

Acknowledgements **xv**

Declaration **xvi**

1 Introduction **1**

1.1 Mathematical biology 1

1.2 Diabetes 2

1.3 Ultradian oscillations 3

1.4 Aims and objectives 4

1.4.1 Proposed questions 5

1.4.2 Motivation 5

1.4.3 Methodology 7

1.4.4 Statement of original contribution 8

1.5 Thesis structure 9

2 Mathematical modelling of glucose-insulin regulation: an overview 10

2.1 Non-oscillatory models of the glucose-insulin system 11

2.1.1 Minimal model 11

2.1.2 Further models of the IVGTT 12

2.2 Models of the ultradian rhythms 14

2.2.1 ODE models 14

2.2.2 DDE models 16

2.2.3 Modelling the effect of diabetes 17

3 Models of glucose-insulin regulation 19

3.1 The two-delay model 19

3.1.1 The effect of insulin resistance on the glucose and insulin levels 24

3.1.2 The effect of insulin resistance on the ultradian oscillations . . 28

3.2 Reduced polynomial model 31

3.2.1 Local stability analysis of the reduced model 33

3.3 Periodic solutions in the linear system 45

4 Strategies for stabilising glucose levels and restoring oscillations 51

4.1 Clinical and Theoretical Treatments for Diabetes 51

4.1.1 Background 51

4.1.2 Insulin Therapy 52

4.1.3 Metformin 52

4.1.4 Insulin Degradation 52

4.2 Strategies 53

4.2.1 Using insulin injections to stabilise the glucose level 54

4.2.2 Reducing hepatic glucose production to stabilise the glucose level 55

4.2.3 Altering insulin degradation to stabilise the glucose level . . . 58

4.2.4 Reintroducing oscillations 59

4.2.5 Combining strategies 60

5 Amplitude and frequency variation 62

5.1 Hopf-bifurcation formulae 62

5.1.1 Constant hepatic glucose production 63

5.1.2 Linear hepatic glucose production 68

5.2 Parameter analysis 75

5.2.1 Constant hepatic glucose production 75

5.2.2 Non-constant hepatic glucose production 78

6 Discussion and Conclusions 82

Bibliography 88

List of Figures

1.1 Profiles of the glucose and insulin blood concentrations for a non-diabetic (left) and a T2DM patient (right) under a constant glucose infusion. Figure from O'Meara et al. (1993). 5

3.1 Flow diagram for model (3.1.1). 20

3.2 Functional forms of f_1, f_2, f_3, f_4 and f_5, using the parameter values given in Tables 3.1 and 3.2. 23

3.3 Solution to system 3.1.1 when $\alpha = \beta = \gamma = 1$, with $d_i = 0.06$, $G_{in} = 1.35$ mg/dl min and $\tau_1 = 6$ min, $\tau_2 = 36$ min. 25

3.4 Curve of Hopf bifurcations in the optimal non-diabetic case $\alpha = \beta = \gamma = 1$, with $d_i = 0.06$ and $G_{in} = 1.35$ mg/dl min. 26

3.5 Graphs of the functions $A(\beta), B(\beta), C(\beta), D(\beta)$ for parameter values from Tables 3.1 and 3.2, with $d_i = 0.06$ and $I_{in} = 0$. 27

3.6 Effect on the steady state of reducing insulin production (left) and reducing insulin-dependent glucose utilisation (right), for $d_i = 0.06$. The glucose and insulin steady states are represented by the blue and red curves, respectively. 27

3.7 The derivative $\frac{d\eta}{d\beta}$ as a function of τ_1, with parameter values from Tables 3.1 and 3.2, with $d_i = 0.06$, $I_{in} = 0$ and $\beta = 1$. Typical values for τ_1 are to be chosen between 5 and 20 minutes. 31

3.8 Effect of insulin resistance on the curve of Hopf bifurcations in the (τ_1, τ_2) space. 31

3.9 Eigenvalues of the linearised system for $\tau_1 = 6$, $\tau_2 = 36$ and $d_i = 0.06$, when $\beta = 1$ (left) and $\beta = 0.8$ (right). 32

3.10 Flow diagram for model (3.2.16). 33

3.11 Range of values of τ_0 which can be attained by varying a_1 and a_2 for each given value of b_2. Here, we used the fixed values $\bar{G} = 97.87$ mg/dl and $\bar{I} = 30$ mU/l. Any value of τ above the range leads to an oscillatory solution. 37

3.12 Oscillations described by the minimal model (3.2.17) using Parameter Set 1 from Table 5.1, with $a_2 = 0.0017$. 38

3.13 Simple closed curve, χ, in the complex plane. 39

3.14 Hopf bifurcation curve for model (9) in the space of delays, along with expansion lines $\tau_2 = k\tau_1$, $k \in \mathbb{Z}^+$. 40

3.15 Solutions to (3.2.24) with $a_0 = 285$, $a_1 = 2.02981789884309 \times 10^{-4}$, $b_1 = 9.3 \times 10^{-8}$, $b_2 = 0.06$, $\tau = 15.8$, $k = 1$, $G(0) = 10000$ and $I(0) = 90$. 42

3.16 Unbounded solution of (3.2.24) with $a_0 = 10$, $a_1 = 0.01$, $a_2 = 0.01$, $a_3 = 2.2$, $b_1 = 0.001$, $b_2 = 0.05$, $k = 5$, $\tau = 10$, $p = 2$, $G(0) = 10000$ and $I(0) = 90$. 43

3.17 Values of r which satisfy the conditions of Proposition 5 for $c_4 \in [-1, 1]$. 49

3.18 Existence of oscillatory solutions in the (τ_1, τ_2) domain for $c_4 = 0.00001$ (left) and $c_4 = 0.1$ (right). Given the periodicity of equations (3.3.41), only the curves which provide the minimal values for τ_2 are reported. 50

4.1 Oscillatory region (in red) in the α, β domain for $d_i = 0.06$ with I_{in} as defined by (4.2.1) with $\gamma = 0.7$ (left) and $\gamma = 1$ (right). The blue region represents values of (α, β) for which $\bar{G}$ remains constant at 97.87, but the system is stable. The white region represents values of (α, β) where the resulting value of I_{in} is negative. 54

4.2 Oscillatory regions in the α, β domain for various values of τ_1 and τ_2. The red, blue and white regions are as defined in Fig. 4.1. 56

4.3 Oscillatory regions in the α, β domain for various values of τ_1 and τ_2 with $G_{in} = 0.54\ mg/dl\ min$. The red, blue and white regions are as defined in Fig. 4.1, although it is noted that $\bar{G}$ is now stabilised to 89 which is the value of the steady state when $\alpha = \beta = \gamma = 1$ for $G_{in} = 0.54$. 57

4.4 Value of γ, as defined by (4.2.2), that enables the stabilisation of $\bar{G} = 97.87$ mg/dl for each β with $\alpha = 1$ (left) and the resulting oscillatory region in the α, β domain with $d_i = 0.06, I_{in} = 0$ (right, red). The blue region represents values of (α,β) such that $\bar{G} = 97.87$ but oscillations do not occur. Finally, the white region corresponds to negative values of γ, which are physiologically impossible. 58

4.5 Clearance rate which allows to stabilise $\bar{G} = 97.87 mg/dl$ and the resulting $\bar{I}$ when $d_i(1,1) = 0.06$ and $I_{in} = 0$. 59

4.6 Oscillatory region (in red) in the α, β domain for $d_i = 0.06$ (left) and $d_i(\alpha, \beta)$ defined by (4.2.3), with $I_{in} = 0$. 59

4.7 Oscillating regions in the α, β, d_i domain. The solid sections represent the values of d_i for which both oscillations occur, and the fasting glucose levels lay within an acceptable range (70-109 mg/dl). 60

4.8 Values of α and β for which oscillations can be restored with a healthy fasting basal level using a combined strategy. 61

5.1 Amplitudes of the oscillations, $\bar{A}$ and $\bar{B}$, as a function of a_2 using Parameter Set 1 (left) and Parameter Set 2 (right). 76

5.2 Period of the oscillations, as given by (5.1.19), as a function of a_2 using Parameter Set 1 (left) and Parameter Set 2 (right). 77

5.3 Percentage change of the closed form expressions of the amplitude (blue) and period (black) of $Y(t)$, which are given by (5.1.18) and (5.1.19) respectively, vs. the percentage change in a_2 for Parameter Set 1 (left) and Parameter Set 2 (right). The initial value used for a_2 was: 0.0017 (left); and 0.0004 (right). 77

5.4 Amplitude of $X(t)$, as given by (5.1.17), vs. b_1 for Parameter Set 1 (left) and Parameter Set 2 (right). 79

5.5 Amplitude of $X(t)$ (left) and $Y(t)$ (right), as given by (5.1.17) and (5.1.18) respectively, vs. b_2 for Parameter Set 1. 79

5.6 Amplitude of $X(t)$ (left) and $Y(t)$ (right), as given by (5.1.17) and (5.1.18) respectively, vs. b_2 for Parameter Set 2. 80

5.7 Amplitude of $X(t)$ (left) and $Y(t)$ (right), as defined by (5.1.39) and (5.1.32) respectively, as a function of k for Parameter Set 1 with $a_2 = 0.0017$. 81

5.8 Amplitude of $X(t)$ (left) and $Y(t)$ (right), as defined by (5.1.39) and (5.1.32) respectively, vs. k for Parameter Set 3. 81

5.9 Amplitude of $X(t)$ (left) and $Y(t)$ (right), as given by (5.1.39) and (5.1.32) respectively, vs. k for fixed ϵ. All other parameters are as defined in Table (5.2). 81

6.1 Ultradian oscillations with a 5% noise on α and β around $\alpha = \beta = 1$. The middle band represents the associated variability of $\bar{G}$. A similar effect can be observed on insulin patterns. Simulation performed with 500 repetitions. 84

6.2 Comparison of two methods for calculating the amplitude of $X(t)$ from model (5.1.1) using Parameter Set 1. The blue line represents the P-L approximation given by (5.1.17) and the black dots represent the numerical approximations obtained using a Runge - Kutta method. 86

6.3 Comparison of the limit cycles corresponding to the P-L approximation, given by (5.1.17), (5.1.18) and (5.1.19), and the numerical solution of system (5.1.1). Parameter values are as defined in Parameter Set 1, with $a_2 = 0.002$. 87

List of Tables

2.1 Parameters used in the functions $f_1 - f_5$. They were originally determined by fitting the functions f_1 - f_5 to published clinical experiments of individual subsystems (see Sturis et al. (1991) and references therein). 15

3.1 Values used for the Hill coefficients h_i, k_i, taken from (Huard, Easton & Angelova 2015). 24

3.2 Parameters used in model (3.1.1). They were originally determined by fitting the functions f_1 - f_5 to published clinical experiments of individual subsystems (see Sturis et al. (1991) and references therein). 24

3.3 Units for the parameters in model (3.2.16). 34

5.1 Parameter Sets 1 and 2 which are used in numerical simulations throughout Section 5.2.1. 76

5.2 Parameter Set 3. 80

List of Abbreviations

Type 1 diabetes mellitus	T1DM
Type 2 diabetes mellitus	T2DM
Hypothalamic pituitary adrenal	HPA
Artificial pancreas	AP
Continuous glucose monitors	CGM
Delay differential equation	DDE
Ordinary differential equation	ODE
Stochastic differential equation	SDE
Intravenous glucose tolerance test	IVGTT
Insulin degrading enzyme	IDE
Poincaré-Lindstedt	P-L

Acknowledgements

First and foremost, I would like to thank my mum and dad for all the love and support that they have given me over the years. Without you, and the belief that you have had in me, I would not be the man that I am today. Sarah, thank you for being there for me. Your kindness, love and support has been invaluable. To Maddy, I really appreciate all of your encouraging words, and for the games of badminton which have been a much needed distraction.

Dr Benoit Huard, your knowledge, guidance, and willingness to help over the last three years has been priceless, and I deeply appreciate all of the opportunities and responsibilities that you have given me. It has been an absolute privilege to work with you, and I hope that we can continue to do so in the years to come. I must also thank Professor Maia Angelova, who has always been supportive and willing to help. Indeed, your insight into the work has been invaluable, and I look forward to future collaborations. I also acknowledge a PhD studentship from Northumbria University.

I would also like to thank my fellow PGR students for the support, encouragement and needed distractions. You have all made the last three years a great experience. In particular, I'd like to thank my former office-mate and friend, David Brazier for all of the support, much needed coffee breaks and conversations. Finally, I'd like to thank all my friends for providing a much needed distraction when I have needed it the most.

Declaration

I declare that the work contained in this thesis has not been submitted for any other award and that it is all my own work. I also confirm that this work fully acknowledges opinions, ideas and contributions from the work of others.

Any ethical clearance for the research presented in this thesis has been approved. Approval has been sought and granted by the Faculty Ethics Committee on 30/08/2017.

I declare that the Word Count of this Thesis is 29580 words (excluding bibliography)

Date: 25/04/2019

Chapter 1

Introduction

1.1 Mathematical biology

Mathematical biology is a research area that combines significant mathematical problems with intriguing biology (Hoppensteadt 1995). While there is no exact formula to detail how to make a successful collaboration between a biologist and a mathematician, generally one could assume the former would describe a set of experiments or propose a biological question, while the latter would formulate a model replicating the experiment/biological system and simulate to ensure physiological accuracy (Friedman 2010). The model may then to be able to identify important mechanisms within the biological system or suggest new biological testable hypotheses (Friedman 2010). However, interdisciplinary research has its challenges and mathematical biology is no exception. It could even be asserted that mathematical biology faces additional challenges when compared to other areas of interdisciplinary research (Reed 2004). For example, while there exists fundamental central principles in mathematical physics (i.e. Newton's laws of motion), no such fundamental principles exist for mathematical biology, with each problem containing assumptions that are context specific (Reed 2004). It can therefore be argued that pure mathematicians wanting to work on biological problems must have motivation for the study of biology, and not just for developing mathematical principles (Reed 2004).

There are many instances of successful collaborations in the field of mathematical biology (Hoppensteadt 1995, Friedman 2010). Indeed, mathematics has affected

many areas of biology and is a growing field (Hoppensteadt 1995, Friedman 2010). One such area where mathematics has brought a significant contribution is the study of diabetes (Ajmera et al. 2013).

1.2 Diabetes

Diabetes mellitus is a chronic metabolic disorder which impairs the regulation of the glucose and insulin blood levels (Centers for Disease Control and Prevention et al. 2011), and it can be thought of as a failure of homoeostasis (Nguyen 2018). Homoeostasis refers to the body's ability to maintain certain variables, called regulated variables (Fossion et al. 2018), at, or close to, a healthy value, or steady state (Cannon 1932, Thomas, Thieffry & Kaufman 1995). The steady state may be stable, leading to constant levels over time, or unstable, leading to sustained oscillations (Thomas et al. 1995). The maintenance of these regulated variables is achieved through the physiological responses triggered by effector variables (Fossion et al. 2018), and is highly influenced by negative feedback loops which occur within the body (Cannon 1932, Thomas et al. 1995, Woods & Ramsay 2007). In the case of the glucose-insulin regulatory system, it is the glucose level that is the regulator variable and the insulin level is the effector variable (Fossion et al. 2018). Indeed, glucose levels should be maintained between $72 - 99\ mg/dl$ under fasting conditions (National Institute for Clinical Excellence 2012), while the insulin levels should vary between $0 - 30\ mU/l$ (Kraft et al. 1975). Fasting levels of glucose between $99 - 124\ mg/dl$ indicate a high risk of diabetes (National Institute for Clinical Excellence 2012).

While it can be argued that there are 5 clusters of diabetes (Ahlqvist et al. 2018), it is generally accepted that there are two main types: type 1 diabetes (T1DM); and type 2 diabetes (T2DM) (Centers for Disease Control and Prevention et al. 2011). T1DM is a condition where the β-cells in the pancreas are destroyed, almost completely removing the body's ability to secrete insulin (World Health Organization et al. 1999, NHS 2014). This destruction of β-cells is usually considered the result

of an autoimmune process (American Diabetes Association 2014), although in some T1DM patients there is no evidence of an autoimmune disorder (World Health Organization et al. 1999, Ahlqvist et al. 2018). Either way, it is a lifelong condition and cannot currently be prevented. In the UK, there are approximately 369,000 people who have been diagnosed with T1DM (Diabetes UK 2017). T2DM is where the muscle cells start to become insulin resistant, hindering the body's ability to utilise glucose correctly (NHS 2014). Unlike T1DM, approximately three fifths of cases of T2DM can be prevented or at least delayed (Diabetes UK 2018). However, this form of diabetes is more common than T1DM, accounting for around 90% of cases in the UK (Diabetes UK 2017). Furthermore, it is estimated that almost 1 million people in the UK have T2DM, but have not yet been diagnosed (Diabetes UK 2017).

Initially, diabetes mellitus causes hyperglycaemia and diabetic ketoacidosis, and can lead to many other long term health problems, such as, retinopathy, cardiovascular disease, nephropathy and neuropathy (Centers for Disease Control and Prevention et al. 2011). This makes it a significant financial burden, costing the NHS £9.8 bn in 2010/2011 (Hex et al. 2012). It also accounted for a further £13.9 bn in indirect costs (e.g. social and productivity costs) (Hex et al. 2012). These costs are expected to increase to £16.9 bn and £22.9 bn respectively in 2035/2036 (Hex et al. 2012). Furthermore, it was predicted by Mathers & Loncar (2006) to increase from the 11th to the 7th leading cause of death in the world by the year 2030. In reality, it had reached this milestone by 2016 (World Health Organization 2016).

1.3 Ultradian oscillations

Within the glucose-insulin regulatory system, both rapid (period $\approx$ 6-15 minutes) and ultradian (period $\approx$ 80-180 minutes) oscillations of insulin have been observed (Satin et al. 2015), along with glucose oscillations (period $\approx$ 80-150 minutes) that are tightly coupled to the insulin oscillations of similar period (Scheen et al. 1996). These ultradian oscillations were first observed by Hansen (1923) and have been observed during fasting (O'Meara et al. 1993), meal ingestion, continuous enteral

nutrition, and under a constant glucose infusion (Simon & Brandenberger 2002). As was highlighted by O'Meara et al. (1993), insulin resistance leads to a lack of control of the ultradian rhythms in the glucose-insulin regulatory system, with the main effect of dampening the oscillations (Fig. 1.1). Indeed, when under the effect of a constant glucose infusion, the absolute amplitude of the insulin levels declines when moving from a group of patients without diabetes to patients with T2DM (O'Meara et al. 1993). Although the role of ultradian rhythms is not fully understood, there exists clinical evidence that an oscillatory insulin secretion is more efficient in managing a sustained glucose stimulation than a continuous one (Sturis et al. 1995). It is worth mentioning that ultradian rhythms are also found in other endocrine systems such as the hypothalamic pituitary adrenal (HPA) axis, which is responsible for the secretion of cortisol (Walker, Terry & Lightman 2010). In this system, it has also been demonstrated that rhythmic secretion improves the reaction to stress (Lightman et al. 2008).

A current hypothesis for explaining the advantages conferred by oscillatory regulation is the avoidance of downregulation (Walker et al. 2010), in which signalling receptors would become exhausted when submitted to a constant stress. As such, oscillations offer a more sustainable response to a continuous stimulus, periodically reducing the load on receptors and enabling their replenishment.

The consideration of these rhythms is currently not embedded in the diagnostic or treatment of diabetes. Therapies for diabetic individuals typically focus on keeping glucose levels within an acceptable range using a variety of medical strategies.

1.4 Aims and objectives

In this thesis, we aim to investigate the impact of deficiencies in either the pancreatic insulin secretion or glucose utilisation on the production of ultradian oscillations in the glucose-insulin regulatory system through the use of two mathematical models. Indeed, the primary focus will be on the stability analysis of models of ultradian rhythms, which are based on a system of first order nonlinear differential equations with multiple time delays. The sensitivity of the regulation in the time-delay domain

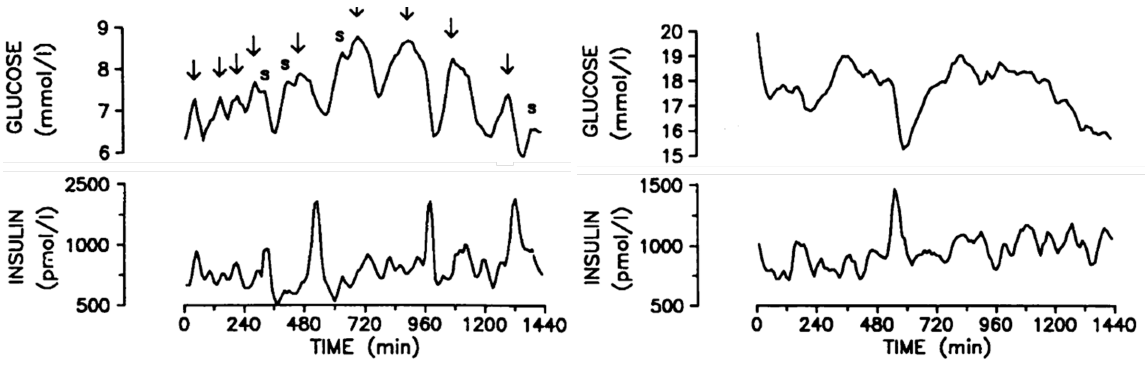

Figure 1.1: Profiles of the glucose and insulin blood concentrations for a non-diabetic (left) and a T2DM patient (right) under a constant glucose infusion. Figure from O'Meara et al. (1993).

with respect to various physiological parameters will be explored analytically and numerically. This will permit the introduction of measurable indicators of deficiency in the system as well as a description of the contribution of clinical treatments to reintroducing the oscillatory behaviour. Furthermore, a perturbation of periodic solutions in the reduced model will be explored in order to investigate the effect of model parameters on the amplitude and period of the oscillations.

1.4.1 Proposed questions

The primary questions we address in this project are:

> *What is the effect of reduced insulin production and/or sensitivity on the ultradian rhythms in an individual and what mechanisms can be used to restore the ultradian oscillatory regime to an acceptable physiological behaviour?*
>
> *What is the effect of diabetic parameters on the amplitude and period of the ultradian rhythms?*

1.4.2 Motivation

One of the main queries (see Atkinson, Eisenbarth & Michels (2014, p. 13) for a detailed list) regarding the treatment of diabetes is:

"Can a safe and effective closed-loop therapy system be developed?"

A closed-loop therapy system is a system that combines a glucose sensor, a control algorithm (based around a mathematical model), and an insulin infusion device (Cobelli, Renard & Kovatchev 2011). This type of system is most commonly referred to as an artificial pancreas (AP). The end aim of the AP is to fully automate/regulate glucose control, with the result of delaying (or preventing) the complications of diabetes, lowering the risk of hyperglycaemic episodes, and reducing the time spent and discomfort of multiple daily insulin injections and glucose tests (Jaremko & Rorstad 1998). In its current state, the AP may decrease the number of extreme variations in the blood glucose by calculating the optimal doses of insulin to be administered (Turksoy & Cinar 2015). As it stands, one of the main challenges in creating a safe and effective AP is the (commercial) integration of high tech continuous glucose monitors (CGM) and insulin infusion systems, along with closed-loop algorithms (Peyser et al. 2014). The algorithms must be able to accurately maintain normoglycemia, by ordering just the right amount of insulin, while adjusting for inaccuracies in the glucose data (Jaremko & Rorstad 1998). To accelerate the development of the AP, a suitable mathematical model which can be used as the basis of the control algorithm needs to be developed and made widely available (Steil & Reifman 2009, Cobelli et al. 2011).

Why modelling is important

Along with the need as the basis of a control algorithm in an AP, a dynamical mathematical model which takes into account several important physiological features of this system, as well as the various delays in the reactions, has been shown to be important in the precise description of the glucose-insulin oscillations (Sturis et al. 1991, Tolic, Mosekilde & Sturis 2000, Li, Kuang & Mason 2006). Through analytical characterisation of the favourable conditions leading to the onset of an oscillatory regime in an appropriate mathematical model, the underlying mechanisms which are most responsible for this regulation can be highlighted (Ajmera et al. 2013).

1.4.3 Methodology

We propose and study two two-compartment nonlinear delay differential equation (DDE) models for representing the ultradian oscillations which are known to occur within the glucose-insulin regulatory system. They are based on the one introduced by Li et al. (2006), which is of the form

$$\begin{aligned} \frac{d}{dt}G(t) &= F_1\left(G(t), I(t), I(t-\tau_2), \beta\right), \\ \frac{d}{dt}I(t) &= F_2\left(G(t), G(t-\tau_1), I(t), \alpha\right), \end{aligned} \tag{1.4.1}$$

where $G(t)$ and $I(t)$ represent the glucose and insulin blood levels respectively, $\tau_1, \tau_2 > 0$ are discrete delays within the system, and α and β represent deficiencies in the glucose-insulin regulatory system (see Section 3.1 for a more in-depth description). The steady state is defined as the equilibrium point in the state space for which $G(t) = \bar{G}$, $I(t) = \bar{I}$ satisfies $F_1\left(\bar{G}, \bar{I}, \beta\right) = 0$, $F_2\left(\bar{G}, \bar{I}, \alpha\right) = 0$ and thus depends on the parameters α and β. Hence, the effect of the diabetic parameters on the steady state of the system is then described. Next, a linear stability analysis is performed by noting that system (1.4.1) can be linearised as follows to characterise the nature of the equilibrium

$$\begin{aligned} \begin{pmatrix} \dot{u} \\ \dot{v} \end{pmatrix} = &\begin{pmatrix} \frac{\partial F_1}{\partial X(t)} & \frac{\partial F_1}{\partial Y(t)} \\ \frac{\partial F_2}{\partial X(t)} & \frac{\partial F_2}{\partial Y(t)} \end{pmatrix}\Bigg|_{X(t)=\bar{X},Y(t)=\bar{Y}} \begin{pmatrix} u(t) \\ v(t) \end{pmatrix} \\ &+ \begin{pmatrix} \frac{\partial F_1}{\partial X(t-\tau_1)} & \frac{\partial F_1}{\partial Y(t-\tau_1)} \\ \frac{\partial F_2}{\partial X(t-\tau_1)} & \frac{\partial F_2}{\partial Y(t-\tau_1)} \end{pmatrix}\Bigg|_{X(t-\tau_1)=\bar{X},Y(t-\tau_1)=\bar{Y}} \begin{pmatrix} u(t-\tau_1) \\ v(t-\tau_1) \end{pmatrix} \\ &+ \begin{pmatrix} \frac{\partial F_1}{\partial X(t-\tau_2)} & \frac{\partial F_1}{\partial Y(t-\tau_2)} \\ \frac{\partial F_2}{\partial X(t-\tau_2)} & \frac{\partial F_2}{\partial Y(t-\tau_2)} \end{pmatrix}\Bigg|_{X(t-\tau_2)=\bar{X},Y(t-\tau_2)=\bar{Y}} \begin{pmatrix} u(t-\tau_2) \\ v(t-\tau_2) \end{pmatrix}, \end{aligned} \tag{1.4.2}$$

where $u(t) = X(t) - \bar{X}$, $v(t) = Y(t) - \bar{Y}$. By looking for exponential solutions i.e.

$$\begin{pmatrix} u(t) \\ v(t) \end{pmatrix} = \begin{pmatrix} u_0 \\ v_0 \end{pmatrix} e^{\lambda t},$$

a transcendental characteristic equation of the form

$$\lambda^2 + A\lambda + B + Ce^{-\lambda\tau_1} + De^{-\lambda(\tau_1+\tau_2)} = 0, \tag{1.4.3}$$

is found. Here A, B, C, D are functions of the model parameters. This is then used to investigate the stability of the system with respect to the diabetic parameters (see Section 3.1.2). Additionally, due to the existence of a curve of supercritical Hopf bifurcations in the (τ_1, τ_2) space, the characteristic equation is used to mathematically investigate treatment strategies for restoring oscillations within the system by looking at the location of its rightmost eigenvalue (Section 4.2). Indeed, it is known that quasi-polynomials of the form (1.4.3) only possess a finite number of roots in the right half-plane (see, e.g. Smith (2011, pp. 17)). It is also shown that pairs of purely imaginary roots of (1.4.3) can be characterised using Chebyshev polynomials (Section 3.2.1).

Finally, a Poincaré-Lindstedt (P-L) perturbation method is applied to investigate the effect of model parameters on the amplitude and frequency of periodic solutions in a reduced nonlinear polynomial model. Indeed, by removing long term non-periodic variation (secular terms) through the rescaling of time, the periodic solutions can be studied in more depth (Casal & Freedman 1980). Initially, the hepatic glucose production term is considered constant, i.e., only one delay is present. Then by assuming $\tau_2 = k\tau_1$ with $k \in \mathbb{Z}^+$, that is, that τ_2 is commensurate with τ_1, the method is applied to the reduced model with a linear hepatic term. See Chapter 5 for more details.

1.4.4 Statement of original contribution

- A local stability analysis is used to investigate the effect of diabetic parameters on the stability of a two delay model of the glucose-insulin regulatory system.
- The restoration of an oscillatory regime within the system is explored mathematically using four treatment strategies.
- Analytical expressions for the amplitude and period of the ultradian rhythms are obtained.

As mentioned in the preamble, some of the material presented in this thesis, namely parts of Sections 1.3, 1.4.1, 3.1, and 3.3, as well as elements of Chapters 4 and 6, is based on Huard, Bridgewater & Angelova (2017).

1.5 Thesis structure

Chapters 2 - 5 of this thesis focus on the mathematical modelling of the glucose-insulin regulatory system using DDEs. More specifically, Chapter 2 highlights key existing literature in the modelling of glucose and insulin dynamics. In Chapter 3, two two-compartment DDE models are introduced, and analysed using a local stability analysis. Chapter 4 investigates the use of four treatment strategies in the restoration of the ultradian oscillations. In Chapter 5, analytical expressions for the amplitude and period of the periodic solutions in the simplified non-linear model are obtained. Finally, in Chapter 6 a conclusion for the work is presented, and possible future avenues are explored.

Chapter 2

Mathematical modelling of glucose-insulin regulation: an overview

Mathematical modelling and computer simulation have become a key means for researchers to investigate and develop new understandings of biological processes (Barnes & Chu 2015). Indeed, mathematical models have been used to describe and investigate a variety of biological concepts and systems, for example: dynamics of infectious diseases (Anderson & May 1992); tumour growth (Roose et al. 2007); epilepsy (Lytton 2008); and the HPA axis (Rankin et al. 2012). With regards to the glucose-insulin regulatory system, it is known that the mathematical modelling of diabetes enables a deeper understanding of the underlying mechanisms involved (Ajmera et al. 2013).

In this chapter, existing models of the glucose-insulin regulatory system are discussed. As highlighted by Boutayeb & Chetouani (2006), there exists a breadth of literature on the modelling of the subject. Indeed, models of the glucose-insulin system can be broken down into many categories, such as: whole body glucose-insulin dynamics (Boutayeb & Chetouani 2006, Ajmera et al. 2013); glucose-insulin oscillations (Palumbo et al. 2013); insulin release (Ajmera et al. 2013); and diagnosis (Ajmera et al. 2013). They can also be grouped mathematically, for example as: ordinary differential equations (ODEs); delay differential equations (DDEs); and

stochastic differential equations (SDEs) (see Makroglou, Li & Kuang (2006) for a detailed list). Therefore, the aim of this chapter is not to provide an exhaustive overview of the available models, but rather the background for which the models presented in Chapter 3 are based. Hence, the primary focus will be on the review of existing models of the ultradian oscillations in the glucose-insulin regulatory system.

2.1 Non-oscillatory models of the glucose-insulin system

Here, we give a brief overview of glucose-insulin models in which: (1) no oscillations are produced; or (2) oscillations are not the primary focus of the model. While some of these models will not directly influence the formulation of the models presented in Chapter 3, their relevance in the field of diabetic modelling warrants their inclusion.

2.1.1 Minimal model

According to Derouich & Boutayeb (2002), Bolie (1961) was one of the pioneering papers in glucose-insulin regulation modelling, and many mathematical models have been proposed since in order to help understand the mechanisms within the system (Makroglou et al. 2006). One of the most commonly used models in research (De Gaetano & Arino 2000, Bergman 2005, Cobelli et al. 2011), is Bergman's *minimal model* (Bergman et al. 1979), which is an ODE model with two compartments. It is given by the following equations (Bergman 2005)

$$\frac{dG(t)}{dt} = -\left(S_G - X(t)\right) G(t),$$
$$\frac{dX(t)}{dt} = p_2 I(t) - p_3 X(t),$$

where $G(t)$ is the plasma glucose concentration, $X(t)$ is the remote insulin (i.e. insulin in the interstitial fluid (Bergman 2005)) , $I(t)$ is the plasma insulin concentration, p_2 represents the fractional rate at which insulin appears in the interstitial fluid, p_3 represents the rate at which insulin is cleared from interstitial fluid and S_G represents the effectiveness of glucose (Bergman 2005). Each of the parameters can be measured using the intravenous glucose tolerance test (IVGTT)

(Bergman et al. 1979). By looking at the partial derivative of $I(t)$ and $G(t)$ upon $\frac{dG}{dt}$ (Bergman 2005), the insulin sensitivity index (Bergman et al. 1979), S_I, was defined as

$$S_I = \frac{p_3}{p_2}.$$

This has enabled estimates of the insulin sensitivity to be calculated using the IVGTT rather than the more invasive glucose clamp method (Bergman et al. 1979).

Bergman (2005) indicates that the *minimal model's* long use in clinical trials may be attributed to its simplicity, and robustness. While possible flaws have been highlighted by some authors (De Gaetano & Arino 2000, Makroglou et al. 2006), its importance in physiological research for diabetic research is strongly acknowledged. However, due to the fact that it does not lead to oscillations, Bergman's *minimal model* will not be used in the formulation of the models introduced in Chapter 3.

2.1.2 Further models of the IVGTT

De Gaetano & Arino (2000) proposed the following DDE model for representing plasma glucose $G(t)$ and insulin $I(t)$ dynamics

$$\frac{dG(t)}{dt} = -b_1 G(t) - b_4 G(t) I(t) + b_7, \quad \frac{dI(t)}{dt} = -b_2 I(t) + \frac{b_6}{b_5} \int_{t-b_5}^{t} G(s) ds, \quad (2.1.1)$$

with

$$G(0) = G_b + b_0, \quad I(0) = I_b + b_0 b_3, \text{and} \quad G(t) = G_b, \quad t \in [-b_5, 0),$$

where the coefficients are defined as

G_b : Pre-intravenous glucose bolus plasma glucose concentration.

b_0 : Theoretical increase in plasma glucose after the intravenous glucose bolus.

b_1 : Glucose effectiveness.

b_2 : Rate of insulin degradation.

b_3 : Insulin concentration increase due to the intravenous glucose bolus.

b_4 : Insulin sensitivity/resistance.

b_5 : Time delay in insulin secretion.

b_6 : Glucose stimulated maximal insulin secretion.

b_7 : Hepatic glucose production.

The solutions of the model were shown to be positive, bounded, and globally asymptotically stable around a unique steady state (De Gaetano & Arino 2000). Li, Kuang & Li (2001) generalised the model of De Gaetano & Arino (2000) as follows

$$\frac{dG(t)}{dt} = -f\left(G(t)\right) - g\left(G(t), I(t)\right) + b_7, \quad \frac{dI(t)}{dt} = q\left(L(G_t)\right) - p\left(I(t)\right),$$

where $f(G(t))$ is the insulin independent glucose uptake, $g(G(t), I(t))$ represents the insulin dependent glucose utilisation, $p(I(t))$ represents the insulin degradation, and $q(L(G_t))$ is the insulin secretion stimulated by glucose. Two types of delay were considered in the process of insulin secretion, discrete and distributed. In both cases it was shown that a Hopf bifurcation occurs, although it should be noted that for a physiological choice of parameters that the solutions were always in the stable regime (Li et al. 2001). Further developing the *minimal model*, Panunzi, Palumbo & De Gaetano (2007) introduced a single delay model based on (2.1.1), with the ranges of the delay being explored by Li et al. (2012). More recently, Shi et al. (2017) introduced a IVGTT model with a delayed effect in the past sub-interval centered at $t - \tau$ with radius ϵ. This delayed effect represented the delay of glucose stimulated insulin secretion. The model is given as follows

$$\frac{dG(t)}{dt} = b - S_g G(t) - S_i G(t) I(t), \quad \frac{dI(t)}{dt} = \sigma f\left(\frac{1}{2\epsilon}\int_{-\tau-\epsilon}^{-\tau+\epsilon} G(t+\theta)d\theta\right) - d_i I(t),$$

with

$$f(z) = \frac{z^n}{z^n + \alpha^n} \quad \text{for} \quad z, \alpha \geq 0 \quad \text{and} \quad n \geq 2, \quad G(t) = \phi(t), \quad t \in [-\tau - \epsilon, 0],$$

where b, S_g, S_i, σ and $d_i > 0$ are parameters representing the hepatic glucose production, insulin independent glucose utilisation, insulin sensitivity/resistance, rate of insulin secretion stimulated by glucose and insulin degradation rate, respectively. Depending on the values of τ and ϵ it was shown that the system could switch from

stable to unstable (Shi et al. 2017). Indeed, using parameter estimates based on patient data, it was numerically shown that a smooth monotonic curve of Hopf bifurcation points split the (τ, ϵ) plane into two regions, one in which the equilibrium point was stable, and one where the limit cycle existed (Shi et al. 2017). However, the values of τ and ϵ required to generate the limit cycle were considered to be non-physiological (Shi et al. 2017) and hence, as with the previous models discussed in this section, stable solutions are predicted when using physiological meaningful parameter values (Shi et al. 2017).

2.2 Models of the ultradian rhythms

Many biological systems are modelled by autonomous systems without delay (Thomas et al. 1995). However, the use of delays is often justified in realistically replicating core aspects of these systems (Thomas et al. 1995). Indeed, models with delays are largely accepted as a source of instabilities and periodic oscillations (Bocharov & Rihan 2000). In this section, first ODE models of the ultradian oscillations in the glucose-insulin system are explored. While the models do not contain explicit delays, subsystems are used to replicate delayed effects. Next, DDE models of the ultradian rhythms are studied. Finally, models that are used to investigate treatment strategies and that can replicate the ultradian oscillations are highlighted.

2.2.1 ODE models

In a pioneering series of clinical investigations of ultradian oscillations conducted in the early 1990s, Sturis et al. (1991) designed the following three compartment ODE model that was based on two negative feedback loops in the glucose-insulin system

$$\begin{aligned}
\frac{dx}{dt} &= f_1(z) - E\left(\frac{x}{V_1} - \frac{y}{V_2}\right) - \frac{x}{t_1}, \\
\frac{dy}{dt} &= E\left(\frac{x}{V_1} - \frac{y}{V_2}\right) - \frac{y}{t_2}, \\
\frac{dz}{dt} &= f_5(h_3) + I - f_2(z) - f_3(z)f_4(y), \\
\frac{dh_1}{dt} = 3\left(\frac{x - h_1}{t_3}\right), &\quad \frac{dh_2}{dt} = 3\left(\frac{h_1 - h_2}{t_3}\right), \quad \frac{dh_3}{dt} = 3\left(\frac{h_2 - h_3}{t_3}\right),
\end{aligned}$$

where $x(t)$, $y(t)$ and $z(t)$ are the plasma insulin, insulin in the interstitial fluid, and mass of glucose, respectively. The two delays in the system are the insulin production delay, and the hepatic glucose production delay, which are represented by the separation of the insulin into two compartments and the three-tiered system of auxiliary variables, h_1, h_2 and h_3, respectively. The functions f_1 to f_5 are given by

$$f_1(G) = \frac{R_m}{1 + e^{\frac{C_1 - GV_g^{-1}}{a_1}}}, \quad f_2(G) = U_b\left(1 - e^{-\frac{-G}{C_2 V_g}}\right), \quad f_3(G) = \frac{G}{C_3 V_g},$$

$$f_4(I) = U_0 + \frac{U_m - U_0}{1 + e^{-\beta \log\left(\frac{I}{C_4\left(V_i^{-1} + (Et_i)^{-1}\right)}\right)}}, \quad f_5(I) = \frac{R_g}{1 + e^{\alpha(IV_p^{-1} - C_5)}},$$

where f_1 is the pancreatic insulin production, f_2 and $f_3 f_4$ are the glucose utilisation by the brain, and muscle/fat cells, respectively, and f_5 is the hepatic glucose production. The values of the parameters in the functions $f_1 - f_5$ are given in Tables 2.1 and 3.2. For more details regarding the formulation of these functions, see Section

Constant	Value	Units
a_1	300	mg/l
C_1	2000	mg/l
C_2	144	mg/l
C_4	80	mU/l
C_5	26	mU/l
α	0.29	lm/U
β	1.77	

Table 2.1: Parameters used in the functions $f_1 - f_5$. They were originally determined by fitting the functions f_1 - f_5 to published clinical experiments of individual subsystems (see Sturis et al. (1991) and references therein).

3.1.

Ultradian insulin secretion oscillations were reproduced using the model, and this led to the proposition that there is no need to postulate the existence of an intra-pancreatic pacemaker (Sturis et al. 1991). The model was later simplified by Tolic et al. (2000).

2.2.2 DDE models

The model of Sturis et al. (1991) has become the basis of multiple DDE models (Drozdov & Khanina 1995, Engelborghs et al. 2001, Bennett & Gourley 2004*a*). Indeed, Li et al. (2006) proposed the following two compartment DDE model incorporating two time delays

$$\frac{dG(t)}{dt} = G_{in} - f_2\left(G(t)\right) - f_3(G(t))f_4(I(t)) + f_5(I(t-\tau_2)),$$
$$\frac{dI(t)}{dt} = f_1(G(t-\tau_1)) - d_i I(t),$$

where the functions $f_1 - f_5$ are as defined by Sturis et al. (1991). The two delays, τ_1 and τ_2, can be interpreted as the time taken for an elevated glucose concentration to stimulate insulin release and be transported to the interstitial space, and the time taken for insulin to have an observed effect on the liver, respectively (Li et al. 2006). It is important to note that the incorporation of the delay in hepatic glucose production was originally based on observed data, rather than from a physiological perspective. Indeed, a suitable method to estimate and study the effect of the delays on the endocrine system does not yet exist (Wu et al. 2011). However, they remain physiologically plausible, and from a mathematical perspective they are crucial in the production of an oscillatory regime (Li et al. 2006). Li & Kuang (2007) studied the model in more depth analytically, and then Song, Huang & Li (2014) adapted the model in order to be incorporated within an AP, through the addition of external insulin at regular time intervals. Analytical characterisation of this adapted model led to an inequality for ensuring periodic solutions within the system.

In Huard et al. (2015), the models proposed by Sturis et al. (1991) and Li et al. (2006) were further developed through the introduction of Hill equations to model the functions f_1, f_2, f_4 and f_5, all of which represent crucial features of the regulatory system. This enabled the use of parameters within the model that have physiological meaning (Huard et al. 2015). These parameters were then related to the apparition of an oscillatory regime. A further analytical characterisation of the two-delay model was also carried out, through an analysis of its local and global stability properties using a Lyapunov functional, thus extending the results obtained by Bennett & Gourley (2004*b*) to the two-delay case.

2.2.3 Modelling the effect of diabetes

To model the dynamics of insulin therapies in T1DM patients, Wang, Li & Kuang (2007) proposed the following DDE model

$$\begin{aligned}\frac{dG(t)}{dt} =& G_{in}(t) - f_2\left(G(t)\right) - f_3\left(G(t)\right) f_4\left(I(t-\tau_3)\right) + f_5\left(I(t-\tau_2)\right),\\ \frac{dI(t)}{dt} =& I_{in}(t) - d_i I(t),\end{aligned}$$

where the functions $f_1 - f_5$, are as defined by Sturis et al. (1991), τ_2 is as defined by Li et al. (2006), and $G_{in}(t)$ and $I_{in}(t)$ are positive ω-periodic functions representing glucose and insulin infusions, respectively. τ_3 is defined as the time taken for insulin-dependent glucose utilisation by the cells to occur. The effects of different types of insulin were explored. Due to the periodicity of the two infusions, a unique and globally asymptotically stable solution $(G(t), I(t))$ was always shown to exist. Chen, Tsai & Wong (2010) introduced the following model to extend the model developed by Li et al. (2006)

$$\begin{aligned}\frac{dG(t)}{dt} =& \left[G_{in}(t) + f_5\left(I(t-\theta_2)\right) f_6\left(G(t)\right)\right]\\ &- \left[f_2\left(G(t)\right) + f_7\left(G(t) - 330\right) + \beta f_3\left(G(t)\right) f_4\left(I(t)\right)\right],\\ \frac{dI(t)}{dt} =& \alpha f_1\left(G(t-\theta_1)\right) - d_i I(t),\end{aligned}$$

where $f_6(G(t))$ and $f_7\left(G(t) - 330\right)$ are functions used to model the effects of hyperglycaemia, θ_1 and θ_2 correspond to the delays defined by Li et al. (2006), and $G_{in}(t)$ is a variable glucose infusion to model food uptake. The functions $f_1 - f_5$ are as defined by Sturis et al. (1991), and the parameters α, β represent insulin release from the pancreas and insulin resistance, respectively. The effect of these parameters on the oscillatory regime was explored numerically.

Kissler et al. (2014) proposed the following two-delay model, which features Michaelis-Menten dynamics for quantifying the insulin degradation

$$\begin{aligned}\frac{dG(t)}{dt} =& G_{in} + f_5\left(I(t-\tau_2)\right) - f_2\left(G(t)\right) - \gamma[1 + s(m - m_b)] f_3\left(G(t)\right) f_4\left(I(t)\right),\\ \frac{dI(t)}{dt} =& I_{in} + \beta f_1\left(G(t-\tau_1)\right) - \frac{V_{max} I(t)}{K_M + I(t)},\end{aligned}$$

where the functions $f_1 - f_5$, are as defined by Sturis et al. (1991), and τ_1 and τ_2 are as defined by Li et al. (2006). The constants β and γ represent β-cell function and

insulin resistance, respectively. As in Chen et al. (2010), these parameters reflecting the effect of diabetes ranged between 0 and 1. The model was used to investigate personalised treatment options for diabetics. While the authors noted whether the resulting solution was oscillatory, the restoration of an oscillatory regime was not the focus of the work.

Chapter 3

Models of glucose-insulin regulation

This chapter focuses on the delayed models of ultradian glucose-insulin regulation which form the core of our investigations. Firstly, the most general form of the two-delay model is presented along with a description of the main physiological functions entering the system. Then, local stability analysis is used to investigate the contribution of various parameters on the oscillatory behaviour of the model, with a special emphasis on the effect of insulin resistance. Secondly, a simplified polynomial version of the first model is introduced to facilitate the characterisation of the periodic solutions. Conditions for stability are identified through local stability analysis and it is shown that points of Hopf bifurcations can be investigated using Chebyshev polynomials. Finally, the periodic solutions of a third (linear) model, in which a non delayed, glucose stimulated, insulin response is included, are explored.

3.1 The two-delay model

In its most general form, the model proposed is given by the following system of DDEs with two delays

$$\begin{aligned} \dot{G} &= G_{in} - f_2(G) - \beta f_3(G) f_4(I) + \gamma f_5(I(t-\tau_2)), \\ \dot{I} &= I_{in} + \alpha f_1(G(t-\tau_1)) - d_i(\alpha,\beta) I, \end{aligned} \tag{3.1.1}$$

and it is based on the framework represented in Fig. 3.1. Here $G(t)$ and $I(t)$ represent plasma glucose and plasma insulin concentrations in mg and mU, respectively. Note, for the purpose of all Figures, $G(t)$ and $I(t)$ will be converted to mg/dl and mU/l, respectively. Model (3.1.1) follows the ones introduced by Kissler et al. (2014) and Huard et al. (2015), which were based on the works of Sturis et al. (1991), Tolic et al. (2000), Engelborghs et al. (2001), Bennett & Gourley (2004a), and Li et al. (2006). Indeed, as in Kissler et al. (2014), model (3.1.1) incorporates parameters for insulin resistance and insulin secretion capacity, as well as the use of Hill functions for system functions, as done by Huard et al. (2015). In contrast to the models of Kissler et al. (2014) and Huard et al. (2015), it incorporates a parameter for the effect of medication on the hepatic glucose production. Additionally, it takes the degradation term to be a function of the insulin resistance and insulin secretion capacity.

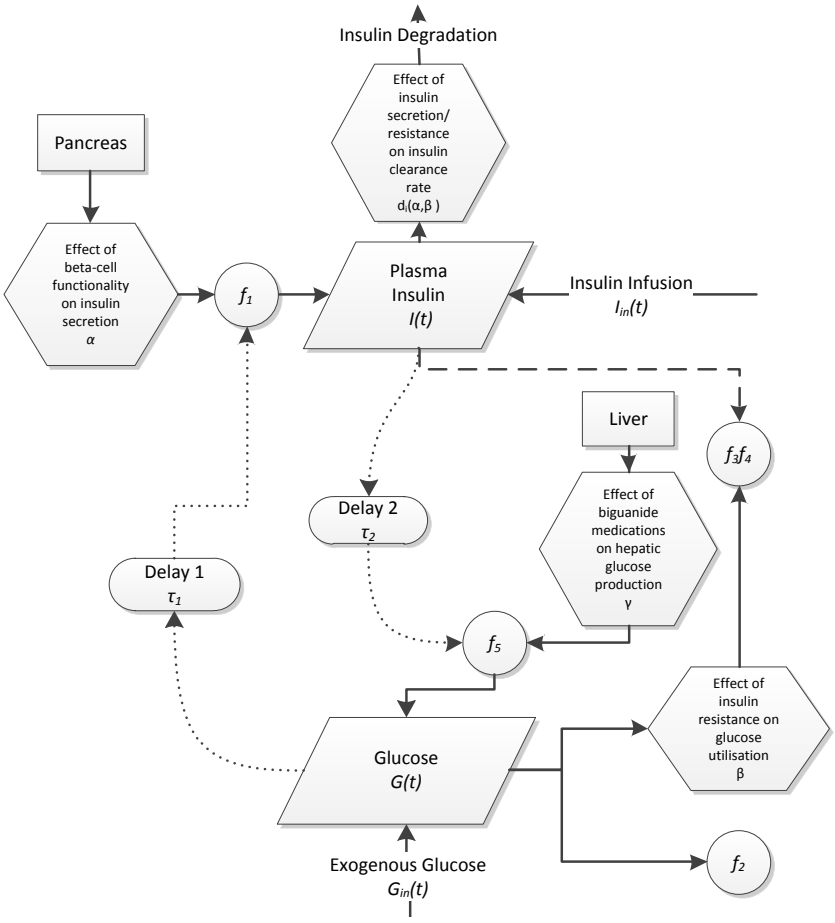

Figure 3.1: Flow diagram for model (3.1.1).

The relevant features of the model can be summarised as follows.

$\alpha f_1(G(t-\tau_1))$ **:** Insulin production/secretion. It is represented by a sigmoidal function (Grodsky 1972) (Fig. 3.2a). A delay τ_1 is present in this process. It accounts for the time lag, in minutes, between when high glucose levels trigger the *production* of insulin within the pancreas and when it becomes available (Li et al. 2006). Clinical experiments have provided a time range of $[5, 20]$ minutes for this reaction. The parameter α modulates this secretion, with low levels being typical of T1DM.

$f_2(G)$ **:** Insulin-independent glucose utilisation, mainly by the brain. As seen in Fig. 3.2b it is also sigmoidal and is based on the function used by Turner et al. (1979).

$\beta f_3(G) f_4(I)$ **:** Insulin-dependent glucose utilisation, by the muscles. As in Sturis et al. (1991), $f_3(G)$ is linear (Fig. 3.2c) and $f_4(I)$ is sigmoidal (Fig. 3.2d). Values of $\beta < 1$ indicate a reduced capacity of utilising insulin to degrade glucose, also called insulin resistance, which is seen in T2DM.

$\gamma f_5(I(t-\tau_2))$ **:** Glucose production by the liver. The shape of the function is based on the work of Rizza, Mandarino & Gerich (1981) and can be seen in Fig. 3.2e. Indeed, large values of insulin induce an inhibitory effect on the glucose production, whereas glucose output increases at lower insulin concentrations (Rizza et al. 1981). The delay in this reaction, denoted by τ_2, denotes the time between hepatic glucose production and insulin stimulation and is typically between 20 and 50 minutes (Li et al. 2006). This production is controlled by the parameter γ, to account for effect of biguanide medications which act by lowering it to keep glucose levels low (Hundal et al. 2000).

$d_i(\alpha, \beta)$ **:** Combined rate of degradation of insulin, especially by the liver and kidneys. In Chapter 4, we consider it as a combination of natural (for example, exercise (Tuominen, Ebeling & Koivisto 1997)) and artificial (for example, through the inhibition of insulin degrading enzyme (IDE) (Costes & Butler 2014, Maianti et al. 2014)) mechanisms, and as a function of α and β

to investigate how it can be used to compensate for the effects of a reduced insulin secretion (α) and/or an increased insulin resistance (β) on an appropriate oscillatory regime.

Here, we represent these functions in terms of Hill functions,

$$f_1 = \frac{R_m(G/V_g)^{h_1}}{(G/V_g)^{h_1} + k_1^{h_1}}, \quad f_2 = \frac{U_b(G/V_g)^{h_2}}{(G/V_g)^{h_2} + k_2^{h_2}}, \quad f_3 = \frac{G}{C_3 V_g}, \tag{3.1.2}$$
$$f_4 = U_0 + (U_m - U_0)\frac{[(1/V_i + 1/(Et_i))I]^{h_4}}{[(1/V_i + 1/(Et_i))I]^{h_4} + k_4^{h_4}}, \quad f_5 = R_g\frac{(I/V_p)^{h_5}}{(I/V_p)^{h_5} + k_5^{h_5}},$$

as defined by Huard et al. (2015). This gives the advantage of introducing new parameters in the model which bear physiological meaning (a list of which can be found in Tables 3.1 and 3.2), and hence allows for more adequate modelling of the underlying physiological dynamics of the glucose-insulin system (Huard et al. 2015). These values were selected in Huard et al. (2015) to ensure the system produces an oscillatory regime in a physiologically suitable range for a non-diabetic patient. The functions are all strictly positive and f_1, f_2, f_4 are increasing while f_5 is decreasing. Here the parameters α and β play a crucial role in modelling the capacity of an individual to produce insulin or use it to utilise glucose, respectively. Values of $\alpha = \beta = \gamma = 1$ represent an optimal non-diabetic patient. Therefore, a value of $\alpha < 1$ represents a reduced insulin production capability, which is seen in T1DM (NHS 2014) (as well as after the onset of T2DM (Pories & Dohm 2012)). A value greater than 1 implies an increased insulin production capacity, observed in the very early stages of T2DM (although the reason for its occurrence is debated (Pories & Dohm 2012)). Likewise, if β is smaller than 1, this indicates a reduced insulin-dependent glucose utilisation which is typical of insulin resistance and related to both T1DM and T2DM (Greenbaum 2002). A value greater than 1 represents an increased sensitivity to insulin, which can pose the risk of hypoglycaemia in T1DM. Finally, values of $\gamma < 1$ represent a reduced glucose hepatic production which can result from the usage of drugs such as Metformin (Hundal et al. 2000), while $\gamma = 1$ corresponds to a typical non-diabetic production. For these reasons, the coefficients α, β and γ will be referred to as the *diabetic parameters*.

The constant value of G_{in} is typically between 1 - 3 mg/dl min, a range where ultradian oscillations have been observed (Simon & Brandenberger 2002). As seen

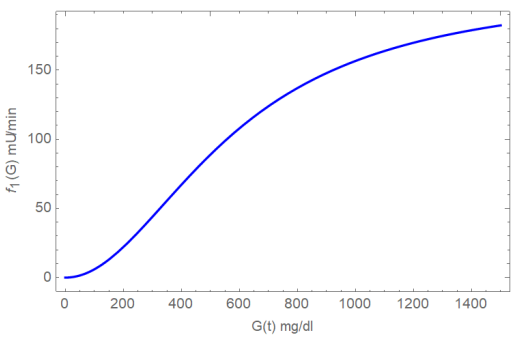

(a) Pancreatic insulin secretion function, f_1.

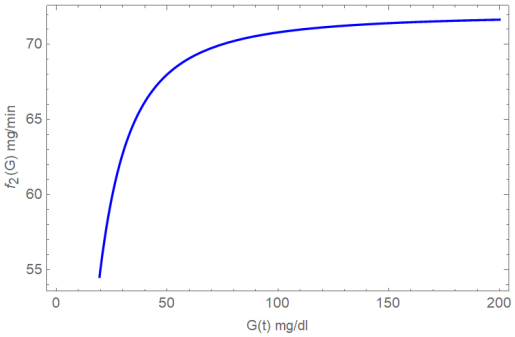

(b) Insulin independent glucose utilisation, f_2.

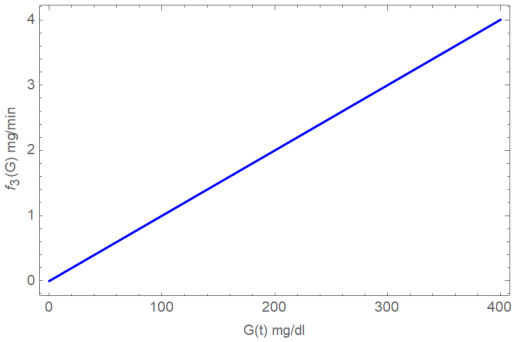

(c) Insulin dependent glucose utilisation, f_3.

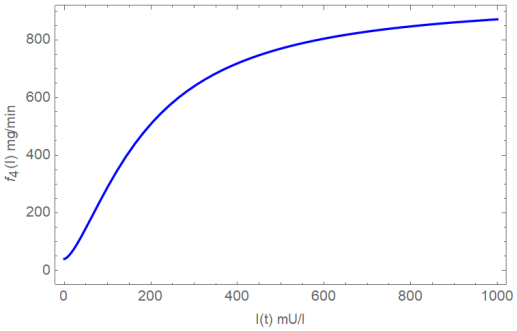

(d) Insulin dependent glucose utilisation, f_4.

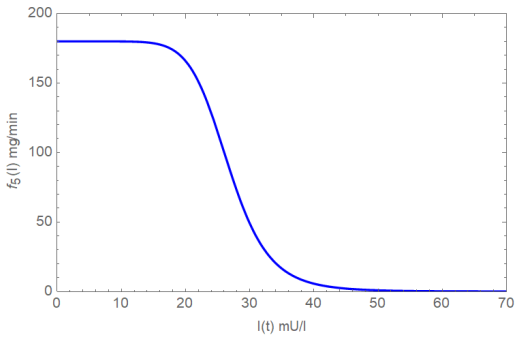

(e) Hepatic glucose production, f_5.

Figure 3.2: Functional forms of f_1, f_2, f_3, f_4 and f_5, using the parameter values given in Tables 3.1 and 3.2.

in Fig. 3.3, solutions to system (3.1.1) when $\alpha = \beta = \gamma = 1$, $I_{in} = 0$ and $\tau_1 = 6$, $\tau_2 = 36$ are oscillatory. Indeed, the joint role of the physiological delays in producing oscillations in the non-diabetic case has already been highlighted (Li & Kuang 2007, Huard et al. 2015). As was shown by Li & Kuang (2007), for any $\tau_1 > 0$ there exists a τ_2 such that the system undergoes a supercritical Hopf bifurcation at

Hill coefficient	Value	Hill coefficient	Value
h_1	2	k_1	5830
h_2	1.8	k_2	103.5
h_4	1.5	k_4	80
h_5	-8.5	k_5	26.72

Table 3.1: Values used for the Hill coefficients h_i, k_i, taken from (Huard et al. 2015).

Constant	Value	Units	Constant	Value	Units
R_m	210	mU/min	V_i	11	l
V_g	10	l	E	0.2	l/min
U_b	72	mg/min	t_i	100	min
C_3	1000	mg/l	R_g	180	mg/min
U_0	40	mg/min	V_p	3	l
U_m	940	mg/min	G_{in}	1.35	mg/dl min

Table 3.2: Parameters used in model (3.1.1). They were originally determined by fitting the functions f_1 - f_5 to published clinical experiments of individual subsystems (see Sturis et al. (1991) and references therein).

the point (τ_1, τ_2). This situation is illustrated in Fig. 3.4, where the threshold curve corresponds to the points where the system possesses a pair of pure imaginary eigenvalues.

3.1.1 The effect of insulin resistance on the glucose and insulin levels

In this section, we investigate the effect of the diabetic parameter β on the steady state $(\bar{G}, \bar{I})$ of model (3.1.1), which is governed by the following system of algebraic equations

$$G_{in} - f_2(\bar{G}) - \beta f_3(\bar{G}) f_4(\bar{I}) + \gamma f_5(\bar{I}) = 0, \tag{3.1.3}$$

$$I_{in} + \alpha f_1(\bar{G}) - d_i(\alpha, \beta)\bar{I} = 0. \tag{3.1.4}$$

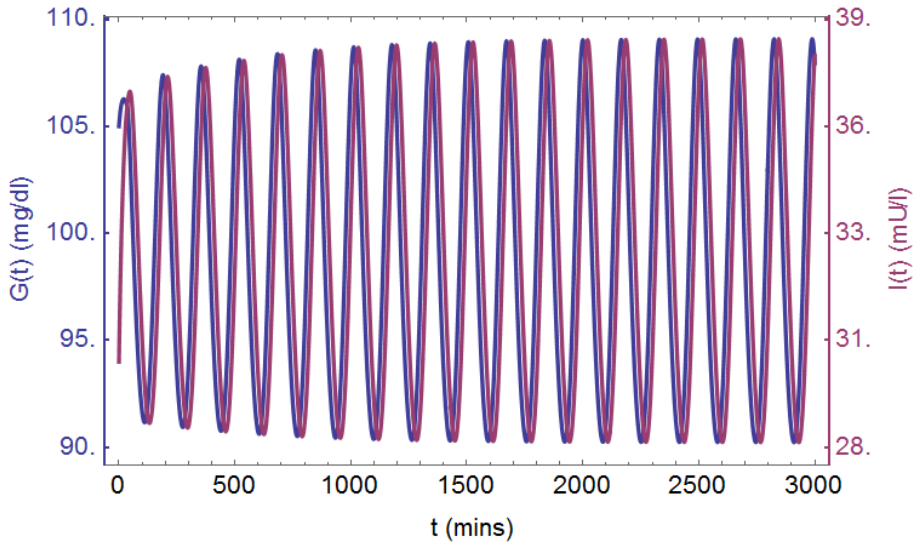

Figure 3.3: Solution to system 3.1.1 when $\alpha = \beta = \gamma = 1$, with $d_i = 0.06$, $G_{in} = 1.35$ mg/dl min and $\tau_1 = 6$ min, $\tau_2 = 36$ min.

To match physiological values, the values for the steady state should fit the ranges $90 < \bar{G} < 120$ and $25 < \bar{I} < 40$ respectively (Sturis et al. 1991). Given the assumptions on the functions and the parameters of the model, it can be shown that this system has a unique solution (see e.g. Bennett & Gourley (2004*b*)). The dependence upon β can be made more explicit in the following way. Differentiating implicitly equations (3.1.3) and (3.1.4) with respect to β leads to the following expressions

$$-f_2'(\bar{G})\bar{G}_\beta - f_3(\bar{G})f_4(\bar{I}) - \beta\left(f_3'(\bar{G})f_4(\bar{I})\bar{G}_\beta + f_3(\bar{G})f_4'(\bar{I})\bar{I}_\beta\right) + \gamma f_5'(\bar{I})\bar{I}_\beta = 0,$$
$$\alpha f_1'(\bar{G})\bar{G}_\beta - d_i(\alpha,\beta)_\beta \bar{I} - d_i(\alpha,\beta)\bar{I}_\beta = 0,$$

where the β subscript stands for the derivative. In matrix form, these can be written as

$$\begin{pmatrix} -A & -(B+C) \\ D & -d_i(\alpha,\beta) \end{pmatrix} \begin{pmatrix} \bar{G}_\beta \\ \bar{I}_\beta \end{pmatrix} = \begin{pmatrix} f_3(\bar{G})f_4(\bar{I}) \\ d_i(\alpha,\beta)_\beta \bar{I} \end{pmatrix}, \tag{3.1.5}$$

where we have introduced the following positive β-dependent quantities

$$A = f_2'(\bar{G}) + \beta f_3'(\bar{G})f_4(\bar{I}), \quad B = \beta f_3(\bar{G})f_4'(\bar{I}), \quad C = -\gamma f_5'(\bar{I}), \quad D = \alpha f_1'(\bar{G}), \tag{3.1.6}$$

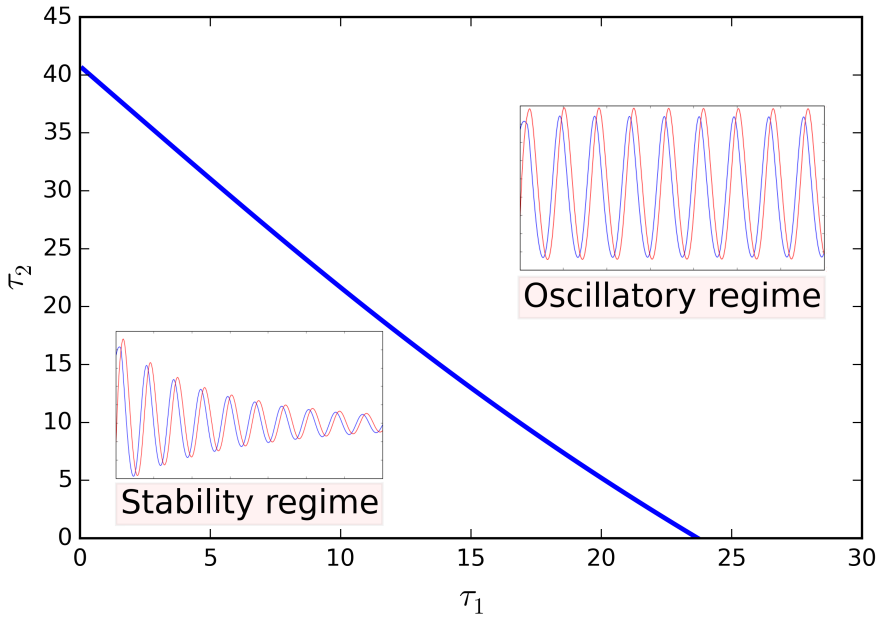

Figure 3.4: Curve of Hopf bifurcations in the optimal non-diabetic case $\alpha = \beta = \gamma = 1$, with $d_i = 0.06$ and $G_{in} = 1.35$ mg/dl min.

with the prime $'$ denoting the derivative with respect to the argument. The dependence of these functions on β is illustrated in Fig. 3.5.

Hence,

$$\begin{pmatrix} \bar{G}_\beta \\ \bar{I}_\beta \end{pmatrix} = \frac{1}{\Delta} \begin{pmatrix} d_i(\alpha,\beta)_\beta \bar{I}(B+C) - d_i(\alpha,\beta) f_3(\bar{G}) f_4(\bar{I}) \\ -D f_3(\bar{G}) f_4(\bar{I}) - A d_i(\alpha,\beta)_\beta \end{pmatrix}, \tag{3.1.7}$$

with

$$\Delta = A d_i(\alpha,\beta) + D(B+C) > 0.$$

The location of the system's steady state is linked to the level of insulin resistance and the clearance rate. Assuming no correlation between insulin degradation and insulin resistance, i.e. assuming d_i is constant, the effect of reduced insulin regulation capacity on the steady state $(\bar{G}, \bar{I})$ of system (3.1.1) is depicted in Fig. 3.6.

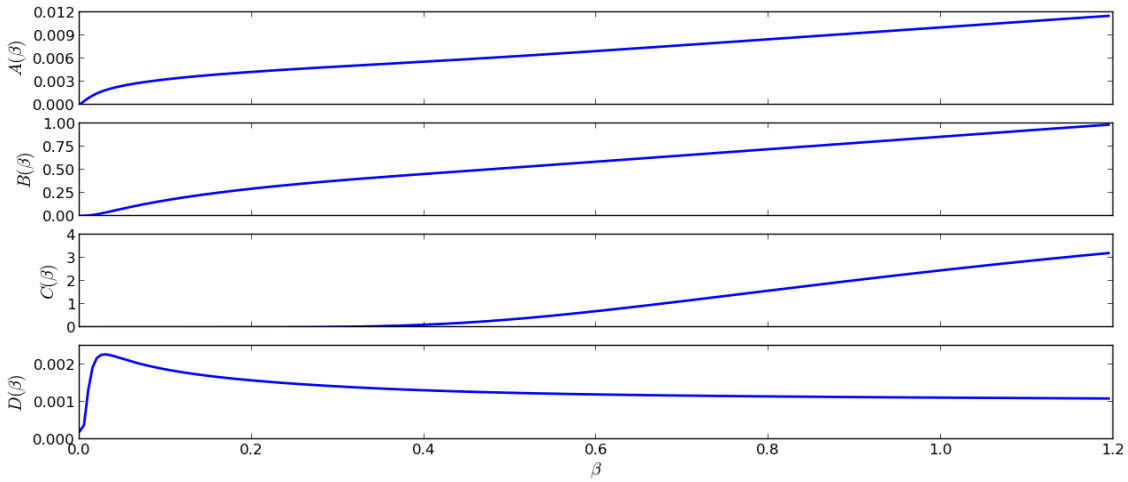

Figure 3.5: Graphs of the functions $A(\beta), B(\beta), C(\beta), D(\beta)$ for parameter values from Tables 3.1 and 3.2, with $d_i = 0.06$ and $I_{in} = 0$.

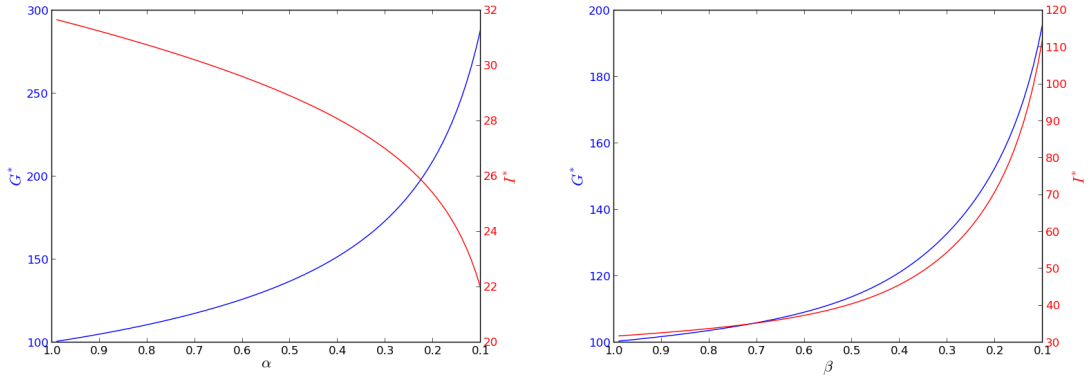

Figure 3.6: Effect on the steady state of reducing insulin production (left) and reducing insulin-dependent glucose utilisation (right), for $d_i = 0.06$. The glucose and insulin steady states are represented by the blue and red curves, respectively.

This picture is already instructive. As expected, reducing insulin production ($\alpha < 1$) leads to lower insulin and higher glucose levels. Additionally, introducing insulin resistance (or equivalently decreasing β) leads to both higher glucose and insulin levels, as observed physiologically in the early stages of T2DM (Pories & Dohm 2012). An investigation of strategies for improving the steady states by altering $d_i(\alpha, \beta)$ will be performed in Section 4.2.3.

3.1.2 The effect of insulin resistance on the ultradian oscillations

We now look at the effect of β on the production of oscillations in (3.1.1). In Kissler et al. (2014), the effect of a parameter, representing insulin sensitivity, on the real part of the dominant eigenvalue of the characteristic equation (for the linearised system) was investigated numerically. It was observed that larger values of the insulin sensitivity parameter were more likely to give rise to values of the real part of the dominant eigenvalue in the right half plane, and hence oscillatory solutions (Kissler et al. 2014). Here, we take a more analytic approach and look to derive a constraint such that oscillatory solutions are lost.

The linearisation of system (3.1.1) about $(\bar{G}, \bar{I})$ is given by

$$\begin{pmatrix} \dot{u} \\ \dot{v} \end{pmatrix} = \begin{pmatrix} -A & -B \\ 0 & -d_i(\alpha,\beta) \end{pmatrix} \begin{pmatrix} u(t) \\ v(t) \end{pmatrix} + \begin{pmatrix} 0 & 0 \\ D & 0 \end{pmatrix} \begin{pmatrix} u(t-\tau_1) \\ v(t-\tau_1) \end{pmatrix} + \begin{pmatrix} 0 & -C \\ 0 & 0 \end{pmatrix} \begin{pmatrix} u(t-\tau_2) \\ v(t-\tau_2) \end{pmatrix}. \tag{3.1.8}$$

A complex exponential solution $e^{\lambda t}$ of system (3.1.8) exists if and only if λ satisfies the following characteristic quasi-polynomial

$$(\lambda + A)(\lambda + d_i(\alpha,\beta)) + D\left[Be^{-\lambda\tau_1} + Ce^{-\lambda(\tau_1+\tau_2)}\right] = 0, \tag{3.1.9}$$

where it is important to note that A, B, C, D are functions of β. We now show that the characteristic equation (3.1.9) implies that the introduction of insulin resistance leads to the loss of oscillations. To do achieve this, we first note that it has been shown that (3.1.9) undergoes a supercritical Hopf bifurcation in the (τ_1, τ_2) space (Li & Kuang 2007). By defining $\lambda(\beta) = \eta(\beta) + \phi(\beta)$, it can therefore be seen that for the oscillations to be lost when insulin resistance is introduced, we must have that η decreases when β decreases from 1. In other words, we wish to prove that

$$\left.\frac{d\eta}{d\beta}\right|_{\beta=1} > 0.$$

Splitting the real and imaginary parts of (3.1.9) and differentiating with respect to β, we get expressions of the type

$$\frac{d\phi}{d\beta}c = \frac{d\eta}{d\beta}a + b, \quad \frac{d\phi}{d\beta}a = -\frac{d\eta}{d\beta}c - d, \tag{3.1.10}$$

where we introduced the following definitions

$$\begin{aligned}
a &= 2\eta + A + d_i - \tau_1 e^{-\eta\tau_1} BD\cos\phi\tau_1 - (\tau_1+\tau_2)\, e^{-\eta(\tau_1+\tau_2)} CD\cos\phi\,(\tau_1+\tau_2),\\
b &= A_\beta\eta + d_i'\eta + (d_i A)_\beta + e^{-\eta\tau_1}\cos\phi\tau_1\,(BD)_\beta + e^{-\eta(\tau_1+\tau_2)}\cos\phi\,(\tau_1+\tau_2)\,(CD)_\beta\,,\\
c &= 2\phi + \tau_1\sin\phi\tau_1 BDe^{-\eta\tau_1} + (\tau_1+\tau_2)\sin\phi\,(\tau_1+\tau_2) CDe^{-\eta(\tau_1+\tau_2)},\\
d &= \phi\,(A_\beta + d_i') - e^{-\eta\tau_1}\sin\phi\tau_1\,(BD)_\beta - e^{-\eta(\tau_1+\tau_2)}\sin\phi\,(\tau_1+\tau_2)\,(CD)_\beta\,.
\end{aligned} \tag{3.1.11}$$

Rearranging equations (3.1.10) and eliminating $\frac{d\phi}{d\beta}$ leads to an explicit expression for $\frac{d\eta}{d\beta}$, given by

$$\frac{d\eta}{d\beta} = -\frac{ab+cd}{a^2+c^2}. \tag{3.1.12}$$

We then obtain the following

Proposition 1 *Let $\lambda(\beta) = \eta(\beta) + i\phi(\beta)$ be a solution of the characteristic equation (3.1.9). Then $\frac{d\eta}{d\beta} > 0$ if and only if $ab + cd < 0$, with a, b, c, d as defined in (3.1.11).*

We now assume that an oscillatory regulation takes place when $\beta = 1$, which is when the system is in normal regulation. We consider the case on the threshold curve, that is $\lambda|_{\beta=1} = (\eta + i\phi)|_{\beta=1} = i\omega$, where $\omega > 0$ satisfies a transcendental equation. Indeed, setting $\lambda = i\omega$ in (3.1.9) and separating the real and imaginary parts leads to the following equation

$$\cos(\tau_2\omega) = \frac{(\omega^2+A^2)(\omega^2+d_i^2) - D^2(B^2+C^2)}{2BCD^2}, \tag{3.1.13}$$

while ω can be seen as a function of τ_1 through the following transcendental equation

$$\begin{aligned}
&(\omega^2+A^2)(\omega^2+d_i^2) + D^2(B^2-C^2)\\
&+ 2BD\left((Ad_i-\omega^2)\cos(\tau_1\omega) - \omega(A+d_i)\sin(\tau_1\omega)\right) = 0,
\end{aligned} \tag{3.1.14}$$

which can also be expressed as

$$\cos(\tau_1\omega + \phi) = -\frac{(\omega^2 + A^2)(\omega^2 + d_i^2) + D^2(B^2 - C^2)}{2BD}, \tag{3.1.15}$$

with

$$\phi = \arctan\left(-\frac{\omega(A + d_i)}{Ad_i - \omega^2}\right) + 2\pi.$$

Using (3.1.13) and (3.1.15), the critical values of τ_1 and τ_2 can then be algebraically calculated simultaneously (Gu et al. 2005, Nguimdo 2018, An et al. 2019).

It can be seen from Fig. 3.7 that $\frac{d\eta}{d\beta}|_{\beta=1} > 0$ when τ_1 is within a physiological range, between 5 and 20 minutes. Indeed, this implies that η decreases when β decreases from 1 or, in other words, that the oscillations are lost as β decreases from 1. The overall effect of β on the production of oscillations can then be seen in Fig. 3.8. As an example, the distribution of eigenvalues λ in the prototypical case $\tau_1 = 6$ and $\tau_2 = 36$ is depicted in Fig. 3.9, for cases with ($\beta = 1$) and without ($\beta = 0.8$) oscillations. This loss of oscillations with decreased β partly reflects what is observed physiologically. Indeed, as mentioned in Section 1.3, the loss of amplitude in the insulin oscillations that occurs with insulin resistance is observed experimentally (O'Meara et al. 1993). On the other hand, the loss of amplitude in the glucose oscillations is not directly observed physiologically when a constant glucose infusion is present (O'Meara et al. 1993). However, the observed decrease of entrainment of insulin secretion by glucose (O'Meara et al. 1993) can be locally seen through a stretching of the period, which has also been noted. Therefore, we shall interpret this loss of oscillations in the model with decreased β as the lack of control observed in patients with T2DM.

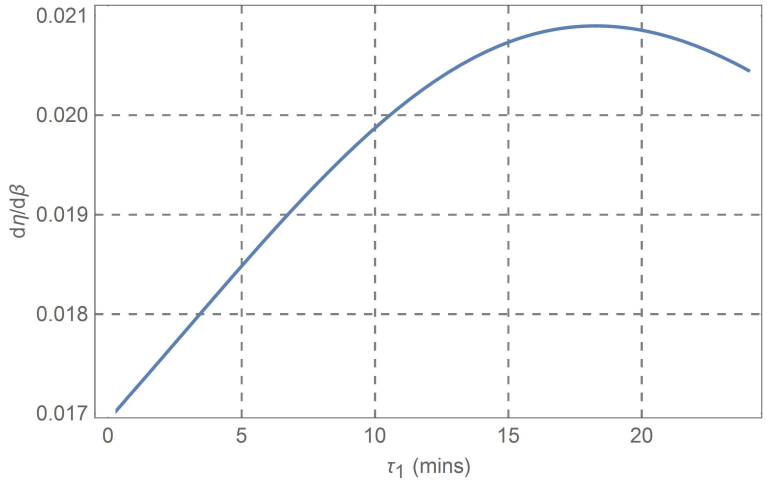

Figure 3.7: The derivative $\frac{d\eta}{d\beta}$ as a function of τ_1, with parameter values from Tables 3.1 and 3.2, with $d_i = 0.06$, $I_{in} = 0$ and $\beta = 1$. Typical values for τ_1 are to be chosen between 5 and 20 minutes.

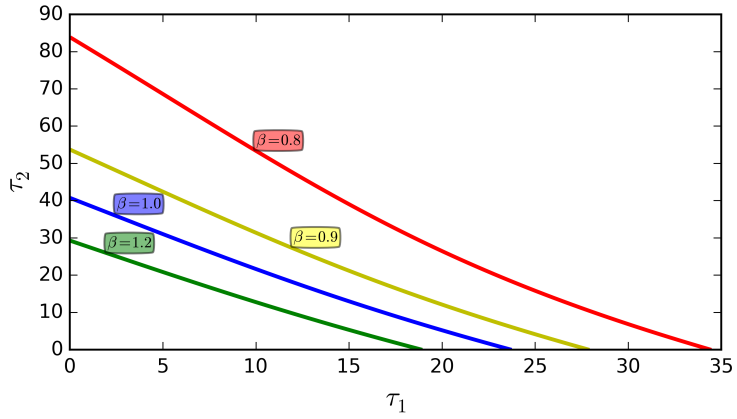

Figure 3.8: Effect of insulin resistance on the curve of Hopf bifurcations in the (τ_1, τ_2) space.

3.2 Reduced polynomial model

We now formulate a reduced polynomial model which is based on system (3.1.1), and follows the framework given in Fig. 3.10. It is given by

$$\dot{G}(t) = a_0 - a_1 G(t) - a_2 G(t) I(t) - a_3 I(t - \tau_2)^p, \tag{3.2.16}$$
$$\dot{I}(t) = b_1 G(t - \tau_1)^n - b_2 I(t), \quad n \in 2\mathbb{Z}, \quad p \in \mathbb{Z}^+,$$

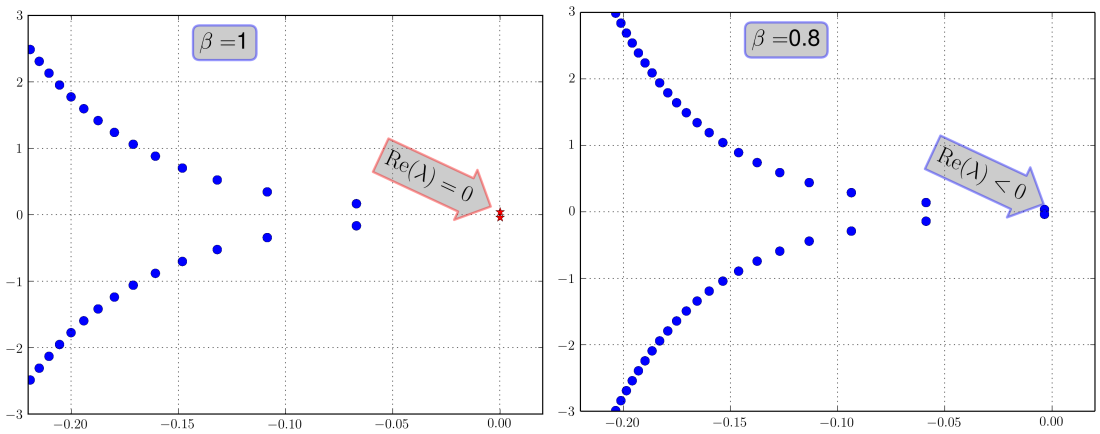

Figure 3.9: Eigenvalues of the linearised system for $\tau_1 = 6$, $\tau_2 = 36$ and $d_i = 0.06$, when $\beta = 1$ (left) and $\beta = 0.8$ (right).

where $G(t)$ is the plasma glucose concentration (measured in mg), and $I(t)$ is the plasma insulin concentration (measured in mU). For the purpose of all Figures, $G(t)$ and $I(t)$ will be converted to mg/dl and mU/l, respectively. All parameters are assumed to be non-zero, and have units as defined in Table 3.3. The coefficients a_1 and a_2 describe the insulin independent and dependent glucose utilisations, respectively. The term $a_0 := G_{in} + C$ comprises two contributions: G_{in}, which corresponds to a constant glucose infusion; and C, which originates from the hepatic glucose production. Indeed, as seen in equation (3.1.2), the hepatic glucose production can be represented by a function of the type

$$\text{Hepatic} \approx \frac{K_0}{K_1 + I(t-\tau_2)^p} \approx C - a_3 I(t-\tau_2)^p,$$

where τ_2 corresponds to the time taken for hepatic glucose to have an effect on the glucose levels. In order to explore the effect of different delay values on the limit cycle, we take τ_2 to be a commensurate delay. In the insulin balance equation, b_1 denotes the insulin production capability of the individual, and b_2 the insulin degradation rate. While the insulin secretion term appears to be unbounded, we note that

$$\text{Secretion} \approx \frac{G(t-\tau_1)^n}{G(t-\tau_1)^n + K_2^n} \approx \frac{G(t-\tau_1)^n}{K_2^n} = b_1 G(t-\tau_1)^n,$$

where τ_1 is the time taken for insulin to be released and have an effect on the glucose levels. Hence, the secretion function is a polynomial approximation of the bounded

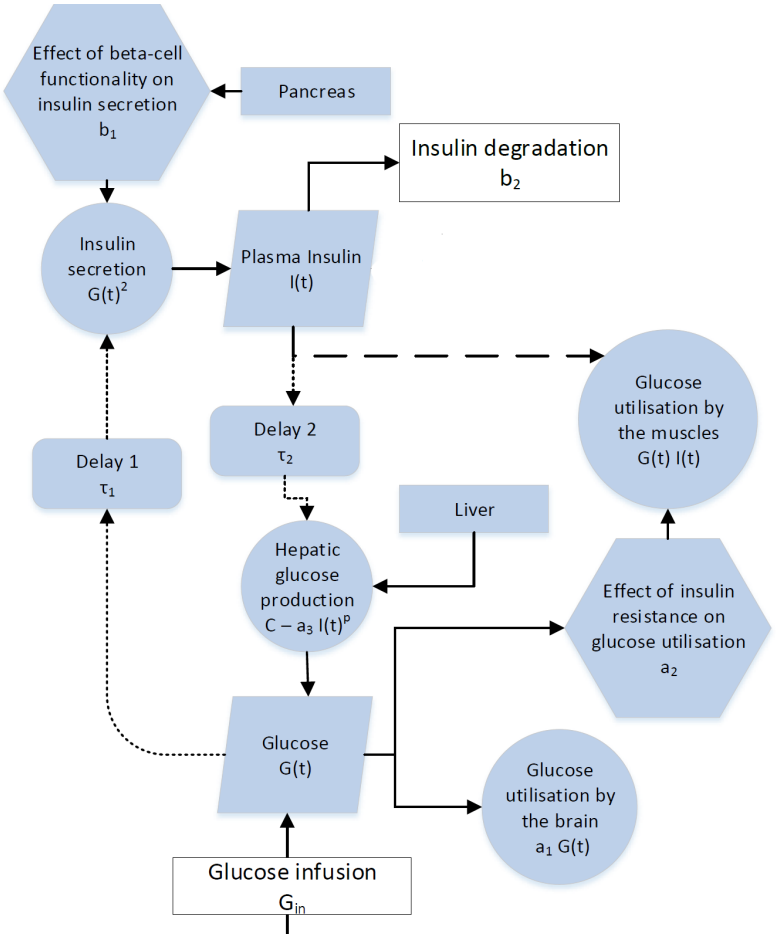

Figure 3.10: Flow diagram for model (3.2.16).

function representing insulin secretion. A consequence of this is that it does not provide the means to investigate the convergence speed of the trajectories to the limit cycle. However, it does allow for the accurate study of the amplitude and period of the periodic solutions, which is the focus of Chapter 5.

3.2.1 Local stability analysis of the reduced model

Constant hepatic glucose production

Here we look to find conditions on the parameter values in the reduced model when $p > 2$. Hence, as a second-order approximation, only the constant term of the hepatic production remains (see (3.2.17)).

$$\begin{aligned} \dot{G}(t) &= G_{in} - a_1 G(t) - a_2 G(t) I(t) + C, \\ \dot{I}(t) &= b_1 G(t-\tau)^n - b_2 I(t), \quad \tau = \tau_1. \end{aligned} \tag{3.2.17}$$

Parameter	Units
a_0	mg min^{-1}
a_1	min^{-1}
a_2	mU^{-1} min^{-1}
a_3	mg mU^{-p} min^{-1}
b_1	mU mg^{-n} min^{-1}
b_2	min^{-1}
τ_1	min
τ_2	min

Table 3.3: Units for the parameters in model (3.2.16).

This is not to say that the delayed term does not have an effect on the oscillations. In fact, its role on the production of an oscillatory regime has been highlighted and made explicit in several studies (Li et al. 2006, Huard et al. 2015). However, in this model, its impact on the amplitude and period of the oscillations is known to be much less than that of τ_1 (see Fig. 6.1. in Li & Kuang (2007)).
Following the arguments made by Shi et al. (2017), it can be shown that trajectories of model (3.2.17) are positive and bounded whenever $G(0) > 0$ and $I(0) > 0$. Indeed, the arguments for boundedness and positivity for the solutions of the minimal model (3.2.17) can be summarised as follows:

1. First, let $G(0) = G_0 > 0$ be a positive initial condition and suppose that $\exists$ $t_0 > 0$ such that $G(t_0) = 0$. Then, at time t_0, we have

$$\dot{G}(t_0) = G_{in} + C > 0,$$

which is a contradiction, and hence $G(t)$ is always positive if $G_0 > 0$. Similarly, letting $I(0) = I_0 > 0$ be a positive initial condition and supposing that $\exists\, t_0 > 0$ such that $I(t_0) = 0$ we have

$$\dot{I}(t_0) = b_0 + b_1 G(t_0 - \tau)^n > 0,$$

which is also a contradiction, and hence $I(t)$ is always positive if $I_0 > 0$.

2. One can then prove boundedness of $G(t)$ by noting that

$$\dot{G}(t) \leq a_0 - a_1 G(t)$$

since $G(t), I(t) > 0$. Denoting $G(t) = X(t) + a_0/a_1$, this implies that

$$\dot{X}(t) \leq -a_1 X(t) \quad \rightarrow \quad e^{-a_1 t}\frac{d}{dt}\left(e^{a_1 t}X(t)\right) \leq 0,$$

which in turn leads to

$$e^{a_1 t}X(t) \leq X(0) \quad \rightarrow \quad G(t) \leq \left(G(0) - \frac{a_0}{a_1}\right)e^{-a_1 t} + \frac{a_0}{a_1}.$$

Therefore

$$G(t) \leq G_+ = \max\left\{G(0), \frac{a_0}{a_1}\right\} < \infty,$$

and hence $G(t)$ is bounded for all $t > 0$.

3. As $G(t) < G_+$ for all $t > 0$, the second equation of (3.2.17) implies that

$$\dot{I}(t) \leq b_1 G_+^n - b_2 I(t)$$

from which it can be shown that

$$I(t) \leq I(0)e^{-b_2 t} + \frac{b_1 G_+^n}{b_2}\left(1 - e^{-b_2 t}\right) \leq I_+ = \max\left\{I(0), \frac{b_1 G_+^n}{b_2}\right\} < \infty,$$

thus establishing the boundedness of $I(t)$.

Value of the parameters

Given an oscillatory solution, the inverse problem of choosing parameters in model (3.2.17) can be addressed in the following way. We note that the system's steady state ($\bar{G}$,$\bar{I}$) is given by

$$\bar{I} = \frac{b_1 \bar{G}^n}{b_2}, \quad a_2 b_1 \left(\bar{G}\right)^{n+1} + (a_1 b_2)\,\bar{G} - a_0 b_2 = 0. \tag{3.2.18}$$

By Descartes' rule of signs, (3.2.18) has exactly one positive root for $\bar{G}$, and so one can always find a positive $(\bar{G}, \bar{I})$. Here we assume that the target basal levels can be identified with the steady state of the system.

1. It has been shown that the insulin clearance is proportional to the insulin concentration (Topp et al. 2000, Koschorreck & Gilles 2008). Numerical fitting procedures have rendered values in the range $(0.03, 0.3)$ (Chen et al. 2010). As in Li et al. (2006) and Huard et al. (2015), we shall choose an initial value of $b_2 = 0.06$ for most numerical computations with the reduced model.

2. From the knowledge of b_2, the value of b_1 is then given by

$$b_1 = b_2 \bar{I} \bar{G}^{-n}.$$

3. The system must be in an oscillatory state. Therefore the delay $\tau \in \mathbb{R}^+$ must be larger than the critical value τ_0 such that the characteristic equation

$$(\lambda + b_2)(\lambda + a_1 + a_2\bar{I}) + n a_2 b_2 \bar{I} e^{-\lambda\tau_0} = 0 \tag{3.2.19}$$

possesses a set of conjugate purely imaginary root $\lambda = \pm i\omega_0$. This requirement implies that ω_0 and τ_0 satisfy the system

$$n a_2 b_2 \bar{I} \cos(\omega_0\tau_0) = \omega_0^2 - b_2(a_1 + a_2\bar{I}), \quad n a_2 b_2 \bar{I} \sin(\omega_0\tau_0) = (b_2 + a_1 a_2 \bar{I})\omega_0, \tag{3.2.20}$$

or equivalently,

$$\cos(\omega_0\tau_0) = \frac{\omega_0^2 - b_2(a_1 + a_2\bar{I})}{n a_2 b_2 \bar{I}}, \quad \sin(\omega_0\tau_0) = \frac{(b_2 + a_1 a_2 \bar{I})\omega_0}{n a_2 b_2 \bar{I}}. \tag{3.2.21}$$

This in turns implies that ω_0 satisfies a quartic equation

$$\omega_0^4 + \omega_0^2\left((a_1 + a_2\bar{I})^2 + b_2^2\right) + b_2^2\left(\left(a_1 + a_2\bar{I}\right)^2 - \left(n a_2 \bar{I}\right)^2\right) = 0. \tag{3.2.22}$$

Requiring that equation (3.2.22) possesses a positive root for ω_0 gives explicit conditions on the coefficients for the existence of a Hopf bifurcation. Since the middle term in (3.2.22) is always positive, one must have

$$n > \frac{a_1}{a_2\bar{I}} + 1 > 1,$$

in order to have a bifurcation. We shall therefore choose $n = 2$ in all subsequent calculations, which in turn implies that $a_1 < a_2\bar{I}$. The value of τ_0 is then obtained from (3.2.21) as

$$\tau_0 = \frac{1}{\omega_0}\left(\arccos\left(\frac{\omega_0^2 - b_2(a_1 + a_2\bar{I})}{2a_2 b_1 \bar{G}^2}\right) + 2K\pi\right), \tag{3.2.23}$$

where $K \in \mathbb{Z}^+$ is the smallest integer such that (3.2.23) defines a positive value. Larger values of K gives successive values of τ_0 for which stability switches may occur in the linear system. However, for the nonlinear system (3.2.17), it is numerically observed that oscillations are present whenever $\tau \geq \tau_0$.

For a more robust approach on the restrictions on the parameter n such that a bifurcation occurs, readers are referred to the next subsection.

4. The constant $a_0 := G_{in} + C$ is obtained from

$$a_0 = a_1\bar{G} + a_2\bar{G}\bar{I}.$$

The parameters a_1 and a_2 can be chosen such that oscillations are present for a physiologically relevant value of the critical delay τ_0. For different values of b_2, one can numerically compute the range of achievable values for τ_0 using equation (3.2.23). This gives the graph shown in Fig. 3.11.

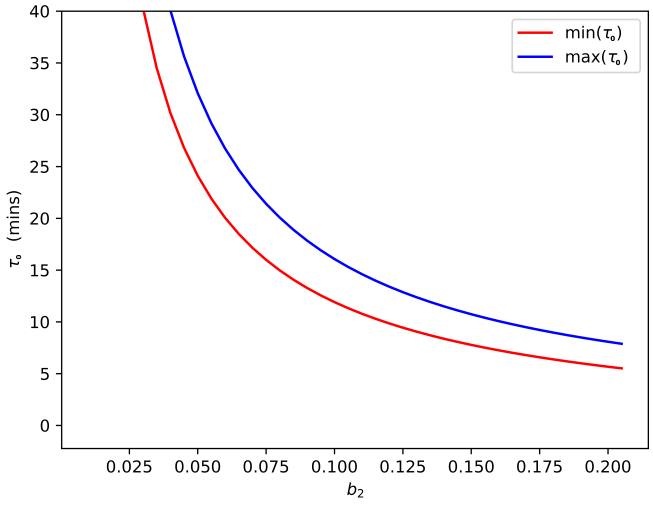

Figure 3.11: Range of values of τ_0 which can be attained by varying a_1 and a_2 for each given value of b_2. Here, we used the fixed values $\bar{G} = 97.87\ mg/dl$ and $\bar{I} = 30\ mU/l$. Any value of τ above the range leads to an oscillatory solution.

As observed in Shi et al. (2017), the model leads to slightly higher values of τ_0 than in the two-delay model (3.1.1), although it is comparable with the value one obtains when formally setting $\tau_2 = 0$ in (3.1.1) (see Fig. 3.4 on page

26). This highlights the importance of both delays in generating a negative feedback loop. Nevertheless, this approach provides a model able to replicate the nonlinear oscillations within an appropriate physiological range (Fig. 3.12).

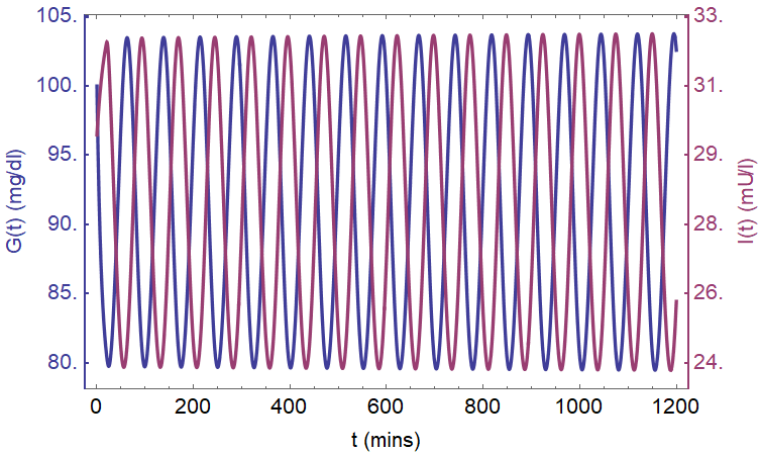

Figure 3.12: Oscillations described by the minimal model (3.2.17) using Parameter Set 1 from Table 5.1, with $a_2 = 0.0017$.

Stability of the steady state

Here we use the following formulation of *Rouché's theorem* to investigate the conditions needed for stability on the parameter n in (3.2.17).

Theorem 1 (Rouché's theorem (Lang 2013)) *For two given functions $f(z)$ and $g(z)$ which are analytic in $\mathcal{A}$, if $|f(z)| > |g(z)|$ on χ, where χ is a simple loop homotopic to a point in $\mathcal{A}$, then $f(z)$ and $f(z) + g(z)$ have the same number of roots inside χ.*

Choosing χ as a semicircle in the right half plane with radius r such that $r \to \infty$ (see Fig. 3.13), it is clear that if (3.2.19) has no roots inside χ, then system (3.2.17) is stable. We then have the following proposition.

Proposition 2 *If $n = 1$, then system (3.2.17) is stable for all $a_0, a_1, a_2, b_1, b_2, \tau_1 > 0$.*

Proof. Let us define

$$f(z) = z^2 + (a_1 + a_2\bar{I} + b_2)z + b_2(a_1 + a_2\bar{I}), \quad g(z) = na_2b_2\bar{I}e^{-z\tau_0},$$

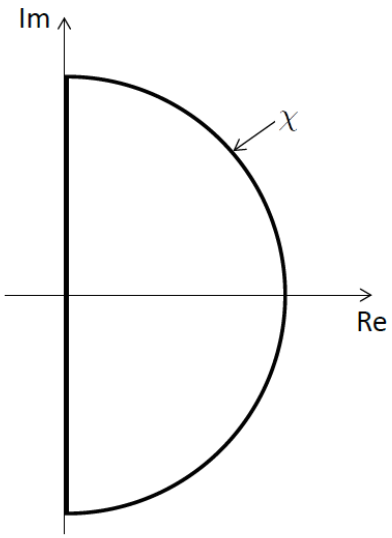

Figure 3.13: Simple closed curve, χ, in the complex plane.

with $z = \eta + i\phi$, $\eta \in \mathbb{R}^+$ and $\phi \in \mathbb{R}$. By Descartes' rule of signs, we can see that $f(z)$ has no roots in χ. As $f(z) + g(z) = 0$ is equivalent to (3.2.19), system (3.2.17) must be stable if $|f(z)| > |g(z)|$. Noting that

1. $|g(z)| = na_2b_2\bar{I}|e^{-\eta\tau_0}|$,

2. $|f(z)| = (\phi^2[a_1^2 + (2a_1 + a_2\bar{I} + 2)(a_2\bar{I} + 2) + b_2(b_2 + 4)]$
$+ [\phi^2 - \eta(a_1 + a_2\bar{I} + b_2 + \eta)]^2 + b_2(a_1 + a_2\bar{I})[(a_1 + a_2\bar{I})(b_2 + 2\eta) + 2\eta(b_2 + \eta)])^{\frac{1}{2}}$,

it can be easily seen that the maximum of $g(z)$ and the minimum of $f(z)$ occur when $z = 0$. Hence it can be shown that

$$n < 1 + \frac{a_1}{a_2\bar{I}}$$

leads to $|f(z)| > |g(z)|$. Therefore, system (3.2.17) is stable for $n = 1$. □

Extension to commensurate delays

We now consider the problem of characterising periodic solutions in system (3.2.16) when the delays are assumed to be commensurate, i.e. $\tau_2 = k\tau_1$, with $k \in \mathbb{Z}^+$. A straightforward generalisation can be made for the case when the delays are rationally related. This assumption allows to perform a perturbative analysis of the periodic solutions, given that the point $(\tau_1, k\tau_1)$ remains sufficiently close to the

threshold curve. Geometrically, this approach provides a discrete set of characteristic frequencies ω_0, corresponding to the intersection between a line and the threshold curve (see Fig. 3.14). We show that these crossing points can be described by using linear combinations of Chebyshev polynomials of the first type.

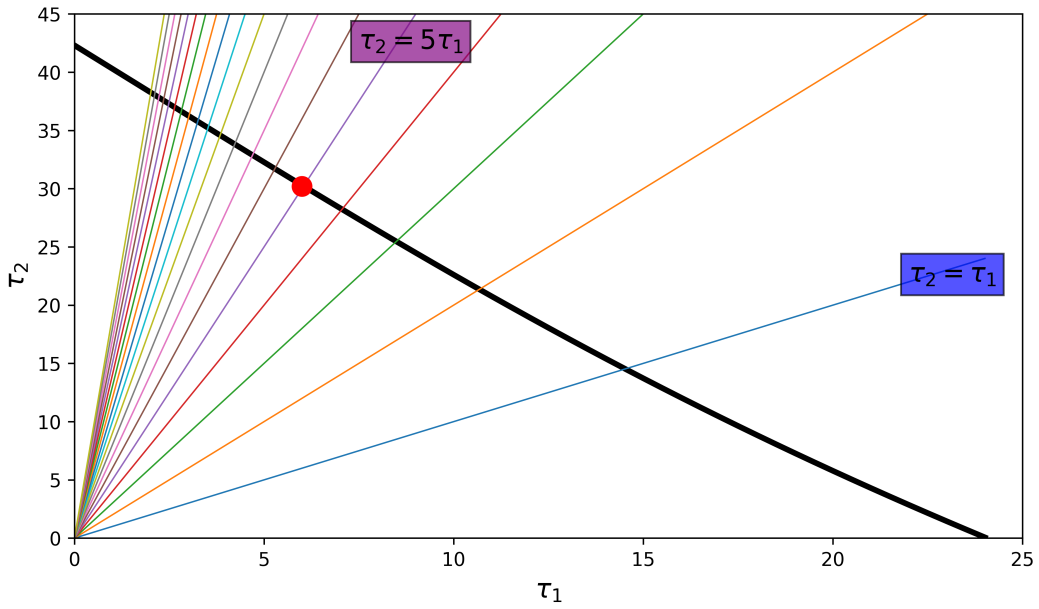

Figure 3.14: Hopf bifurcation curve for model (9) in the space of delays, along with expansion lines $\tau_2 = k\tau_1$, $k \in \mathbb{Z}^+$.

In its most general form, the polynomial model with commensurate delay becomes

$$\dot{G} = a_0 - a_1 G - a_2 GI - a_3 I(t - k\tau)^p, \quad \dot{I} = b_1 G(t-\tau)^2 - b_2 I, \quad \tau = \tau_1. \tag{3.2.24}$$

For $a_0 > 0$, system (3.2.24) always possesses a positive steady state $\bar{G}, \bar{I}$ which satisfies

$$a_3 b_1^p \bar{G}^{2p} + a_2 b_1 b_2^{p-1} \bar{G}^3 + a_1 b_2^p \bar{G} - a_0 b_2^p = 0, \quad \bar{I} = \frac{b_1}{b_2}\bar{G}^2.$$

The linearisation about its unique positive steady state reads as

$$\begin{pmatrix} \dot{X} \\ \dot{Y} \end{pmatrix} = \begin{pmatrix} -(a_1 + a_2\bar{I}) & -a_2\bar{G} \\ 0 & -b_2 \end{pmatrix} \begin{pmatrix} X \\ Y \end{pmatrix} + \begin{pmatrix} 0 & 0 \\ 2b_1\bar{G} & 0 \end{pmatrix} \begin{pmatrix} X_\tau \\ Y_\tau \end{pmatrix} + \begin{pmatrix} 0 & -a_3 p \bar{I}^{p-1} \\ 0 & 0 \end{pmatrix} \begin{pmatrix} X_{k\tau} \\ Y_{k\tau} \end{pmatrix}, \tag{3.2.25}$$

where $X_\tau = X(t-\tau), X_{k\tau} = X(t-k\tau)$ and similarly for Y. The characteristic equation of (3.2.25) is a quasi-polynomial of the form

$$\lambda^2 + A_1\lambda + A_2 + A_3 e^{-\lambda\tau} + A_4 e^{-(k+1)\lambda\tau} = 0, \quad k \in \mathbb{Z}^+, \tag{3.2.26}$$

where

$$A_1 = a_1 + a_2\bar{I} + b_2, \quad A_2 = a_1 b_2 + a_2 b_2 \bar{I}, \quad A_3 = 2a_2 b_1 \bar{G}^2, \quad A_4 = 2p\bar{G}\bar{I}^{p-1} a_3 b_1.$$

Since $A_1, A_2, A_3, A_4 > 0$, equation (3.2.26) is Hurwitz stable for $\tau = 0$ and so we now look for conditions on k and τ ensuring that it undergoes a Hopf bifurcation. Hence, setting $\lambda = i\omega_0$, $\omega_0 > 0$ leads to the system

$$\omega_0^2 = A_2 + A_3\cos(\omega_0\tau_0) + A_4\cos((1+k)\omega_0\tau_0), \tag{3.2.27}$$

$$A_1\omega_0 = A_3\sin(\omega_0\tau_0) + A_4\sin((1+k)\omega_0\tau_0). \tag{3.2.28}$$

Eliminating polynomial occurrences of ω_0, one is led to the following trigonometric equation

$$\begin{aligned} &A_1^2(A_2 + A_3\cos(\omega_0\tau_0) + A_4\cos((1+k)\omega_0\tau_0)) \\ &\quad = (A_3\sin(\omega_0\tau_0) + A_4\sin((1+k)\omega_0\tau_0))^2. \end{aligned} \tag{3.2.29}$$

Setting $z = \cos(\omega_0\tau_0)$, i.e. $\omega_0\tau_0 = \arccos z$, then

$$\cos(n\omega_0\tau_0) = T_n(z), \quad \sin(n\omega_0\tau_0) = \sqrt{1-z^2}U_{n-1}(z),$$

where T_n and U_{n-1} are Chebyshev polynomials of the first and second kinds, respectively. Equation (3.2.29) implies that z satisfies the following polynomial equation

$$A_1^2(A_2 + A_3 z + A_4 T_{1+k}(z)) = (1-z^2)(A_3 + A_4 U_k(z))^2. \tag{3.2.30}$$

Further using that, for $n \geq m$,

$$(1-z^2)U_{n-1}(z) = zT_n(z) - T_{n+1}(z), \quad 2(1-z^2)U_{n-1}(z)U_{m-1}(z) = T_{n-m}(z) - T_{n+m}(z),$$

we obtain that (3.2.30) can be rewritten as a linear combination of Chebyshev polynomials of the first type

$$\begin{aligned} &A_4^2 T_{2k+2}(z) + 2A_3A_4T_{k+2}(z) + 2A_4A_1^2T_{k+1}(z) - 2A_3A_4T_k(z) \\ &\quad + A_3^2T_2(z) + 2A_1^2A_3T_1(z) + 2A_2A_1^2 - (A_3^2 + A_4^2) = 0. \end{aligned} \tag{3.2.31}$$

For a given $k \in \mathbb{Z}^+$, any real root z of (3.2.31) with $|z| < 1$ gives a solution for ω_0. The existence of such values of z can be then assessed using Sturm chains and the fact that $T_n(1) = 1, T_n(-1) = (-1)^n$. From the knowledge of z, one can obtain ω_0 from (3.2.27) and (3.2.28), which can be rewritten as

$$\begin{aligned} \omega_0^2 &= A_2 + A_3 z + A_4 T_{1+k}(z), \\ A_1\omega_0 &= A_3\sqrt{1-z^2} + A_4\sqrt{1-z^2}U_k(z). \end{aligned} \tag{3.2.32}$$

Boundedness and persistence

Contrary to the solutions of (3.2.17), solutions to system (3.2.24) may not necessarily be positive and bounded. Indeed, for certain values of the parameters of the system, $G(t)$ can be negative and/or unbounded, and $I(t)$ can be unbounded (as illustrated in Figs. 3.15a, 3.15b and 3.16). Irrespective of this, we have the following proposition.

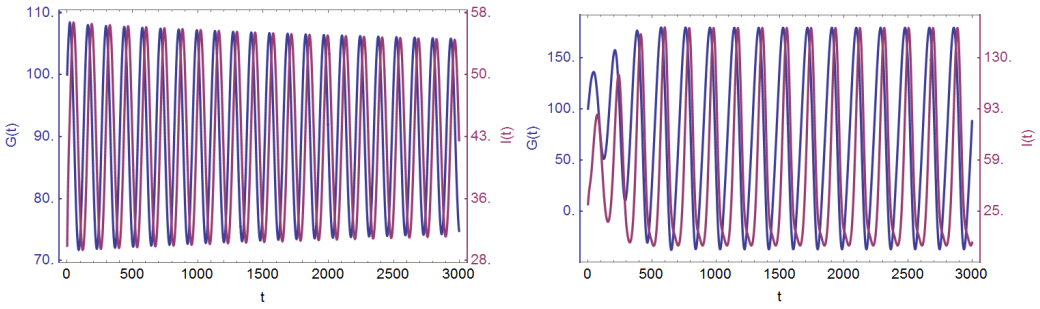

(a) Positive and bounded solutions of (3.2.24) with $a_2 = 0.00009$, $a_3 = 1.415$ and $p = 1$.

(b) Bounded solutions of (3.2.24) with $a_2 = 0.00001$, $a_3 = 1.615$ and $p = 1$.

Figure 3.15: Solutions to (3.2.24) with $a_0 = 285$, $a_1 = 2.02981789884309 \times 10^{-4}$, $b_1 = 9.3 \times 10^{-8}$, $b_2 = 0.06$, $\tau = 15.8$, $k = 1$, $G(0) = 10000$ and $I(0) = 90$.

Proposition 3 *Let $(G(t), I(t))$ be a solution of system (3.2.24). Then $I(0) > 0$ implies $I(t) > 0, \forall t > 0$.*

Proof.

First, let $I(0) = I_0 > 0$ be a positive initial condition and suppose that $\exists\ t_0 > 0$

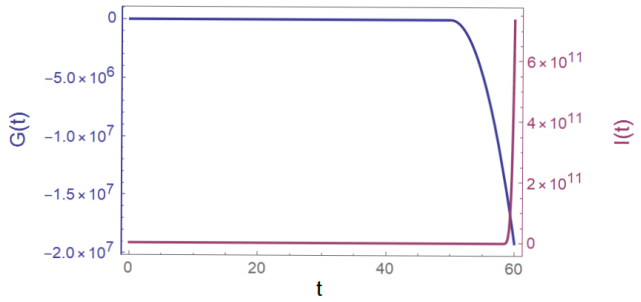

Figure 3.16: Unbounded solution of (3.2.24) with $a_0 = 10$, $a_1 = 0.01$, $a_2 = 0.01$, $a_3 = 2.2$, $b_1 = 0.001$, $b_2 = 0.05$, $k = 5$, $\tau = 10$, $p = 2$, $G(0) = 10000$ and $I(0) = 90$.

such that $I(t_0) = 0$. Then, at time t_0, we have

$$\dot{I}(t_0) = b_1 G(t_0 - \tau)^2.$$

If

1. $G(t_0 - \tau) \neq 0$, then $\dot{I}(t_0) > 0$ and we have a contradiction.

2. $G(t_0 - \tau) = 0$, then $\dot{I} = 0$ and so t_0 is a high order zero. However, by noting that the m^{th} derivative of I is given by

$$I^{(m)}(t_0) = b_1 \sum_{j=0}^{m-1} \binom{m-1}{j} G^{(m-1-j)}(t_0 - \tau) G^{(j)}(t_0 - \tau) - b_2 I^{(m-1)}(t_0),$$

it can be seen that either

(a) $\exists\ j \in \mathbb{N}$ such that

$$I^{(2j)}(t_0) = 0 \ \ \& \ \ I^{(2j+1)}(t_0) > 0,$$

which implies that t_0 is a point of inflection, and hence we have a contradiction, or

(b) $I^{(j)}(t_0) = 0\ \forall j$, which also leads to a contradiction.

Hence, $I(t) > 0$ for all t. □

Due to the nature of this problem, unbounded solutions are not in our current scope and therefore parameter values leading to such solutions will be not be investigated. It is important to note that the introduction of an additional nonlinear term in

the model, namely when $a_3 \neq 0$ and $p > 1$, can give rise to new dominant behaviour which may lead to singularities in the solutions. In particular, the presence of movable poles can be assessed by performing a Painlevé-type analysis on each dominant nonlinear truncation of the system. Here, we restrict ourselves to system (3.2.24) without delays, for which arguments from Painlevé analysis apply (Goriely & Hyde 1998, Goriely & Hyde 2000).

Two such truncations of (3.2.24) can be distinguished

$$\begin{array}{lll} A. & \dot{G} \sim -a_2 G I & \qquad B. \quad \dot{G} \sim -a_3 I^p \\ & \dot{I} \sim b_1 G^2 & \qquad\quad \dot{I} \sim b_1 G^2 \end{array}$$

Looking for dominant terms of the form

$$G(t) \sim \alpha_1 (t - t_0)^{q_1}, \quad I(t) \sim \alpha_2 (t - t_0)^{q_2}, \tag{3.2.33}$$

one is led to the following solutions for each truncation

$$A. \quad G \sim 2^{1/2} \left(\frac{-1}{2 a_2 b_1} \right)^{1/2} (t - t_0)^{-1} \tag{3.2.34}$$

$$I \sim \frac{1}{a_2} (t - t_0)^{-1} \tag{3.2.35}$$

$$B. \quad G \sim \left(\frac{(-1)^p a_3 b_1^p (2p-1)^{p+1}}{3^p (p+1)} \right)^{\frac{1}{1-2p}} (t - t_0)^{\frac{1+p}{1-2p}} \tag{3.2.36}$$

$$I \sim \left(-\frac{b_1 a_3^2 (p+1)^{-2} (2p-1)^3}{3} \right)^{\frac{1}{1-2p}} (t - t_0)^{\frac{3}{1-2p}} \tag{3.2.37}$$

The following conclusions can be drawn.

Truncation A. Since all parameters are assumed to be strictly positive, we see that equation (3.2.34) does not give an expression with real coefficients. Therefore, no open set of initial conditions lead to a movable pole (Goriely & Hyde 1998, Goriely & Hyde 2000).

Truncation B. In order to have a pole, one needs to have that $2p > 1$, which is always satisfied here. This branch can therefore include resonances leading to the presence of a movable pole (Goriely & Hyde 1998, Conte & Musette 2008, Hone 2009).

Therefore, from now on, we shall assume that parameters are selected such that $I(t)$ remains bounded, $I(t) \leq I_+ < \infty$. We then have the following.

Proposition 4 *Let $I(t)$ be bounded from above, $0 \leq I(t) \leq I_+ < \infty$, with $a_0 > a_3 I_+^p$. Then $G(t)$ is positive and bounded for all $t > 0$ if $G(0) > 0$.*

Proof. From the first equation in system (3.2.24), it can be easily seen that

$$[G(s)e^{\int_0^t (a_1+a_2 I(s))ds}]_0^t = \int_0^t e^{\int_0^t (a_1+a_2 I(s))ds}(a_0 - a_3 I(t-k\tau)^p)ds$$

Hence $G(t)$ is strictly positive for all t if $a_0 > a_3 I_+^p$. Since we have that

$$\dot{G} \leq a_0 - a_1 G$$

when $G(t) > 0$ and $a_0 > a_3 I_+^p$, using the arguments from Shi et al. (2017) (and summarised in Subsection (3.2.1)) it can be easily seen that $G(t)$ is bounded for all $t > 0$. □

3.3 Periodic solutions in the linear system

In this section, we derive explicit conditions for the existence of sinusoidal solutions for linear systems with two delays

$$\dot{x}(t) = c_1 x(t) + c_2 y(t) + c_3 y(t-\tau_2), \quad \dot{y}(t) = c_4 x(t) + c_5 y(t) + c_6 x(t-\tau_1). \tag{3.3.38}$$

The purpose of this derivation is twofold. On one hand, contrary to the case $c_4 = 0$ where the solution of a transcendental equation is required, we show that conditions can be formulated when $c_4 \neq 0$ by investigating the roots of a cubic polynomial. On the other hand, in the context of model (3.1.1), the introduction of the coefficient c_4 would correspond to a non-delayed glucose-dependent insulin secretion. Hence our conditions provide a qualitative description of the effect of such an insulin contribution.

We assume here that $c_3, c_6 \neq 0$ to ensure the dependence upon the two delays is preserved and postulate the form of the solution as

$$x(t) = A_1 \cos(\omega t) + A_2 \sin(\omega t), \quad y(t) = B_1 \cos(\omega t) + B_2 \sin(\omega t). \tag{3.3.39}$$

Given that the system is linear, we impose that $x(t)$ and $y(t)$ are normalised such that $A_1^2 + A_2^2 = 1$, $B_1^2 + B_2^2 = r^2$, $r > 0$. Hence we set

$$A_1 = \cos\phi, \quad A_2 = \sin\phi, \quad B_1 = r\cos\theta, \quad B_2 = r\sin\theta. \tag{3.3.40}$$

Substituting (3.3.39) into (3.3.38), one obtains the following system

$$\begin{aligned}
\cos(\tau_1\omega) &= -\frac{1}{c_6}\left[c_4 + c_5\cos z - r\omega\sin z\right], \quad \sin(\tau_1\omega) = -\frac{r}{c_6}\left[c_5\sin z + \omega\cos z\right], \\
\cos(\tau_2\omega) &= -\frac{1}{c_3 r}\left[c_2 r + c_1\cos z + \omega\sin z\right], \quad \sin(\tau_2\omega) = \frac{1}{c_3 r}\left[c_1\sin z - \omega\cos z\right],
\end{aligned} \tag{3.3.41}$$

given that $c_3, c_6 \neq 0$, where we introduced $z = \theta - \phi$. These lead to the following conditions

$$\omega^2 + 2c_2 r\left(\omega\sin z + c_1\cos z\right) + c_1^2 + r^2(c_2^2 - c_3^2) = 0, \tag{3.3.42}$$

$$r^2\omega^2 + 2c_4 r\left(c_5\cos z - \omega\sin z\right) + r^2 c_5^2 + c_4^2 - c_6^2 = 0. \tag{3.3.43}$$

Here, we focus exclusively on the generic case where $c_2, c_4, c_1 + c_5 \neq 0$. Conditions when $c_2 = c_4 = 0$ for the local and global existence of periodic solutions have been discussed, for example in Ruan & Wei (1999) using degree theory. We do not make use of a rational transformation to bring the transcendental equation into a polynomial problem (as done, for example in Sipahi & Olgac (2004) and Gu et al. (2005)) or of geometric switching (see, e.g. Beretta & Kuang (2002) or An et al. (2019)). In the generic case, one can solve (3.3.42) and (3.3.43) for $\sin z$ and $\cos z$ and upon using that $\cos^2 z + \sin^2 z = 1$, obtain a cubic polynomial for $\rho = \omega^2$

$$b_3\rho^3 + b_2\rho^2 + b_1\rho + b_0 = 0, \tag{3.3.44}$$

with

$$
\begin{aligned}
b_0 &= \left(c_1^2c_4c_5 - c_1c_2c_4^2 - c_1c_2c_5^2r^2 + c_1c_2c_6^2 + c_2^2c_4c_5r^2 - c_3^2c_4c_5r^2\right)^2,\\
b_1 &= c_1^4c_4^2 - 2c_1^3c_2c_4c_5r^2 + 2c_1^2c_2^2c_5^2r^4 - 2c_1^2c_2^2c_6^2r^2 + 2c_1^2c_2c_4^3 + 2c_1^2c_2c_4c_5^2r^2\\
&\quad -2c_1^2c_2c_4c_6^2 - 2c_1^2c_3^2c_4^2r^2 + 2c_1^2c_4^2c_5^2 - 2c_1c_2^3c_4c_5r^4 - 8c_1c_2^2c_4^2c_5r^2\\
&\quad +2c_1c_2c_3^2c_4c_5r^4 - 2c_1c_2c_4^3c_5 - 2c_1c_2c_4c_5^3r^2 + 2c_1c_2c_4c_5c_6^2 + c_2^4c_4^2r^4\\
&\quad +2c_2^3c_4^3r^2 + 2c_2^3c_4c_5^2r^4 - 2c_2^3c_4c_6^2r^2 - 2c_2^2c_3^2c_4^2r^4 + c_2^2c_4^4 - 2c_2^2c_4^2c_6^2 + c_2^2c_5^4r^4\\
&\quad -2c_2^2c_5^2c_6^2r^2 + c_2^2c_6^4 - 2c_2c_3^2c_4^3r^2 - 2c_2c_3^2c_4c_5^2r^4 + 2c_2c_3^2c_4c_6^2r^2\\
&\quad +c_3^4c_4^2r^4 - 2c_3^2c_4^2c_5^2r^2,\\
b_2 &= c_1^2c_2^2r^4 + 2c_1^2c_2c_4r^2 + 2c_1^2c_4^2 - 2c_1c_2c_4c_5r^2 + 2c_2^3c_4r^4\\
&\quad +4c_2^2c_4^2r^2 + 2c_2^2c_5^2r^4 - 2c_2^2c_6^2r^2 - 2c_2c_3^2c_4r^4 + 2c_2,\\
b_3 &= \left(c_2r^2 + c_4\right)^2.
\end{aligned}
$$

The polynomial (3.3.44) always possesses at least one real root for ρ. We now investigate conditions which ensure that it possesses at least one positive root and discard the case $b_0 = 0$, which would lead to a constant solution. Assuming a factorisation of the form

$$
\begin{aligned}
&b_3(\rho-\rho_1)(\rho-\rho_2)(\rho-\rho_3)\\
&\qquad = b_3\left[\rho^3 - (\rho_1+\rho_2+\rho_3)\rho^2 + (\rho_1\rho_2+\rho_1\rho_2+\rho_2\rho_3)\rho - \rho_1\rho_2\rho_3\right],
\end{aligned}
$$

the fact that b_0 and b_3 are positive implies that the product of roots $\rho_1\rho_2\rho_3$ is negative. Hence, the polynomial either has 1 or 3 negative roots. Moreover, if two roots are complex, say $\rho_3 = \overline{\rho_2}$, then

$$
\rho_1\rho_2\rho_3 = \rho_1\rho_2\bar{\rho_2} = \rho_1|\rho_2|^2 < 0 \Rightarrow \rho_1 < 0
$$

and the polynomial has no positive root. Hence, for the polynomial (3.3.44) to have at least one positive root, its three roots must be real, or equivalently the discriminant of (3.3.44) must be positive. As a consequence, the only choice is to have 1 negative root and 2 positive ones. According to Descartes' rule of signs, the series of coefficients of polynomial (3.3.44) must exhibit exactly two sign changes,

while the series obtained upon setting $x \to -x$ must have exactly one sign change. This leads to the following proposition.

Proposition 5 *In the generic case $c_2, c_4, c_1 + c_5 \neq 0$, system (3.3.38) possesses at least one sinusoidal solution if the discriminant of (3.3.44),*

$$\Delta = 18b_0b_1b_2b_3 - 4b_2^3b_0 + b_1^2b_2^2 - 4b_3b_1^3 - 27b_0^2b_3^2$$

is positive and either i) $b_2 < 0$ or ii) $b_2 > 0$ and $b_1 < 0$ or iii) $b_1 = 0$ or $b_2 = 0$ holds.

Moreover, values of z can be obtained directly by eliminating ω from (3.3.42) and (3.3.43),

$$\begin{aligned}
&8c_2c_4(c_1+c_5)r^3\left(c_2r^2+c_4\right)\eta^3\\
&-4r^2\Big[c_2r^4\left(c_1^2c_2-c_2^2c_4-c_2c_5^2+c_3^2c_4\right)\\
&\quad+r^2\left(c_2^2c_6^2+c_3^2c_4^2-c_1^2c_2c_4-2c_1c_2c_4c_5-2c_2^2c_4^2-c_2c_4c_5^2\right)\\
&\quad-c_4\left(c_1^2c_4+c_2c_4^2-c_2c_6^2-c_4c_5^2\right)\Big]\eta^2\\
&-4r\Big[c_1c_2(c_2^2-c_3^2)r^6+\left(c_1^3c_2+2c_1c_2^2c_4-c_1c_2c_5^2+c_2^2c_4c_5+c_3^2c_4c_5\right)r^4\\
&\quad\left(c_4c_5^3-c_1^2c_4c_5+c_1c_2c_4^2+c_1c_2c_6^2+2c_2c_4^2c_5\right)r^2+c_4c_5(c_4^2-c_6^2)\Big]\eta\\
&-\Big[(c_2^2-c_3^2)^2r^8+2\left(c_1^2c_2^2-c_1^2c_3^2+2c_2^3c_4+c_2^2c_5^2-2c_2c_3^2c_4+c_3^2c_5^2\right)r^6\\
&\quad(c_1^4+4c_1^2c_2c_4-2c_1^2c_5^2+6c_2^2c_4^2-2c_2^2c_6^2+4c_2c_4c_5^2-2c_3^2c_4^2-2c_3^2c_6^2+c_5^4)r^4\\
&\quad+2\left(c_1^2c_4^2+c_1^2c_6^2+2c_2c_4^3-2c_2c_4c_6^2+c_4^2c_5^2-c_5^2c_6^2\right)r^2+(c_4^2-c_6^2)^2\Big]=0,
\end{aligned} \tag{3.3.45}$$

where $\eta = \cos z$. Using equations (3.3.42) and (3.3.43) one can then obtain the points in the positive (τ_1, τ_2) domain where sinusoidal solutions of the form (3.3.39) exist. We now give an example using as starting point the linearisation of system (3.1.1) in which we introduce the coefficient c_4.

Example 1 Physiological parameters for system (3.1.1) in the non-diabetic case $\alpha = \beta = \gamma = 1$ were obtained in Huard et al. (2015). Note that in that case $c_4 = 0$ and here we assume that c_4 is sufficiently small and represents a first-order approximation of an instantaneous glucose-dependent insulin release. The corresponding

values are given by

$$c_1 = -0.010, \quad c_2 = -0.855, \quad c_3 = -2.457, \quad c_5 = -0.06, \quad c_6 = 0.001. \quad (3.3.46)$$

Following the procedure just highlighted, it can be seen (Fig. 3.17) that for each value of $-1 \leq c_4 \leq 1$, there exists a small range on r for which the conditions of Proposition 5 are satisfied. For example, for $c_1 = 0.00001$, the range of $0.0145619 \leq r \leq 0.0170074$ is determined numerically with corresponding ω's within [0.0253264, 0.0471886]. For each value of r, values of ω and z are obtained from (3.3.44) and (3.3.45). For each trio (r, ω, z), equations (3.3.41) are then used to obtain the resulting values for τ_1 and τ_2. Because of the periodicity of these equations, we report here only the minimal positive values of the delays.

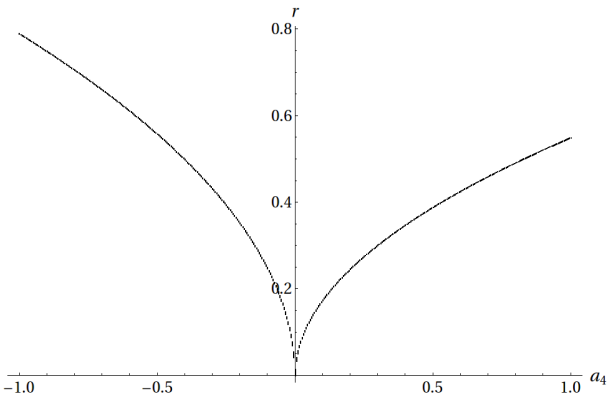

Figure 3.17: Values of r which satisfy the conditions of Proposition 5 for $c_4 \in [-1, 1]$.

Increasing c_4 has a crucial effect of the production of sinusoidal solutions (Fig. 3.18). The lower branch of the graph for $c_4 = 0.00001$ gives an approximation to the transcendental curve of Hopf bifurcations which was presented in Fig. 3.4. The graph in Fig. 3.18 shows that this curve is part of a closed loop in this space. For comparison, increasing c_4 and repeating the analysis shows that it deforms this loop by shrinking it progressively, here represented for $c_4 = 0.1$. We observe numerically that values of c_4 larger than around 39.02 cannot lead to an oscillatory solution. However, in the context of glucose-insulin regulation, it is reasonable to expect that a value above the delayed insulin production or the degradation rate will break the ability of the system to generate oscillations.

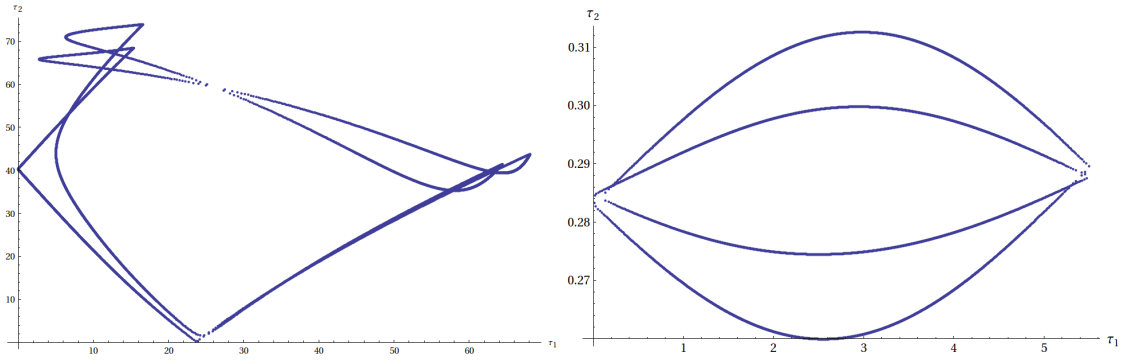

Figure 3.18: Existence of oscillatory solutions in the (τ_1, τ_2) domain for $c_4 = 0.00001$ (left) and $c_4 = 0.1$ (right). Given the periodicity of equations (3.3.41), only the curves which provide the minimal values for τ_2 are reported.

Chapter 4

Strategies for stabilising glucose levels and restoring oscillations

In this chapter, we first look at a variety of different treatment strategies for both T1DM and T2DM. While many of the strategies discussed are used currently used in practice, some are in a more theoretical stage. We then look at using some of the strategies as a way of: (1) maintaining a physiological acceptable blood glucose level; and (2) restoring an accurate oscillatory regime. Finally, we look to combine two of the strategies to investigate whether a combined approach is better at enabling the two objectives.

4.1 Clinical and Theoretical Treatments for Diabetes

4.1.1 Background

Research into the treatment and understanding of diabetes has made significant progress since the hormone insulin was first coined by Sir Edward Albert Sharpey-Schafer in 1910 (American Diabetes Association 2015). The advances made (along with an improvement of patient care) have been shown to have reduced the incidence of diabetic complications significantly over the last 20 years (American Diabetes Association 2015). However, there are still many aspects of the illness that remain

a mystery.

4.1.2 Insulin Therapy

In current practice, daily insulin doses are used as the main treatment for all Type 1 diabetics, as well as for some with T2DM (Centers for Disease Control and Prevention et al. 2011) (although the use of insulin therapy in the initial treatment for T2DM is debated (Pories & Dohm 2012)). These insulin doses can be taken by injection or through an insulin pump (Centers for Disease Control and Prevention et al. 2011).

4.1.3 Metformin

Metformin is a Biguanidine drug which is used in the treatment of T2DM (Centers for Disease Control and Prevention et al. 2011). It has been shown to: lower the fasting plasma glucose concentration (Hundal et al. 2000); inhibit hepatic glucose production (Hundal et al. 2000); and improve insulin resistance (Giannarelli et al. 2003).

4.1.4 Insulin Degradation

In circulation, insulin is known to have a short half-life. This is likely due to the high efficiency of its clearance mechanisms, for example degradation by IDE (Tang 2016). Defects in IDE have long been linked to the development of serious conditions, such as T2DM and Alzheimer's disease (Tang 2016). Indeed, Farris et al. (2003) showed that increased insulin levels resulting from significantly reduced insulin clearance is sufficient enough to lead to glucose intolerance. While the potential role of hyperinsulinemia in the aggravation of insulin resistance is a subject of debate (Pories & Dohm 2012), it appears of crucial importance to identify mechanisms which keep both glucose and insulin levels within a physiologically acceptable range. One such mechanism could be insulin clearance. Indeed, over the years there has been much speculation that reducing insulin degradation may be used to treat T2DM (Mirsky & Broh-Kahn 1949, Duckworth, Bennett & Hamel 1998) and in Maianti et al. (2014)

it was shown that acute inhibition of IDE in mice lead to substantially improved glucose tolerance.

However, there are still many unanswered questions regarding the use of IDE inhibitors in humans (Tang 2016), and a lot of work still needs to be done to see if they can be used prolonged periods of time (Hogan et al. 2016). Nevertheless, their use represents an encouraging avenue for clinical treatment (Tang 2016).

4.2 Strategies

We now investigate strategies allowing the stabilisation of the basal glucose level and/or the restoration of oscillations using the insulin degradation or insulin infusion as a bifurcation parameter. As stated in Section 3.1, $d_i(\alpha, \beta)$ can be viewed as a combination of natural and artificial processes which regulate the clearance of insulin. Indeed, under the assumption that the insulin degradation rate is adjusted in a continuous way, proportionally to the insulin levels, this effect can be incorporated into $d_i(\alpha, \beta)$. Our analysis for the stabilisation processes makes use of equations (3.1.3) and (3.1.4) for the steady state $(\bar{G}, \bar{I})$, as given in Section 3.

In the optimal non-diabetic case $\alpha = \beta = \gamma = 1$, the current choice of parameters from Tables 3.1 and 3.2 gives a value of $\bar{G} \approx 97.87$ mg/dl, which we use as the reference value.

The effect of this stabilisation mechanism on the generation of an oscillatory regime is also investigated as follows. It is known that for all values of A, B, C, D (as defined in (3.1.2)), $d_i(\alpha, \beta)$, and any fixed τ_1, there exists a $\tau_2^*(\tau_1)$ such that the characteristic equation (3.1.9) undergoes a supercritical Hopf bifurcation in the (τ_1, τ_2) space (Li & Kuang 2007). If we then suppose that an individual has fixed secretion time delays (here we use $\tau_1 = 6$ and $\tau_2 = 36$), then for a fixed pair (α,β) one can compute the point of Hopf bifurcation $\tau_2^*(6)$ using formulas (3.1.13) and (3.1.14). Since every $\tau_2 > \tau_2^*(6)$ will lead to an oscillatory regime (see Fig. 3.4), this provides an easy way to verify whether the pair (α,β) is oscillatory, and hence allows to decide whether specific values of α and β for a given individual (with fixed τ_1 and τ_2) lead to an oscillatory regime.

4.2.1 Using insulin injections to stabilise the glucose level

We assume here that a continuous insulin infusion may allow the stabilisation of the basal glucose level. Indeed since the steady state $(\bar{G}, \bar{I})$ satisfies equations (3.1.3) and (3.1.4), it is easily computed that in order to keep $\bar{G}$ constant, for fixed G_{in}, α, β and γ, one can solve equation (3.1.3) numerically to obtain $\bar{I}$ while equation (3.1.4) gives

$$I_{in} = d_i(\alpha, \beta)\bar{I} - \alpha f_1(\bar{G}). \tag{4.2.1}$$

Using the algorithm detailed above, we determine whether each (α,β), with I_{in} as defined by (4.2.1) and $d_i = 0.06$, leads to an oscillatory regime. The result is shown in Fig. 4.1. For physiological accuracy, only values of (α,β) where $I_{in} > 0$ were considered. It can be seen that insulin injections are indeed able to stabilise the basal glucose level for a vast range of diabetic states. However, in the case when $\gamma = 1$, oscillations are only present/restored for a small range of α and β. This range was further reduced when γ was decreased.

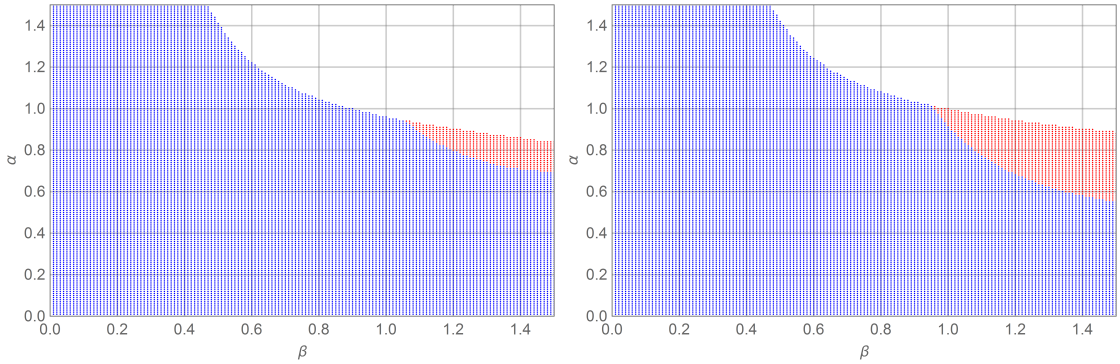

Figure 4.1: Oscillatory region (in red) in the α, β domain for $d_i = 0.06$ with I_{in} as defined by (4.2.1) with $\gamma = 0.7$ (left) and $\gamma = 1$ (right). The blue region represents values of (α, β) for which $\bar{G}$ remains constant at 97.87, but the system is stable. The white region represents values of (α, β) where the resulting value of I_{in} is negative.

As seen from Fig. 4.2, changing τ_1 and τ_2, which is equivalent to looking at different individuals, has very little effect on the range for which oscillations can be restored using a constant insulin infusion. Indeed, when $G_{in} = 1.35$, oscillations cannot be restored when $\beta < 0.9$ irrespective of the value of the delays chosen.

Interestingly, the oscillatory region also remains relatively unchanged for varying delays when $G_{in} = 0.54$. However, unlike when $G_{in} = 1.35$, the oscillations can be restored for a larger range of diabetic states when $G_{in} = 0.54$ (Fig. 4.3). Even so, there still exists a critical value of β such that if $\beta < \beta_{cr}$ then oscillations cannot be restored.

4.2.2 Reducing hepatic glucose production to stabilise the glucose level

Inhibiting hepatic glucose production can also be seen as a mechanism for reducing glucose levels, as employed by several medications occurring in the treatment of T2DM (Hundal et al. 2000). Let us consider a situation where insulin resistance is present, $\beta < 1$, and investigate under which circumstances the reduction of hepatic glucose allows to keep the value of $\bar{G}$ constant. Assuming d_i and I_{in} are fixed, (3.1.3) and (3.1.4) can be rearranged to obtain the stabilising value of γ,

$$\gamma = \frac{G_{in} - f_2(\bar{G}) - \beta f_3(\bar{G}) f_4(\frac{I_{in}+\alpha f_1(\bar{G}))}{d_i})}{f_5(\frac{I_{in}+\alpha f_1(\bar{G}))}{d_i})}. \tag{4.2.2}$$

It can be seen in equation (4.2.2) that there is a linear relationship between β and γ in compensating insulin resistance by reducing hepatic glucose production. Applying the algorithm described previously, one can assess whether the resulting choice leads to an oscillatory regime. The result is illustrated in Fig. 4.4. Indeed, it is seen that there is a small region of (α, β) for which $\bar{G}$ is kept constant and oscillations occur. On the other hand, for the current choice of parameters, neither the restoration of oscillations or the stabilisation of $\bar{G}$ is possible when both $(\alpha, \beta) < 0.8$. Therefore the reduction of the hepatic glucose production on its own may not be an effective strategy for the restoration of oscillations in the diabetic state. However, as mentioned in Subsection 4.1.3, drugs like Metformin lower both the hepatic glucose production and insulin resistance (Hundal et al. 2000). Therefore, physiologically, this strategy may be more effective than Fig. 4.4 suggests.

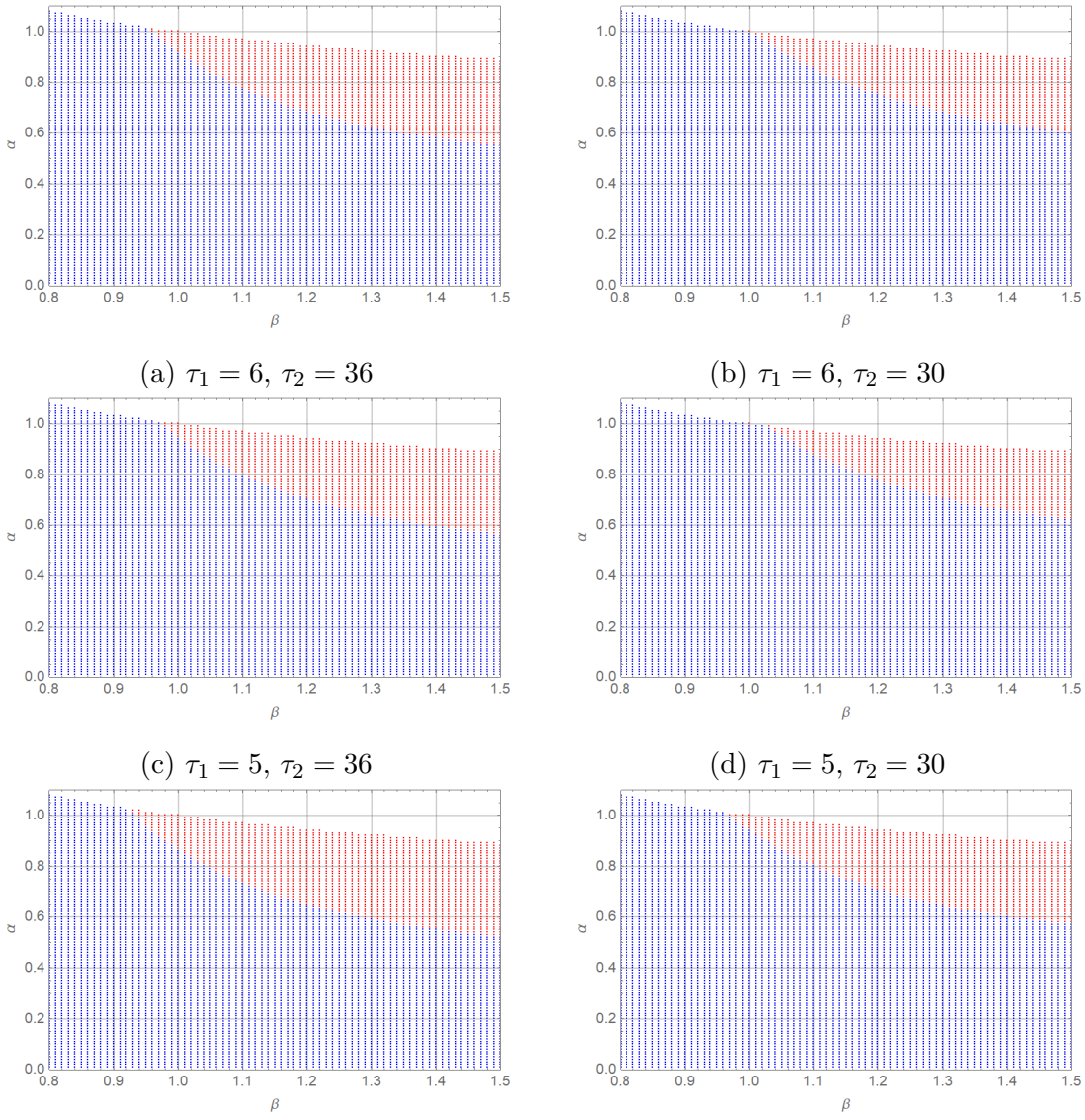

(a) $\tau_1 = 6$, $\tau_2 = 36$

(b) $\tau_1 = 6$, $\tau_2 = 30$

(c) $\tau_1 = 5$, $\tau_2 = 36$

(d) $\tau_1 = 5$, $\tau_2 = 30$

(e) $\tau_1 = 8$, $\tau_2 = 36$

(f) $\tau_1 = 8$, $\tau_2 = 30$

Figure 4.2: Oscillatory regions in the α, β domain for various values of τ_1 and τ_2. The red, blue and white regions are as defined in Fig. 4.1.

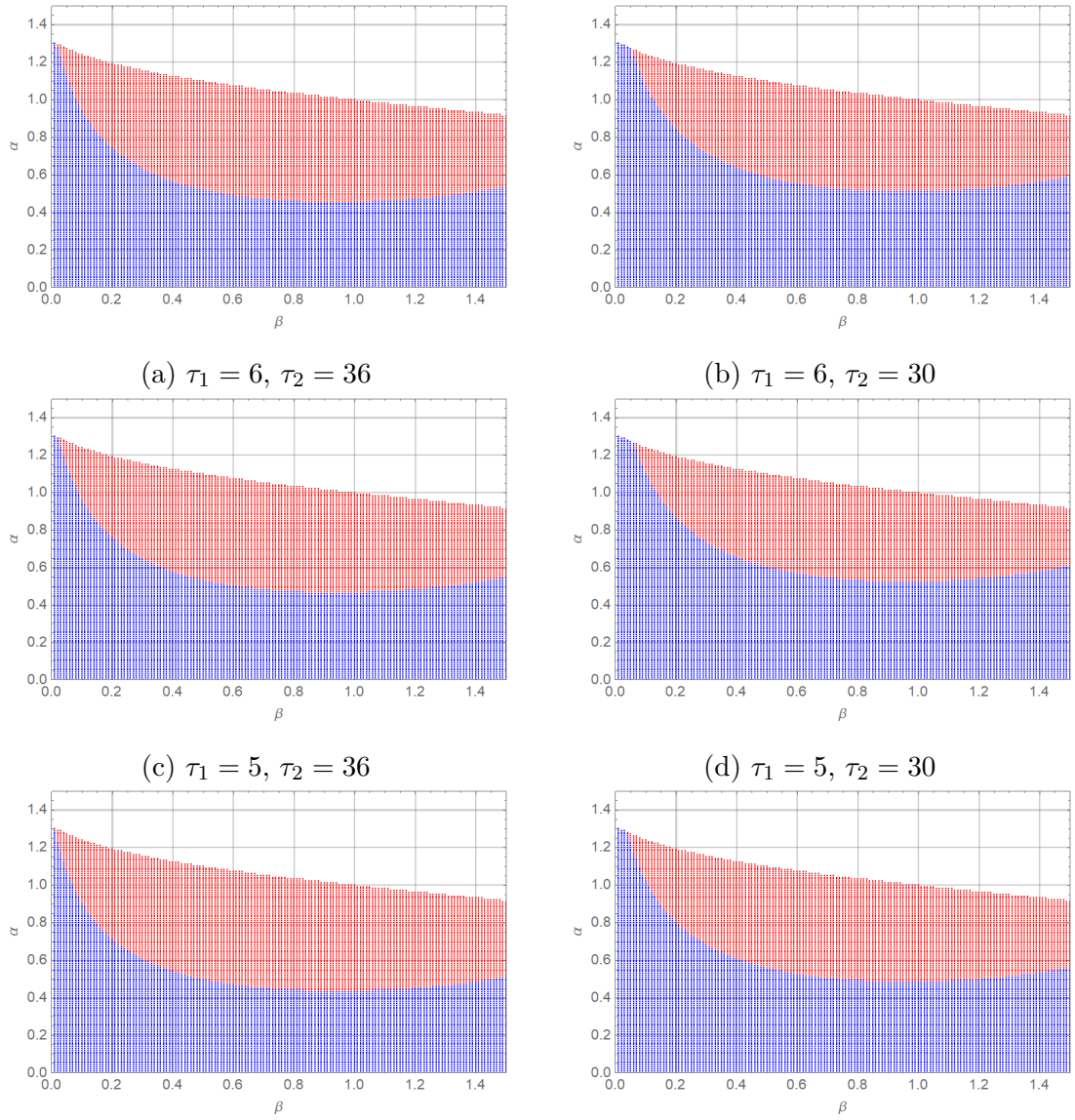

(a) $\tau_1 = 6$, $\tau_2 = 36$

(b) $\tau_1 = 6$, $\tau_2 = 30$

(c) $\tau_1 = 5$, $\tau_2 = 36$

(d) $\tau_1 = 5$, $\tau_2 = 30$

(e) $\tau_1 = 8$, $\tau_2 = 36$

(f) $\tau_1 = 8$, $\tau_2 = 30$

Figure 4.3: Oscillatory regions in the α, β domain for various values of τ_1 and τ_2 with $G_{in} = 0.54\ mg/dl\ min$. The red, blue and white regions are as defined in Fig. 4.1, although it is noted that $\bar{G}$ is now stabilised to 89 which is the value of the steady state when $\alpha = \beta = \gamma = 1$ for $G_{in} = 0.54$.

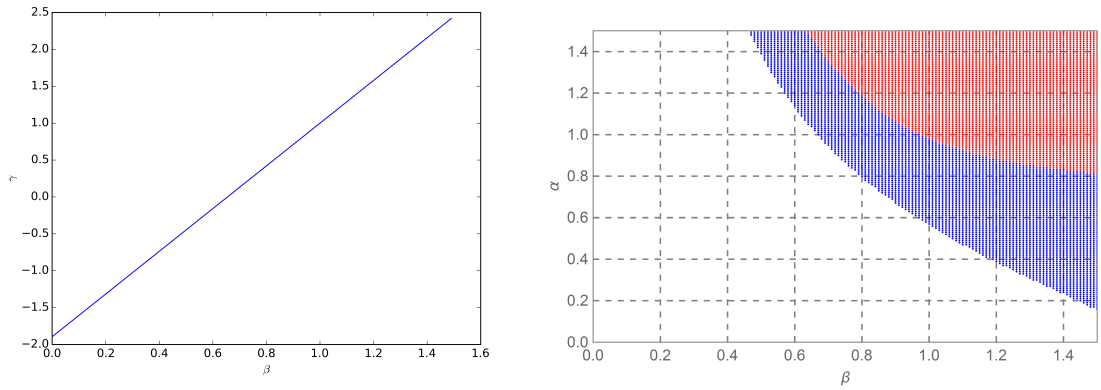

Figure 4.4: Value of γ, as defined by (4.2.2), that enables the stabilisation of $\bar{G} = 97.87$ mg/dl for each β with $\alpha = 1$ (left) and the resulting oscillatory region in the α, β domain with $d_i = 0.06, I_{in} = 0$ (right, red). The blue region represents values of (α,β) such that $\bar{G} = 97.87$ but oscillations do not occur. Finally, the white region corresponds to negative values of γ, which are physiologically impossible.

4.2.3 Altering insulin degradation to stabilise the glucose level

As mentioned in Section 4.2.1, since the steady state $(\bar{G}, \bar{I})$ satisfies equations (3.1.3) and (3.1.4), it can be easily computed that

$$G_{in} - f_2(\bar{G}) - \beta f_3(\bar{G}) f_4(\bar{I}) + \gamma f_5(\bar{I}) = 0, \tag{4.2.3}$$

$$\bar{I} = \frac{I_{in} + \alpha f_1(\bar{G})}{d_i(\alpha, \beta)}. \tag{4.2.4}$$

Using (4.2.3) and (4.2.4), with fixed α, we can determine the function $d_i(\alpha, \beta)$ which stabilises the glucose basal level to 97.87 mg/dl and the resulting insulin basal level, $\bar{I}$. These can be seen in Fig. 4.5.

The graphs clearly show that in the case of moderate insulin resistance ($\beta \in [0.6, 1]$), it is possible to keep both the glucose and insulin basal levels relatively unchanged by altering the insulin clearance rate.

It is readily seen that this strategy can be applied in the case of limited insulin resistance.

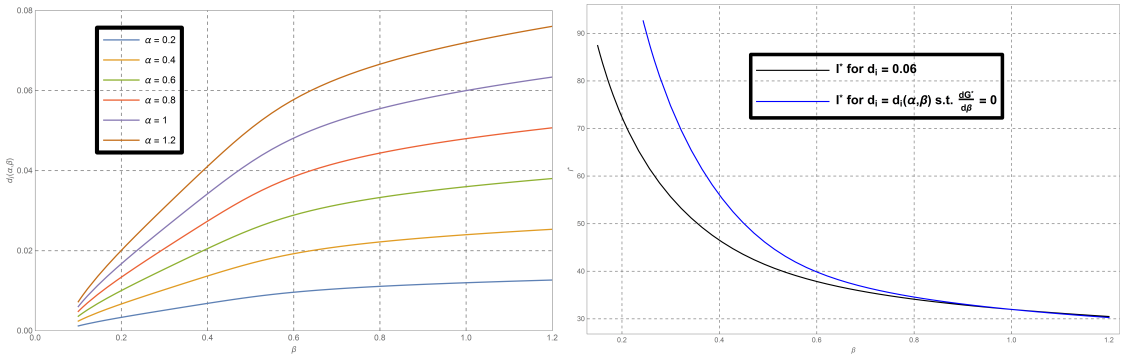

Figure 4.5: Clearance rate which allows to stabilise $\bar{G} = 97.87mg/dl$ and the resulting $\bar{I}$ when $d_i(1,1) = 0.06$ and $I_{in} = 0$.

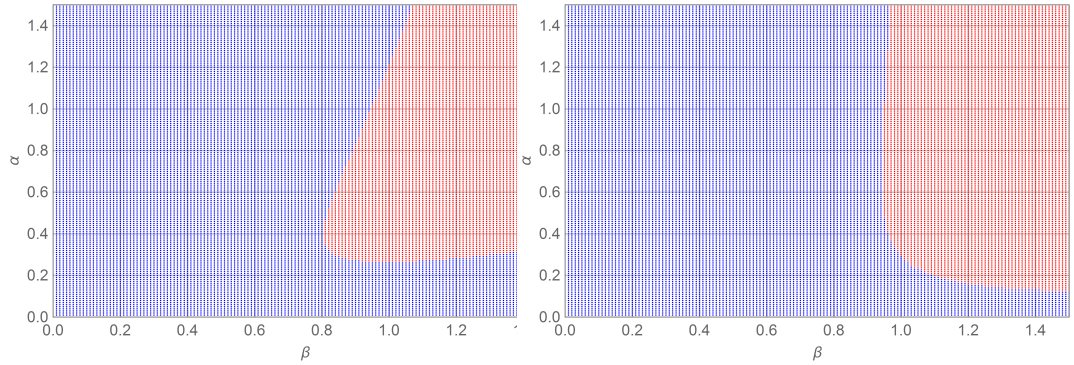

Figure 4.6: Oscillatory region (in red) in the α, β domain for $d_i = 0.06$ (left) and $d_i(\alpha, \beta)$ defined by (4.2.3), with $I_{in} = 0$.

4.2.4 Reintroducing oscillations

This strategy focuses primarily on the reintroduction of an oscillatory regime. To this end, we use d_i as a bifurcation parameter to assess whether altering insulin clearance may be used for this purpose. However, a Hopf bifurcation has only been shown to occur in the (τ_1, τ_2) space, and so we use the algorithm outlined previously in order to determine whether the system oscillates for a given (α, β, d_i), and hence obtain the oscillatory region in the (α, β, d_i) space (shown in Fig. 4.7) . We also verify that the resulting fasting glucose levels fall within an acceptable physiological range. It can be seen from Fig. 4.7 that changing d_i is considerably more effective for restoring oscillations for large variations of α than β. Indeed, for values of $\beta < 0.9$, d_i cannot be used to restore the oscillatory regime of the system and keep the fasting glucose levels within an acceptable range.

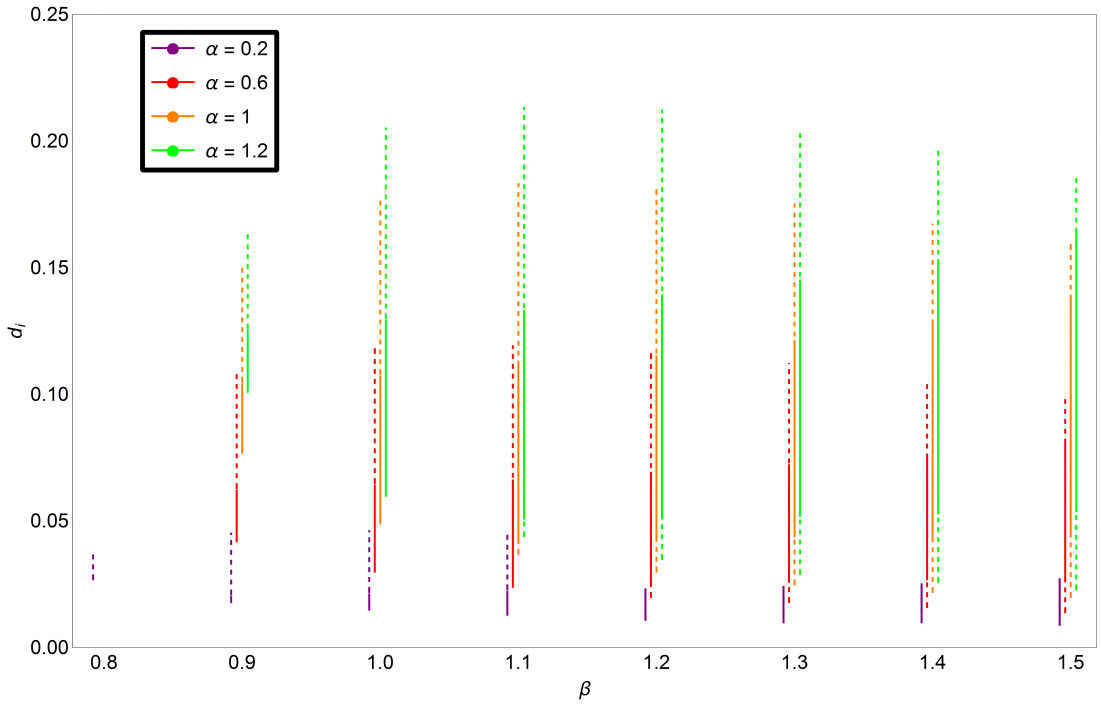

Figure 4.7: Oscillating regions in the α, β, d_i domain. The solid sections represent the values of d_i for which both oscillations occur, and the fasting glucose levels lay within an acceptable range (70-109 mg/dl).

4.2.5 Combining strategies

The final strategy combines the use of both γ and d_i to assess whether a larger range of diabetic states can be successfully recalibrated. We proceed as follows. For fixed values of α, β and delays, we look at whether any value in the ranges $d_i \in [0.01, 0.3]$ and $\gamma \in (0, 1]$ leads to an oscillatory solution with acceptable fasting glucose values. As seen in Fig 4.8, this combination does extend the range of (α, β) values which can be successfully recalibrated. In particular, even in cases where insulin secretion is relatively low, the retuning of insulin degradation and hepatic production enables the restoration of an oscillatory regime.

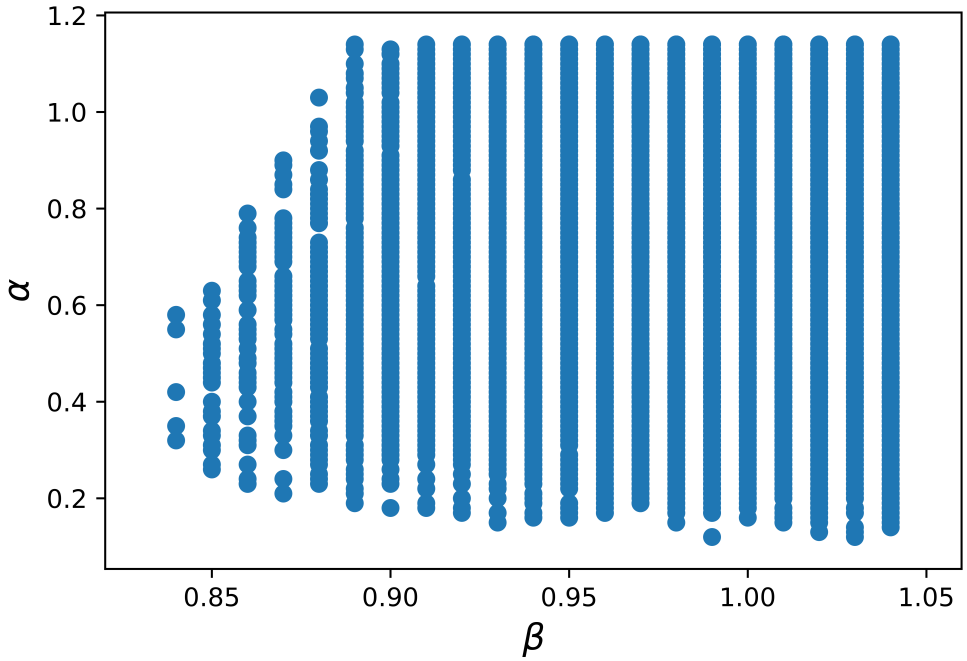

Figure 4.8: Values of α and β for which oscillations can be restored with a healthy fasting basal level using a combined strategy.

Chapter 5

Amplitude and frequency variation

This chapter provides an analysis of the variation of amplitude and frequency in the simplified nonlinear model with respect to the model parameters. This is achieved through the perturbation of periodic solutions in a neighbourhood of the critical manifold. This technique is usually referred to as the Poincaré-Lindstedt (P-L) expansion (Verhulst 2006, pp. 122–127).

In Section 5.1.1 we first consider the case when hepatic glucose production is assumed to be constant (see model (5.1.1)), in which case the small bifurcation parameter $\epsilon > 0$ represents the distance from the critical τ_0. Then in Section 5.1.2 we extend our considerations to the two delay case by assuming that the second delay is a constant multiple of the first one, thus defining a fan of expansion lines in the space of delays (see model (5.1.20)). Finally, the effect of the model parameters on the expressions for the amplitude and period are analysed in Section 5.2, with Subsections 5.2.1 and 5.2.2 focusing on the expressions for models (5.1.1) and (5.1.20), respectively.

5.1 Hopf-bifurcation formulae

The P-L technique is a method for finding approximate expressions for periodic solutions of nonlinear systems through the removal of secular terms. It was extended to differential equations with explicit delay by Casal & Freedman (1980) and has been applied in a limited number of studies to highlight the contribution of parame-

ters to the amplitude of oscillations. For example, Verdugo & Rand (2008) used the P-L technique to predict the amplitude and frequency of a two compartment DDE model of gene expression with one delay, while Brandt, Pelster & Wessel (2006) used it to calculate the frequency of a two compartment DDE model, representing two coupled Hopfield neurons, with two equal delays. The P-L method has also served as a basis for developing a Floquet theory of time periodic states (Simmendinger, Wunderlin & Pelster 1999).

Throughout this section, it is assumed that the frequency of the periodic solution of the linearised system, ω_0, does not satisfy an equation of order lower than the characteristic equation.

5.1.1 Constant hepatic glucose production

Recall from Section 3.2.1 that the simplified model with a constant hepatic glucose production term, with $n = 2$, is given by

$$\begin{aligned} \dot{G}(t) &= G_{in} - a_1 G(t) - a_2 G(t) I(t) + C, \\ \dot{I}(t) &= b_1 G(t-\tau_1)^2 - b_2 I(t), \quad \tau = \tau_1. \end{aligned} \tag{5.1.1}$$

Defining

$$X(t) = X = G(t) - \bar{G}, \quad Y(t) = Y = I(t) - \bar{I},$$

as deviations from the positive equilibrium, and substituting into (5.1.1) leads to

$$\begin{aligned} \dot{X} &= -a_1 X - a_2 \left(XY + \bar{I}X + \bar{G}Y \right), \\ \dot{Y} &= b_1 X_\tau^2 + 2 b_1 \bar{G} X_\tau - b_2 Y. \end{aligned} \tag{5.1.2}$$

Eliminating Y in (5.1.2) allows us to write the following second-order DDE for X

$$\begin{aligned} &\left(\bar{G} + X\right) \ddot{X} - \dot{X}^2 + \left(a_0 + b_2(\bar{G} + X)\right) \dot{X} \\ &+ \left(\bar{G} + X\right) \left(\left(a_1 + a_2 \bar{I}\right) b_2 X + a_2 b_1 \left(\bar{G} + X\right) X_\tau \left(2\bar{G} + X_\tau\right) \right) = 0. \end{aligned} \tag{5.1.3}$$

We now introduce the bifurcation parameter ϵ, which is defined as the distance from the critical delay τ_0 as follows

$$\epsilon = \sqrt{\tau - \tau_0}. \tag{5.1.4}$$

The state variable X is then scaled as

$$X(t) = \epsilon u(s), \tag{5.1.5}$$

where

$$s = \Omega(\epsilon)\, t \tag{5.1.6}$$

corresponds to a new time variable ensuring that $u(s)$ has a period of 2π. Here, Ω is also assumed to have an ϵ-expansion

$$\Omega = \omega_0 + \epsilon\omega_1 + \epsilon^2\omega_2 + \epsilon^3\omega_3 + ..., \tag{5.1.7}$$

where ω_0 is the frequency associated to the critical value τ_0. Finally, we expand the delayed term u_τ

$$\begin{aligned} u(s - \Omega\tau) = u(s - \tau_0\omega_0) - \tau_0\omega_1\epsilon\dot{u}(s - \tau_0\omega_0) \\ + \epsilon^2\left(\frac{1}{2}\tau_0^2\omega_1^2\ddot{u}(s - \tau_0\omega_0) - \dot{u}(s - \tau_0\omega_0)(\omega_0 + \tau_0\omega_2)\right) + O(\epsilon^3), \end{aligned} \tag{5.1.8}$$

along with u and its derivatives

$$u(s) = u_0(s) + \epsilon u_1(s) + \epsilon^2 u_2(s) + ... \tag{5.1.9}$$

Substituting into (5.1.3) and collecting terms (up to and including $O(\epsilon^2)$) gives

$$\omega_0^2\ddot{u}_0 + \dot{u}_0\omega_0(a_2\bar{I} + a_1 + b_2) + b_2u_0(a_2\bar{I} + a_1) + 2a_2b_1\bar{G}^2u_{0\tau} = 0, \tag{5.1.10}$$

$$\begin{aligned}&\omega_0^2\ddot{u}_1 + \dot{u}_1\omega_0(a_2\bar{I} + a_1 + b_2) + b_2u_1(a_2\bar{I} + a_1) + 2a_2b_1\bar{G}^2u_{1\tau}\\ &+ \bar{G}^{-1}(u_0(4a_2b_1\bar{G}^2u_{0\tau} + \omega_0(b_2\dot{u}_0 + \omega_0\ddot{u}_0) - 2a_2b_1\bar{G}^3\omega_1\tau_0\dot{u}_{0\tau}) + a_2b_1\bar{G}^2u_{0\tau}^2\\ &+ b_2u_0^2(a_2\bar{I} + a_1) + a_2\bar{G}\bar{I}\omega_1\dot{u}_0 + a_1\bar{G}\omega_1\dot{u}_0 + b_2\bar{G}\omega_1\dot{u}_0 + 2\bar{G}\omega_1\omega_0\ddot{u}_0 - \omega_0^2\dot{u}_0^2) = 0,\end{aligned} \tag{5.1.11}$$

$$\begin{aligned}&\omega_0^2\ddot{u}_2 + \dot{u}_2\omega_0(a_2\bar{I} + a_1 + b_2) + b_2u_2(a_2\bar{I} + a_1) + 2a_2b_1\bar{G}^2u_{2\tau}\\ &+ \bar{G}^{-1}(a_2b_1\bar{G}^3\omega_1^2\tau_0^2\ddot{u}_{0\tau} - 2a_2b_1\bar{G}^3\omega_2\tau_0\dot{u}_{0\tau} - 2a_2b_1\bar{G}^3\omega_1\tau_0\dot{u}_{1\tau} - 2a_2b_1\bar{G}^3\omega_0\dot{u}_{0\tau}\\ &+ u_0(4a_2b_1\bar{G}^2u_{1\tau} - 4a_2b_1\bar{G}^2\omega_1\tau_0\dot{u}_{0\tau} + 2a_2b_1\bar{G}u_{0\tau}^2 + 2b_2u_1(a_2\bar{I} + a_1) + b_2\omega_1\dot{u}_0\\ &+ b_2\dot{u}_1\omega_0 + 2\omega_1\omega_0\ddot{u}_0 + \omega_0^2\ddot{u}_1) + 2a_2b_1\bar{G}^2u_{0\tau}(u_{1\tau} - \omega_1\tau_0\dot{u}_{0\tau} + 2u_1) + 2a_2b_1\bar{G}u_0^2u_{0\tau}\\ &+ a_2\bar{G}\bar{I}\omega_2\dot{u}_0 + a_2\bar{G}\bar{I}\omega_1\dot{u}_1 + a_1\bar{G}\omega_2\dot{u}_0 + a_1\bar{G}\omega_1\dot{u}_1 + b_2\bar{G}\omega_2\dot{u}_0 + b_2\bar{G}\omega_1\dot{u}_1 + b_2u_1\dot{u}_0\omega_0\\ &+ 2\bar{G}\omega_2\omega_0\ddot{u}_0 + 2\bar{G}\omega_1\omega_0\ddot{u}_1 + \bar{G}\omega_1^2\ddot{u}_0 - 2\omega_1\dot{u}_0^2\omega_0 + u_1\omega_0^2\ddot{u}_0 - 2\dot{u}_0\dot{u}_1\omega_0^2) = 0,\end{aligned} \tag{5.1.12}$$

with $u_{i\tau} = u_i(s - \tau_0\omega_0)$. The seed solution is chosen as

$$u_0(s) = A_0\cos(s) + B_0\sin(s) \tag{5.1.13}$$

and since (5.1.10) is linear, A_0 and B_0 are arbitrary. Without loss of generality, we impose the initial condition $u_0(\frac{\pi}{2}) = 0$, giving

$$u_0(s) = A_0\cos(s) \tag{5.1.14}$$

where, following (5.1.5), A_0 is related to the amplitude of x (denoted by $\bar{A}$) by $\bar{A} = A_0\epsilon$. Choosing

$$u_1(s) = A_1\sin(s) + B_1\cos(s) + C_1\sin(2s) + D_1\cos(2s) + E_1 \tag{5.1.15}$$

and substituting into (5.1.11) and comparing coefficients of the $\cos(s)$ and $\sin(s)$ terms shows that: (1) A_1, B_1 are arbitrary (2) $\omega_1 = 0$. From comparison of the $\cos(2s)$ and $\sin(2s)$ coefficients, it can be shown that

$$C_1 = \frac{A_0^2F}{G}, \quad D_1 = \frac{A_0^2H}{K}, \quad E_1 = \frac{A_0^2(2a_1b_2 - a_2(2b_1\bar{G}^2 - 2b_2\bar{I}))}{4\bar{G}(a_2(2b_1\bar{G}^2 + b_2\bar{I}) + a_1b_2)}$$

where F, G, H and K are some functions of $a_1, a_2, b_1, b_2, \bar{G}, \bar{I}, \omega_0$. Due to their length, they are not reproduced here. By substituting

$$\begin{aligned} u_2(s) =& A_2 \sin(s) + B_2 \cos(s) + C_2 \sin(2s) + D_2 \cos(2s) \\ &+ E_2 \sin(3s) + F_2 \cos(3s) + G_2 \end{aligned} \tag{5.1.16}$$

along with (5.1.15) and (5.1.13) into (5.1.12), and comparing the coefficients of the $\cos(s)$ and $\sin(s)$ terms, the dominant term for the amplitude, $\bar{A}$, of the limit cycle is expressible as

$$\bar{A}^2 = \frac{8\bar{G}^2\rho\left(2a_2b_1\bar{G}^3 + a_0b_2\right)\left(a_0^2 + \bar{G}^2\left(b_2^2 + 2\rho\right)\right)p_1}{\sum_{m=0}^{7}(p_{2,m} + \tau_0 p_{3,m})a_0^m}\epsilon^2, \tag{5.1.17}$$

while the dominant term of the amplitude of the insulin oscillations, $\bar{B}$, and the second-order term for frequency correction, ω_2, are given by

$$\bar{B} = \frac{\bar{A}}{a_2\bar{G}}\sqrt{\rho + \frac{a_0^2}{\bar{G}^2}}, \quad \omega_2 = \frac{-\sqrt{\rho}\sum_{m=0}^{7} p_{3,m}a_0^m}{\sum_{m=0}^{7}(p_{2,m} + \tau_0 p_{3,m})a_0^m}. \tag{5.1.18}$$

Here, we introduced the following definitions

$$
\begin{aligned}
\rho =& \omega_0^2, \\
p_1 =& 4a_2b_1\bar{G}^3\left(b_2^3\left(a_0^3+3a_0\bar{G}^2\rho\right)+3a_0b_2\rho\left(a_0^2+3\bar{G}^2\rho\right)-4\bar{G}^3\rho^3\right)+b_\rho^2\left(a_0^2+\bar{G}^2\rho\right)^2 \\
&+4a_2^2b_1^2\bar{G}^6b_{4\rho}\left(a_0^2+4\bar{G}^2\rho\right), \\
p_{2,0} =& 16a_2b_1b_2\bar{G}^9\rho^2\left(8a_2^2b_1^2\bar{G}^4b_{4\rho}-2a_2b_1\bar{G}^2\left(5b_2^2\rho+b_2^4+12\rho^2\right)+\rho b_\rho^2\right), \\
p_{2,1} =& 2\bar{G}^6\rho(64a_2^3b_1^3\bar{G}^6(2b_2^2+3\rho)b_{4\rho}-4a_2^2b_1^2\bar{G}^4\rho(59b_2^2\rho-5b_2^4+92\rho^2) \\
&+a_2b_1\bar{G}^2\rho(59b_2^2\rho^2+12b_2^4\rho+7b_2^6+22\rho^3)-2b_2^2\rho^2b_\rho^2), \\
p_{2,2} =& b_2\bar{G}^5\rho(320a_2^3b_1^3\bar{G}^6b_{4\rho}+4a_2^2b_1^2\bar{G}^4(97b_2^2\rho+31b_2^4+6\rho^2) \\
&+2a_2b_1\bar{G}^2\rho(b_2^4+39\rho^2)-\rho(3b_2^2+2\rho)b_\rho^2), \\
p_{2,3} =& \bar{G}^4(16a_2^3b_1^3\bar{G}^6(3b_2^2+2\rho)b_{4\rho}+4a_2^2b_1^2\bar{G}^4\rho(85b_2^2\rho+43b_2^4-38\rho^2) \\
&+2a_2b_1\bar{G}^2\rho(28b_2^2\rho^2-59b_2^4\rho-7b_2^6+44\rho^3)-11b_2^2\rho^2b_\rho^2), \\
p_{2,4} =& 2b_2\bar{G}^3(24a_2^3b_1^3\bar{G}^6b_{4\rho}+2a_2^2b_1^2\bar{G}^4(21b_2^2\rho+9b_2^4+16\rho^2) \\
&-a_2b_1b_2^2\bar{G}^2\rho(7b_2^2+59\rho)-\rho(3b_2^2+2\rho)b_\rho^2), \\
p_{2,5} =& 2\bar{G}^2(6a_2^2b_1^2\bar{G}^4(5b_2^2\rho+3b_2^4-6\rho^2)+a_2b_1\bar{G}^2\rho(11b_2^2\rho-15b_2^4+22\rho^2)-5b_2^2\rho b_\rho^2), \\
p_{2,6} =& -b_2\bar{G}(6a_2b_1\bar{G}^2\rho(5b_2^2+\rho)+(3b_2^2+2\rho)b_\rho^2), \\
p_{2,7} =& -3b_2^2b_\rho^2, \\
p_{3,0} =& 16a_2b_1\bar{G}^9\rho^2b_\rho(8a_2^2b_1^2\bar{G}^4b_{4\rho}-12a_2b_1\bar{G}^2\rho^2+\rho b_\rho^2), \\
p_{3,1} =& -4b_2\bar{G}^6\rho^2b_\rho(2a_2^2b_1^2\bar{G}^4(\rho-5b_2^2)-24a_2b_1\bar{G}^2\rho^2+\rho b_\rho^2), \\
p_{3,2} =& 2a_2b_1\bar{G}^7\rho b_\rho(160a_2^2b_1^2\bar{G}^4b_{4\rho}-156a_2b_1\bar{G}^2\rho^2+\rho(-28b_2^2\rho+b_2^4+31\rho^2)), \\
p_{3,3} =& b_2\bar{G}^4\rho b_\rho(4a_2^2b_1^2\bar{G}^4(43b_2^2+85\rho)+132a_2b_1\bar{G}^2\rho^2-11\rho b_\rho^2), \\
p_{3,4} =& 2a_2b_1\bar{G}^5b_\rho(24a_2^2b_1^2\bar{G}^4b_{4\rho}+\rho(36a_2b_1\bar{G}^2\rho-59b_2^2\rho-7b_2^4+38\rho^2)), \\
p_{3,5} =& 2b_2\bar{G}^2b_\rho(6a_2^2b_1^2\bar{G}^4(3b_2^2+5\rho)+18a_2b_1\bar{G}^2\rho^2-5\rho b_\rho^2), \\
p_{3,6} =& 30a_2b_1\bar{G}^3\rho(\rho-b_2^2)b_\rho, \\
p_{3,7} =& -3b_2b_\rho^3,
\end{aligned}
$$

with $b_\rho = b_2^2 + \rho$ and $b_{4\rho} = b_2^2 + 4\rho$. Finally, we note that the period of the limit cycle, T, is given by

$$T = \frac{2\pi}{\omega_0 + \epsilon^2\omega_2}. \tag{5.1.19}$$

Simulations making use of expressions (5.1.17), (5.1.18), and (5.1.19) are presented in Section 5.2.1.

5.1.2 Linear hepatic glucose production

We now turn to study the effect of a non-constant hepatic glucose production, and hence a second delay, on the limit cycles (see model (3.2.24)). As mentioned in the introduction to this section, the P-L method has indeed been used in a limited number of studies to investigate the effect of model parameters on the amplitude of the resulting oscillatory solutions. For example, in Brandt et al. (2006) a coupled first-order DDE model describing a two-neuron system with delay was explored. While the system had two separate delays, these were combined giving a characteristic equation of the form

$$\lambda^2 + A_1\lambda + A_2 + A_3 e^{-\lambda\tau} = 0, \quad \tau = \tau_1 + \tau_2,$$

with A_1, A_2 constant and A_3 a function of the model parameters. In contrast, the characteristic equation of model (3.2.24), given by (3.2.26), contains a second exponential term which leads to additional challenges in finding points of bifurcation, as discussed in Section 3.2.1. For conciseness, we will assume that $p = 1$ in model (3.2.24) for the following P-L calculation, although the technique can be applied to higher orders. The resulting model is hence given by

$$\begin{aligned} \dot{G}(t) &= a_0 - a_1 G(t) - a_2 G(t) I(t) - a_3 I(t - k\tau), \\ \dot{I}(t) &= b_1 G(t-\tau)^2 - b_2 I(t), \end{aligned} \tag{5.1.20}$$

where the dimensionless parameter k is used to represent the commensurateness of the time delays. As with the calculation in the previous section, we state that

$$X = G(t) - \bar{G}, \quad Y = I(t) - \bar{I}.$$

Let (ω_0, τ_0) be a critical pair obtained using the algorithm described in Section 3.2.1. Then by introducing $\epsilon = \sqrt{\tau - \tau_0}$, as in (5.1.4), we can scale the variables X and Y as

$$X(t) = \epsilon u(s), \quad Y(t) = \epsilon v(s), \tag{5.1.21}$$

where s is the scaled time variable as defined in (5.1.6). The expansions for $v(s)$ and $v(s - k\omega\tau)$ are

$$\begin{aligned} v(s-\Omega\tau) =& v(s-k\tau_0\omega_0) - k\tau_0\omega_1\epsilon\dot{v}(s-k\tau_0\omega_0) \\ &+ \frac{1}{2}k\epsilon^2(\tau_0(k\tau_0\omega_1^2\ddot{v}(s-k\tau_0\omega_0) - 2\omega_2\dot{v}(s-k\tau_0\omega_0)) \\ &- 2\omega_0\dot{v}(s-k\tau_0\omega_0)) + O(\epsilon^3), \end{aligned} \tag{5.1.22}$$

$$v(s) = v_0(s) + \epsilon v_1(s) + \epsilon^2 u_2(s) + ... \tag{5.1.23}$$

Following the steps outlined in (5.1.6) - (5.1.9), substituting into (5.1.20) and collecting terms (up to and including $O(\epsilon^3)$) gives

$$\frac{du_m}{ds} = -\frac{(a_1 + a_2\bar{I})}{\omega_0}u_m - \frac{a_2\bar{G}}{\omega_0}v_m - \frac{a_3}{\omega_0}v_{m\tau} + g_m, \tag{5.1.24}$$

$$\frac{dv_m}{ds} = -\frac{b_2}{\omega_0}v_m + \frac{2b_1\bar{G}}{\omega_0}u_{m\tau} + h_m, \tag{5.1.25}$$

with $m = 0, 1, 2$, $u_{m\tau} = u_m(s - \tau_0\omega_0)$, $v_{m\tau} = v_m(s - k\tau_0\omega_0)$ and where the inhomogeneous terms g_m and h_m are related to the solutions of previous orders. Here we have $g_0 = 0$, $h_0 = 0$, and

$$g_1 = - a_2u_0v_0 + a_3k\omega_1\tau_0\dot{v_{0\tau}} - \omega_1\dot{u_0}, \tag{5.1.26}$$

$$h_1 = b_1{u_{0\tau}}^2 - 2b_1\bar{G}\omega_1\tau_0\dot{u_{0\tau}} - \omega_1\dot{v_0}, \tag{5.1.27}$$

$$\begin{aligned} g_2 =& - a_2u_1v_0 - a_2u_0v_1 - \frac{1}{2}a_3k^2\omega_1^2\tau_0^2\ddot{v_{0\tau}} + a_3k\omega_1\tau_0\dot{v_{1\tau}} + a_3k\omega_0\dot{v_{0\tau}} \\ &+ a_3k\omega_2\tau_0\dot{v_{0\tau}} - a_3v_{2\tau} + \omega_1\dot{u_1} - \omega_2\dot{u_0}, \end{aligned} \tag{5.1.28}$$

$$\begin{aligned} h_2 =& 2b_1u_{0\tau}\,(u_{1\tau} - \omega_1\tau_0\dot{u_{0\tau}}) - 2b_1\bar{G}\omega_1\tau_0\dot{u_{1\tau}} - 2b_1\bar{G}\omega_0\dot{u_{0\tau}} - 2b_1\bar{G}\omega_2\tau_0\dot{u_{0\tau}} \\ &+ b_1\bar{G}\omega_1^2\tau_0^2\ddot{u_{0\tau}} - \omega_1\dot{v_1} - \omega_2\dot{v_0}. \end{aligned} \tag{5.1.29}$$

By imposing the initial conditions $u_0(0) = C_0$, $v_0(0) = C_0R_1$ on the solutions of (5.1.24) and (5.1.25), with $m = 0$ we find that

$$u_0(s) = C_0\cos(s), \tag{5.1.30}$$

$$v_0(s) = C_0R_1\cos(s) + C_0R_2\sin(s), \tag{5.1.31}$$

where

$$R_1 = \frac{1}{Q}(-\omega_0(a_1 + a_2\bar{I} - b_2) + a_1 b_2 - 2a_2 b_1 \bar{G}^2 \sin(\tau_0\omega_0) + 2a_2 b_1 \bar{G}^2 \cos(\tau_0\omega_0) + a_2 b_2 \bar{I} + 2a_3 b_1 \bar{G} \sin((k-1)\tau_0\omega_0) + 2a_3 b_1 \bar{G} \cos((k+1)\tau_0\omega_0) - \omega_0^2),$$

$$R_2 = \frac{1}{Q}(\omega_0(a_1 + a_2\bar{I} + b_2) + a_1 b_2 - 2a_2 b_1 \bar{G}^2 \sin(\tau_0\omega_0) + 2a_2 b_1 \bar{G}^2 \cos(\tau_0\omega_0) + a_2 b_2 \bar{I} - 2a_3 b_1 \bar{G} \sin((k+1)\tau_0\omega_0) + 2a_3 b_1 \bar{G} \cos((k-1)\tau_0\omega_0) + \omega_0^2),$$

$$Q = 2(\omega_0(a_2\bar{G} + a_3 \cos(k\tau_0\omega_0)) + a_3 b_2 \sin(k\tau_0\omega_0)).$$

We note that C_0 is related to the amplitude of $X(t)$ (denoted by $\bar{C}$) by $\bar{C} = C_0\epsilon$, and that the amplitude of $Y(t)$ (denoted by $\bar{D}$) is given by

$$\bar{D} = \bar{C}\sqrt{R_1^2 + R_2^2}. \tag{5.1.32}$$

As we necessitate that the solutions u_m and v_m are periodic in s with period 2π, we must find conditions such that the inhomogeneities do not contain secular terms. Hence, we proceed as in Brandt et al. (2006) and expand u_m, v_m, g_m and h_m as Fourier series to get

$$\begin{pmatrix} u_m(s) \\ v_m(s) \end{pmatrix} = \sum_{\kappa=0}^{\infty} \left(\begin{pmatrix} a_{1,\kappa}^{(m)} \\ a_{2,\kappa}^{(m)} \end{pmatrix} \cos(\kappa s) + \begin{pmatrix} b_{1,\kappa}^{(m)} \\ b_{2,\kappa}^{(m)} \end{pmatrix} \sin(\kappa s) \right), \tag{5.1.33}$$

$$\begin{pmatrix} g_m(s) \\ h_m(s) \end{pmatrix} = \sum_{\kappa=0}^{\infty} \left(\begin{pmatrix} \alpha_{1,\kappa}^{(m)} \\ \alpha_{2,\kappa}^{(m)} \end{pmatrix} \cos(\kappa s) + \begin{pmatrix} \beta_{1,\kappa}^{(m)} \\ \beta_{2,\kappa}^{(m)} \end{pmatrix} \sin(\kappa s) \right). \tag{5.1.34}$$

Substituting (5.1.33) and (5.1.34) into (5.1.24) and (5.1.25), it can be seen that the coefficients, $\alpha_{j,1}^{(m)}$, $\beta_{j,1}^{(m)}$ (with $j = 1, 2$), in the inhomogeneities g_m and h_m must satisfy the following conditions

$$-a_2\alpha_{2,1}^{(m)}\bar{G} + \alpha_{1,1}^{(m)} b_2 - \alpha_{2,1}^{(m)} a_3 \cos(\tau_0\omega_0) + a_3\beta_{2,1}^{(m)} \sin(\tau_0\omega_0) + \beta_{1,1}^{(m)}\omega_0 = 0, \tag{5.1.35}$$

$$-\alpha_{1,1}^{(m)}\omega_0 - a_2\beta_{2,1}^{(m)}\bar{G} + b_2\beta_{1,1}^{(m)} - \alpha_{2,1}^{(m)} a_3 \sin(\tau_0\omega_0) - a_3\beta_{2,1}^{(m)} \cos(\tau_0\omega_0) = 0. \tag{5.1.36}$$

For further details of the derivation of these conditions, the reader is referred to the next subsection.

When $\kappa = 1$, the coefficients of the inhomogeneities g_1 and h_1 are

$$\alpha_{1,1}^{(1)} = \frac{kC_0\tau_0\omega_1 v_1}{v_5\omega_0}, \quad \beta_{1,1}^{(1)} = \frac{C_0\omega_1(k\tau_0 v_2 - 2v_1)}{v_5\omega_0}, \quad \alpha_{2,1}^{(1)} = \frac{C_0\omega_1 v_3}{v_5}, \quad \beta_{2,1}^{(1)} = \frac{C_0\omega_1 v_4}{v_5},$$

where

$$\begin{aligned}
v_1 =& a_3\omega_0(a_2\bar{I} + a_1 - b_2)\sin(k\tau_0\omega_0) - a_3(b_2(a_2\bar{I} + a_1) + \omega_0^2)\cos(k\tau_0\omega_0) \\
&+ \bar{G}(-2b_1(a_3 - a_2\bar{G})(a_2\bar{G} + a_3)\cos(\tau_0\omega_0) + a_2b_2(a_2\bar{I} + a_1) - a_2\omega_0^2), \\
v_2 =& -a_3(b_2(a_2\bar{I} + a_1) + \omega_0^2)\sin(k\tau_0\omega_0) - a_3\omega_0(a_2\bar{I} + a_1 - b_2)\cos(k\tau_0\omega_0) \\
&+ 2b_1\bar{G}(a_2^2\bar{G}^2 - a_3^2)\sin(\tau_0\omega_0) - a_2\bar{G}\omega_0(a_2\bar{I} + a_1 + b_2), \\
v_3 =& 2b_1\bar{G}(a_3\cos((k-1)\tau_0\omega_0) + 2\tau_0v_1\sin(\tau_0\omega_0)) + a_2(2b_1\bar{G}^2\cos(\tau_0\omega_0) + b_2\bar{I}) \\
&+ a_1b_2 + \omega_0^2, \\
v_4 =& 2b_1\bar{G}(-a_3\sin((k-1)\tau_0\omega_0) + a_2\bar{G}\sin(\tau_0\omega_0) - 2\tau_0v_1\cos(\tau_0\omega_0)) \\
&+ \omega_0(a_2\bar{I} + a_1 - b_2), \\
v_5 =& 2(a_3b_2\sin(k\tau_0\omega_0) + \omega_0(a_3\cos(k\tau_0\omega_0) + a_2\bar{G})).
\end{aligned}$$

Hence, using (5.1.35), (5.1.36), this implies that

$$\begin{aligned}
C_0\omega_1Z_1(a_1, a_2, a_3, b_1, b_2, k, \bar{G}, \bar{I}, \omega_0, \tau_0) = 0, \\
C_0\omega_1Z_2(a_1, a_2, a_3, b_1, b_2, k, \bar{G}, \bar{I}, \omega_0, \tau_0) = 0,
\end{aligned}$$

where Z_1, Z_2 are functions of $a_1, a_2, a_3, b_1, b_2, k, \bar{G}, \bar{I}, \omega_0, \tau_0$. If $C_0 = 0$, then we obtain the trivial solution. Additionally, it can be seen that Z_1 and Z_2 do not vanish modulo the characteristic curve. Therefore, following our assumption that ω_0 does not satisfy any polynomial equation of lower order, this implies that $\omega_1 = 0$. Substituting this, along with (5.1.30) and (5.1.31), into (5.1.24) and (5.1.25) it can be shown that

$$u_1(s) = a_{1,0}^{(1)} + a_{1,1}^{(1)}\cos(s) + b_{1,1}^{(1)}\sin(s) + C_0^2h_1\cos(2s) + C_0^2h_2\sin(2s), \tag{5.1.37}$$

$$v_1(s) = a_{2,0}^{(1)} + a_{2,1}^{(1)}\cos(s) + b_{2,1}^{(1)}\sin(s) + C_0^2h_3\cos(2s) + C_0^2h_4\sin(2s), \tag{5.1.38}$$

where h_1, h_2, h_3 and h_4 are functions of $a_1, a_2, a_3, b_1, b_2, k, \bar{G}, \bar{I}, \omega_0, \tau_0$. Substituting (5.1.30), (5.1.31) and (5.1.37), (5.1.38) into (5.1.28), (5.1.29), expressions for $\alpha_{1,1}^{(2)}$, $\beta_{1,1}^{(2)}$, $\alpha_{1,2}^{(2)}$ and $\beta_{1,2}^{(2)}$ can be obtained. Finally, using conditions (5.1.35), (5.1.36) and solving the resulting system of equations, it can be shown that the dominant term for the amplitude, $\bar{C}$, the second-order term for frequency correction, ω_2, and the period, T, can be expressed as

$$\bar{C}^2 = \frac{W_1}{V_1}\epsilon^2, \tag{5.1.39}$$

$$\omega_2 = \frac{W_2}{V_2}, \quad T = \frac{2\pi V_2}{\omega_0 V_2 + W_2 \epsilon^2}, \tag{5.1.40}$$

where W_1, W_2, V_1 and V_2 are functions of a_1, a_2, a_3, b_1, b_2, $\bar{G}$, $\bar{I}$, κ, ω_0 and τ_0. Given their length, the expressions are not reproduced here but are used in simulations in Section 5.2.2.

Derivation of the two conditions (5.1.35) and (5.1.36)

Here we show how conditions (5.1.35), (5.1.36) are obtained. First, we note that from (3.2.27) and (3.2.28) it can be seen that

$$\cos((k+1)\omega_0\tau_0) = \frac{-b_2(a_1 + a_2\bar{I}) - 2a_2b_1\bar{G}^2\cos(\tau_0\omega_0) + \omega_0^2}{2a_3b_1\bar{G}}, \tag{5.1.41}$$

$$\sin((k+1)\omega_0\tau_0) = \frac{\omega_0(a_1 + a_2\bar{I} + b_2) - 2a_2b_1\bar{G}^2\sin(\tau_0\omega_0)}{2a_3b_1\bar{G}}. \tag{5.1.42}$$

Through the substitution of the Fourier series decompositions (given by (5.1.33) and (5.1.34)) into (5.1.24), (5.1.25) and comparing the coefficients of $\cos(\kappa s)$ and $\sin(\kappa s)$, we obtain that

$$\begin{aligned} &a_3a_{2,\kappa}^{(m)}\cos(\kappa k\omega_0\tau_0) + a_1a_{1,\kappa}^{(m)} + a_2\bar{G}a_{2,\kappa}^{(m)} + a_2\bar{I}a_{1,\kappa}^{(m)} - a_3b_{2,\kappa}^{(m)}\sin(\kappa k\omega_0\tau_0) \\ &+ \kappa\omega_0 b_{1,\kappa}^{(m)} - \alpha_{1,\kappa}^{(m)} = 0, \end{aligned} \tag{5.1.43}$$

$$\begin{aligned} &a_3a_{2,\kappa}^{(m)}\sin(\kappa k\omega_0\tau_0) + a_3b_{2,\kappa}^{(m)}\cos(\kappa k\omega_0\tau_0) + a_1b_{1,\kappa}^{(m)} + a_2\bar{G}b_{2,\kappa}^{(m)} + a_2\bar{I}b_{1,\kappa}^{(m)} \\ &- \kappa\omega_0 a_{1,\kappa}^{(m)} - \beta_{1,\kappa}^{(m)} = 0, \end{aligned} \tag{5.1.44}$$

$$b_2a_{2,\kappa}^{(m)} - 2b_1\bar{G}a_{1,\kappa}^{(m)}\cos(\kappa\omega_0\tau_0) + 2b_1\bar{G}b_{1,\kappa}^{(m)}\sin(\kappa\omega_0\tau_0) + \kappa\omega_0 b_{2,\kappa}^{(m)} - \alpha_{2,\kappa}^{(m)} = 0, \tag{5.1.45}$$

$$b_2b_{2,\kappa}^{(m)} - 2b_1\bar{G}a_{1,\kappa}^{(m)}\sin(\kappa\omega_0\tau_0) - \kappa\omega_0 a_{2,\kappa}^{(m)} - 2b_1\bar{G}b_{1,\kappa}^{(m)}\cos(\kappa\omega_0\tau_0) - \beta_{2,\kappa}^{(m)} = 0, \tag{5.1.46}$$

which can then be solved for $a_{1,\kappa}^{(m)}$, $a_{2,\kappa}^{(m)}$, $b_{1,\kappa}^{(m)}$ and $b_{2,\kappa}^{(m)}$, with any inhomogeneity, when $\kappa > 1$ (Brandt et al. 2006). The solution of (5.1.43) - (5.1.46) (for $\kappa > 1$) is

$$
\begin{aligned}
a_{1,\kappa}^{(m)} = \frac{1}{D}\{&-a_1a_3b_2\alpha_{2,\kappa}^{(m)}\cos(\kappa k\tau_0\omega_0) + a_1a_3b_2\beta_{2,\kappa}^{(m)}\sin(\kappa k\tau_0\omega_0)\\
&- 2a_2a_3b_1\bar{G}^2\alpha_{2,\kappa}^{(m)}\cos(\kappa(k-1)\tau_0\omega_0) + 2a_2a_3b_1\bar{G}^2\beta_{2,\kappa}^{(m)}\sin(\kappa(k-1)\tau_0\omega_0)\\
&+ \kappa\omega_0(a_3b_2\alpha_{2,\kappa}^{(m)}\sin(\kappa k\tau_0\omega_0) - 2a_3b_1\bar{G}\alpha_{1,\kappa}^{(m)}\sin(\kappa(k+1)\tau_0\omega_0)\\
&+ 2a_3b_1\bar{G}\beta_{1,\kappa}^{(m)}\cos(\kappa(k+1)\tau_0\omega_0) + a_3\beta_{2,\kappa}^{(m)}(a_2\bar{I} + a_1 + b_2)\cos(\kappa k\tau_0\omega_0)\\
&- 2a_2b_1\bar{G}^2\alpha_{1,\kappa}^{(m)}\sin(\kappa\tau_0\omega_0) + 2a_2b_1\bar{G}^2\beta_{1,\kappa}^{(m)}\cos(\kappa\tau_0\omega_0)\\
&+ a_2\bar{G}\beta_{2,\kappa}^{(m)}(a_2\bar{I} + a_1 + b_2) + a_1a_3\alpha_{2,\kappa}^{(m)}\sin(\kappa k\tau_0\omega_0) + \kappa\omega_0(a_1\alpha_{1,\kappa}^{(m)}\\
&+ a_3\alpha_{2,\kappa}^{(m)}\cos(\kappa k\tau_0\omega_0) - a_3\beta_{2,\kappa}^{(m)}\sin(\kappa k\tau_0\omega_0) + a_2\bar{G}\alpha_{2,\kappa}^{(m)} + a_2\bar{I}\alpha_{1,\kappa}^{(m)} - \kappa\omega_0\beta_{1,\kappa}^{(m)})\\
&+ a_2a_3\bar{I}\alpha_{2,\kappa}^{(m)}\sin(\kappa k\tau_0\omega_0) - b_2^2\beta_{1,\kappa}^{(m)}) + b_2(a_2\bar{I} + a_1)(b_2\alpha_{1,\kappa}^{(m)} - a_2\bar{G}\alpha_{2,\kappa}^{(m)})\\
&+ 2a_3b_1\bar{G}\cos(\kappa(k+1)\tau_0\omega_0)(b_2\alpha_{1,\kappa}^{(m)} - a_2\bar{G}\alpha_{2,\kappa}^{(m)})\\
&+ 2a_3b_1\bar{G}\sin(\kappa(k+1)\tau_0\omega_0)(b_2\beta_{1,\kappa}^{(m)} - a_2\bar{G}\beta_{2,\kappa}^{(m)}) - a_2a_3b_2\bar{I}\alpha_{2,\kappa}^{(m)}\cos(\kappa k\tau_0\omega_0)\\
&+ a_2a_3b_2\bar{I}\beta_{2,\kappa}^{(m)}\sin(\kappa k\tau_0\omega_0) - 2a_2^2b_1\bar{G}^3\beta_{2,\kappa}^{(m)}\sin(\kappa\tau_0\omega_0) - 2a_3^2b_1\bar{G}\beta_{2,\kappa}^{(m)}\sin(\kappa\tau_0\omega_0)\\
&- 2b_1\bar{G}\cos(\kappa\tau_0\omega_0)(a_3^2\alpha_{2,\kappa}^{(m)} + a_2\bar{G}(a_2\bar{G}\alpha_{2,\kappa}^{(m)} - b_2\alpha_{1,\kappa}^{(m)}))\\
&+ 2a_2b_1b_2\bar{G}^2\beta_{1,\kappa}^{(m)}\sin(\kappa\tau_0\omega_0)\},
\end{aligned}
$$

$$
\begin{aligned}
b_{1,\kappa}^{(m)} = \frac{1}{D}\{&a_1a_3b_2\alpha_{2,\kappa}^{m}\sin(\kappa k\tau_0\omega_0) + a_1a_3b_2\beta_{2,\kappa}^{m}\cos(\kappa k\tau_0\omega_0)\\
&+ 2a_2a_3b_1\bar{G}^2\alpha_{2,\kappa}^{m}\sin(\kappa(k-1)\tau_0\omega_0) + 2a_2a_3b_1\bar{G}^2\beta_{2,\kappa}^{m}\cos(\kappa(k-1)\tau_0\omega_0)\\
&- \kappa\omega_0(a_3b_2\beta_{2,\kappa}^{m}\sin(\kappa k\tau_0\omega_0) - 2a_3b_1\bar{G}\alpha_{1,\kappa}^{m}\cos(\kappa(k+1)\tau_0\omega_0)\\
&- 2a_3b_1\bar{G}\beta_{1,\kappa}^{m}\sin(\kappa(k+1)\tau_0\omega_0) - a_3\alpha_{2,\kappa}^{m}(a_2\bar{I} + a_1 + b_2)\cos(\kappa k\tau_0\omega_0)\\
&- 2a_2b_1\bar{G}^2\alpha_{1,\kappa}^{m}\cos(\kappa\tau_0\omega_0) - 2a_2b_1\bar{G}^2\beta_{1,\kappa}^{m}\sin(\kappa\tau_0\omega_0) - a_2\bar{G}\alpha_{2,\kappa}^{m}(a_2\bar{I} + a_1 + b_2)\\
&+ a_1a_3\beta_{2,\kappa}^{m}\sin(\kappa k\tau_0\omega_0) + \kappa\omega_0(a_1\beta_{1,\kappa}^{m} + \kappa\omega_0\alpha_{1,\kappa}^{m} + a_3\alpha_{2,\kappa}^{m}\sin(\kappa k\tau_0\omega_0)\\
&+ a_3\beta_{2,\kappa}^{m}\cos(\kappa k\tau_0\omega_0) + a_2\bar{G}\beta_{2,\kappa}^{m} + a_2\bar{I}\beta_{1,\kappa}^{m}) + a_2a_3\bar{I}\beta_{2,\kappa}^{m}\sin(\kappa k\tau_0\omega_0) + b_2^2\alpha_{1,\kappa}^{m})\\
&+ 2a_3b_1\bar{G}\sin(\kappa(k+1)\tau_0\omega_0)(b_2\alpha_{1,\kappa}^{m} - a_2\bar{G}\alpha_{2,\kappa}^{m}) + 2a_2b_1b_2\bar{G}^2\alpha_{1,\kappa}^{m}\sin(\kappa\tau_0\omega_0)\\
&+ 2a_3b_1\bar{G}\cos(\kappa(k+1)\tau_0\omega_0)(a_2\bar{G}\beta_{2,\kappa}^{m} - b_2\beta_{1,\kappa}^{m}) + a_2a_3b_2\bar{I}\alpha_{2,\kappa}^{m}\sin(\kappa k\tau_0\omega_0)\\
&+ a_2a_3b_2\bar{I}\beta_{2,\kappa}^{m}\cos(\kappa k\tau_0\omega_0) - 2a_2^2b_1\bar{G}^3\alpha_{2,\kappa}^{m}\sin(\kappa\tau_0\omega_0)\\
&- 2a_3^2b_1\bar{G}\alpha_{2,\kappa}^{m}\sin(\kappa\tau_0\omega_0) + 2b_1\bar{G}\cos(\kappa\tau_0\omega_0)(a_3^2\beta_{2,\kappa}^{m} + a_2\bar{G}(a_2\bar{G}\beta_{2,\kappa}^{m} - b_2\beta_{1,\kappa}^{m}))\\
&+ b_2(a_2\bar{I} + a_1)(a_2\bar{G}\beta_{2,\kappa}^{m} - b_2\beta_{1,\kappa}^{m})\},
\end{aligned}
$$

$$
\begin{aligned}
a_{2,\kappa}^{(m)} = \frac{1}{D}\{&2b_1\bar{G}(-a_1b_2\beta_{1,\kappa}^m\sin(\kappa\tau_0\omega_0) + 2a_3b_1\bar{G}\alpha_{1,\kappa}^m\cos(\kappa k\tau_0\omega_0)\\
&+ 2a_3b_1\bar{G}\beta_{1,\kappa}^m\sin(\kappa k\tau_0\omega_0) + (a_2\bar{I}+a_1)\cos(\kappa\tau_0\omega_0)(a_2\bar{G}\alpha_{2,\kappa}^m + b_2\alpha_{1,\kappa}^m)\\
&- a_2b_2\bar{I}\beta_{1,\kappa}^m\sin(\kappa\tau_0\omega_0) + a_3(a_2\bar{I}+a_1)\alpha_{2,\kappa}^m\cos(\kappa(k+1)\tau_0\omega_0)\\
&+ a_3(a_2\bar{I}+a_1)\beta_{2,\kappa}^m\sin(\kappa(k+1)\tau_0\omega_0) + a_1a_2\bar{G}\beta_{2,\kappa}^m\sin(\kappa\tau_0\omega_0)\\
&+ a_2^2\bar{G}\bar{I}\beta_{2,\kappa}^m\sin(\kappa\tau_0\omega_0)) - \kappa\omega_0(2b_1\bar{G}(\sin(\kappa\tau_0\omega_0)(\alpha_{1,\kappa}^m(a_2\bar{I}+a_1+b_2)\\
&+ a_2\bar{G}\alpha_{2,\kappa}^m) + \cos(\kappa\tau_0\omega_0)(\beta_{1,\kappa}^m(a_2\bar{I}+a_1+b_2) - a_2\bar{G}\beta_{2,\kappa}^m)\\
&+ a_3\alpha_{2,\kappa}^m\sin(\kappa(k+1)\tau_0\omega_0) - a_3\beta_{2,\kappa}^m\cos(\kappa(k+1)\tau_0\omega_0)) + (a_2\bar{I}+a_1)^2\beta_{2,\kappa}^m\\
&+ \kappa\omega_0(-b_2\alpha_{2,\kappa}^m + \kappa\omega_0\beta_{2,\kappa}^m + 2b_1\bar{G}\alpha_{1,\kappa}^m\cos(\kappa\tau_0\omega_0) - 2b_1\bar{G}\beta_{1,\kappa}^m\sin(\kappa\tau_0\omega_0)))\\
&+ 4a_2b_1^2\bar{G}^3\alpha_{1,\kappa}^m + b_2(a_2\bar{I}+a_1)^2\alpha_{2,\kappa}^m\},
\end{aligned}
$$

$$
\begin{aligned}
b_{2,\kappa}^{(m)} = \frac{1}{D}\{&2b_1\bar{G}(a_1b_2\alpha_{1,\kappa}^m\sin(\kappa\tau_0\omega_0) - 2a_3b_1\bar{G}\alpha_{1,\kappa}^m\sin(\kappa k\tau_0\omega_0)\\
&+ (a_2\bar{I}+a_1)\cos(\kappa\tau_0\omega_0)(a_2\bar{G}\beta_{2,\kappa}^m + b_2\beta_{1,\kappa}^m) + a_2b_2\bar{I}\alpha_{1,\kappa}^m\sin(\kappa\tau_0\omega_0)\\
&- a_3(a_2\bar{I}+a_1)\alpha_{2,\kappa}^m\sin(\kappa(k+1)\tau_0\omega_0) + a_3(a_2\bar{I}+a_1)\beta_{2,\kappa}^m\cos(\kappa(k+1)\tau_0\omega_0)\\
&- a_1a_2\bar{G}\alpha_{2,\kappa}^m\sin(\kappa\tau_0\omega_0) - a_2^2\bar{G}\bar{I}\alpha_{2,\kappa}^m\sin(\kappa\tau_0\omega_0) + 2a_3b_1\bar{G}\beta_{1,\kappa}^m\cos(\kappa k\tau_0\omega_0))\\
&+ \kappa\omega_0(-2b_1\bar{G}(-\cos(\kappa\tau_0\omega_0)(\alpha_{1,\kappa}^m(a_2\bar{I}+a_1+b_2) - a_2\bar{G}\alpha_{2,\kappa}^m)\\
&+ \sin(\kappa\tau_0\omega_0)(\beta_{1,\kappa}^m(a_2\bar{I}+a_1+b_2) + a_2\bar{G}\beta_{2,\kappa}^m) + a_3\alpha_{2,\kappa}^m\cos(\kappa(k+1)\tau_0\omega_0)\\
&+ a_3\beta_{2,\kappa}^m\sin(\kappa(k+1)\tau_0\omega_0)) + (a_2\bar{I}+a_1)^2\alpha_{2,\kappa}^m + \kappa\omega_0(\kappa\omega_0\alpha_{2,\kappa}^m + b_2\beta_{2,\kappa}^m\\
&- 2b_1\bar{G}(\alpha_{1,\kappa}^m\sin(\kappa\tau_0\omega_0) + \beta_{1,\kappa}^m\cos(\kappa\tau_0\omega_0)))) + 4a_2b_1^2\bar{G}^3\beta_{1,\kappa}^m\\
&+ b_2(a_2\bar{I}+a_1)^2\beta_{2,\kappa}^m\},
\end{aligned}
\tag{5.1.47}
$$

where

$$
\begin{aligned}
D = &\kappa\omega_0(-4b_1\bar{G}(a_2\bar{I}+a_1+b_2)(a_3\sin(\kappa(k+1)\tau_0\omega_0) + a_2\bar{G}\sin(\kappa\tau_0\omega_0))\\
&+ \kappa\omega_0(-4b_1\bar{G}(a_3\cos(\kappa(k+1)\tau_0\omega_0) + a_2\bar{G}\cos(\kappa\tau_0\omega_0)) + (a_2\bar{I}+a_1)^2 + b_2^2)\\
&+ \kappa^3\omega_0^3) + 4b_1\bar{G}(a_2\bar{G}(2a_3b_1\bar{G}\cos(\kappa k\tau_0\omega_0) + b_2(a_2\bar{I}+a_1)\cos(\kappa\tau_0\omega_0))\\
&+ a_3b_2(a_2\bar{I}+a_1)\cos(\kappa(k+1)\tau_0\omega_0)) + 4b_1^2\bar{G}^2(a_2^2\bar{G}^2 + a_3^2) + b_2^2(a_2\bar{I}+a_1)^2.
\end{aligned}
$$

Note that when $\kappa = 1$, $D = 0$, and therefore we must re-examine (5.1.43) - (5.1.46) for $\kappa = 1$. By taking (ω_0 (5.1.43) + ($a_2\bar{G} + a_3\cos k\tau_0\omega_0$) (5.1.46)) − ($b_2$ (5.1.44) − ($a_3\sin k\tau_0\omega_0$) (5.1.45)) we obtain (5.1.35). Similarly, by taking (b_2 (5.1.43) −

$(a_2\bar{G} + a_3 \cos k\tau_0\omega_0)$ (5.1.45)) + (ω_0 (5.1.44) + $(a_3 \sin k\tau_0\omega_0)$ (5.1.46)) we obtain (5.1.36).

5.2 Parameter analysis

The closed form expressions for the limit cycles presented in Sections 5.1.1 and 5.1.2 allow for the effect of changes in each of the model parameters on the amplitude and period to be more easily studied. This section is split into two parts. Firstly, the effect of changes in a_2 (insulin resistance), b_1 (insulin secretion) and b_2 (insulin degradation) on the important characteristics of the waveforms for the constant hepatic production model solutions are explored. Secondly, we investigate how the amplitude and period of model (5.1.20) vary with respect to the commensurate delay parameter k.

5.2.1 Constant hepatic glucose production

In this section, the closed form expressions for the amplitude and period of model (5.1.1), as given by (5.1.17), (5.1.18) and (5.1.19), will be analysed using two different Parameter Sets, which are given in Table 5.1. The values used in Parameter Set 1 are based off the values used in Sturis et al. (1991), Li et al. (2006), and Huard et al. (2015), and represent a patient under a constant glucose infusion. Parameter Set 2 looks to replicate the values that may be observed in a patient under a larger constant glucose infusion.

On the quantification of insulin sensitivity

To begin, we analysed the relationship between the insulin sensitivity parameter, a_2, and the closed form expressions for the amplitude and period of model (5.1.1). It can be seen from Fig. 5.1 that the amplitude of $X(t)$, as given by (5.1.17), varies between 4 and 15 for Parameter Set 1, and 1 and 38 mg/dl for Parameter Set 2. Additionally, the amplitude of $Y(t)$ from (5.1.18) is observed to be approximately between either 1 and 5, or 1 and 29 mU/l. These values are within a physiologically acceptable range. Furthermore, in Figure 5.2 we note that the values of the period,

	Parameter Set 1	Parameter Set 2	Units
a_0	1300	1800	mg min^{-1}
a_1	2.02982×10^{-4}	2.02982×10^{-4}	min^{-1}
b_1	6.01344×10^{-8}	9.01344×10^{-8}	mU mg^{-2} min^{-1}
b_2	0.06	0.064	min^{-1}
τ	20	20	min

Table 5.1: Parameter Sets 1 and 2 which are used in numerical simulations throughout Section 5.2.1.

as defined by (5.1.19), vary between 74.5 and 76 minutes for Parameter Set 1, and 76 and 78 minutes for Parameter Set 2, and hence are also within an acceptable range.

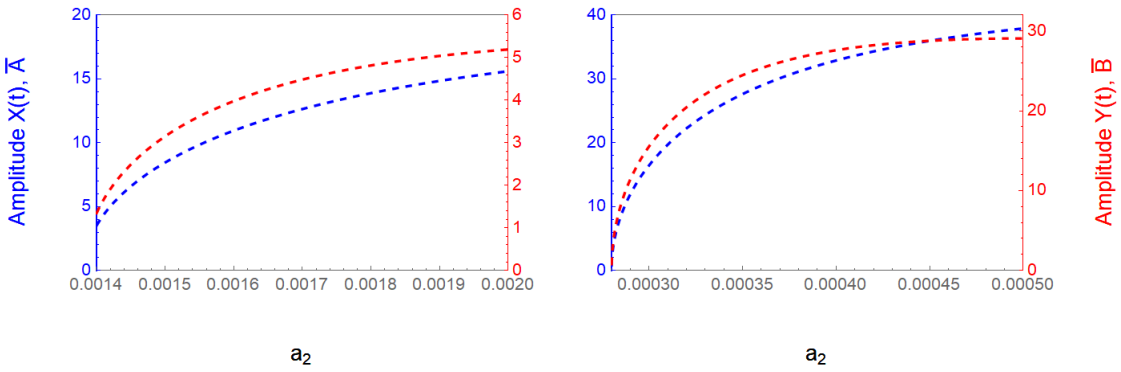

Figure 5.1: Amplitudes of the oscillations, $\bar{A}$ and $\bar{B}$, as a function of a_2 using Parameter Set 1 (left) and Parameter Set 2 (right).

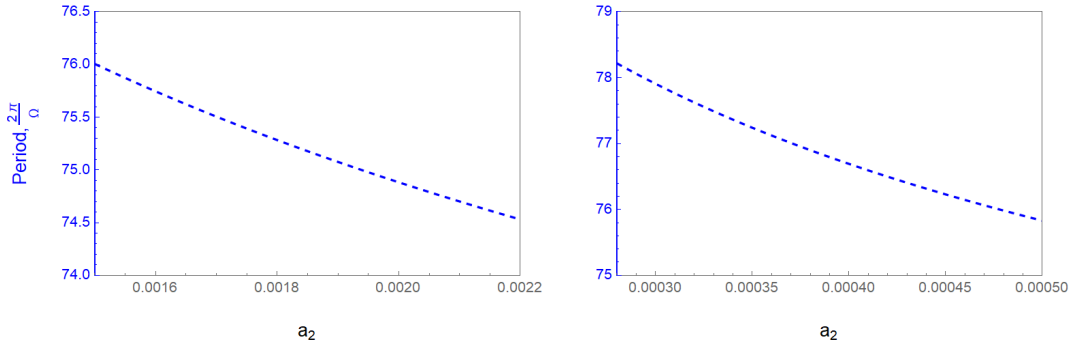

Figure 5.2: Period of the oscillations, as given by (5.1.19), as a function of a_2 using Parameter Set 1 (left) and Parameter Set 2 (right).

It can be seen in Fig. 5.3 that increasing a_2 has little consequence on the oscillations, while decreasing a_2 has a more profound effect. For example, for Parameter Set 1 a 20% increase in a_2 from 0.0017 increases the amplitude by 15%. However, a 20% decrease in a_2 reduces the amplitude by almost 80%. Similarly for Parameter Set 2, a 20% increase in a_2 from 0.0004 increases the amplitude by less than 5% while a 20% decrease in a_2 reduces the amplitude by approximately 30%. It is noted that a_2 has a much deeper influence on the amplitude of the oscillations compared to the period.

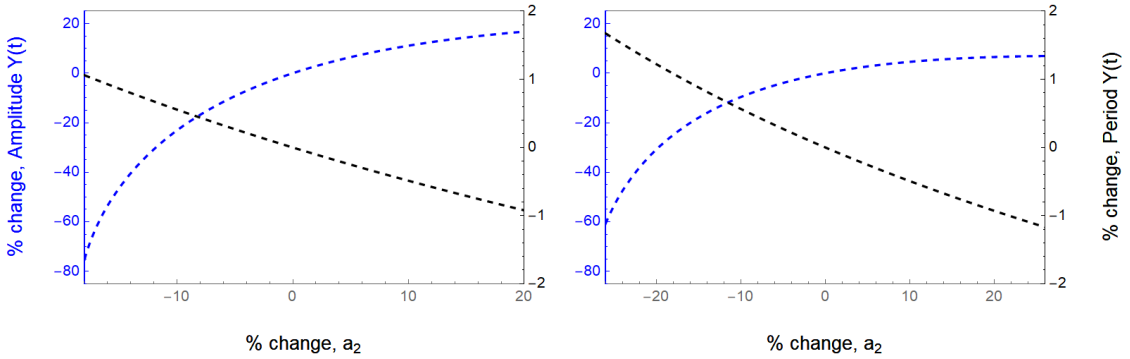

Figure 5.3: Percentage change of the closed form expressions of the amplitude (blue) and period (black) of $Y(t)$, which are given by (5.1.18) and (5.1.19) respectively, vs. the percentage change in a_2 for Parameter Set 1 (left) and Parameter Set 2 (right). The initial value used for a_2 was: 0.0017 (left); and 0.0004 (right).

Insulin secretion capacity b_1 and insulin degradation b_2 vs. amplitude of $X(t)$ and $Y(t)$

Next, we look at the relationship between the insulin secretion capacity, b_1, and the closed form expression of the amplitude of $X(t)$ defined by (5.1.17). As shown in Fig. 5.4, the amplitude variation with respect to b_1 is between 0 and 19 for Parameter Set 1, regardless of the value of a_2 used. However, a_2 does have an effect on the decline of amplitude observed with an increased b_1. Indeed, as a_2 increases, the observed value of b_1 such that the amplitude begins to decrease, decreases. This effect is also observed with Parameter Set 2.

Fig. 5.5 shows the effect of b_2 on the amplitude of $X(t)$ and $Y(t)$, respectively, for Parameter Set 1. It is observed from both that the oscillations are lost when b_2 drops below ≈ 0.059 regardless of the value of a_2. Indeed when looking at the amplitude as a function of b_2, a_2 has very little effect of $\bar{A}$ and only a small effect on $\bar{B}$ for Parameter Set 1. However, as seen in Fig. 5.6, this is not true for Parameter Set 2, where a_2 has a more profound effect on both the amplitude of $X(t)$ and $Y(t)$. Irrespective of this, it is observed for both Parameter Sets that an increase in b_2 leads to an increase in the amplitude of the oscillations. This was also observed by Li et al. (2006, Fig. 12). While the size of the oscillations of $Y(t)$ in Fig. 5.5 and Fig. 5.6 are plausible for all values of b_2, the size of the oscillations of $X(t)$ become too large with b_2. Indeed, eventually the value of $\bar{G} - \bar{A}$ drops below 70 mg/dl in both cases. Physiologically, this would mean the onset of hypoglycaemia. The ranges $0.06 < b_2 < 0.062$ for Parameter Set 1, and $0.064 < b_2 < 0.075$ for Parameter Set 2 ensure that glucose levels are kept within a realistic physiological range.

5.2.2 Non-constant hepatic glucose production

We now move on to investigate the effect of the two delays on the closed form expressions for the amplitude and period of model (5.1.20). In particular, we focus on the relationship between the amplitudes of $X(t)$ and $Y(t)$, given by (5.1.39) and (5.1.32) respectively, and the commensurate delay parameter k. Using Parameter Set 1 with $a_2 = 0.0017$, it can be seen in Fig. 5.7 that when a_3 is small, k has

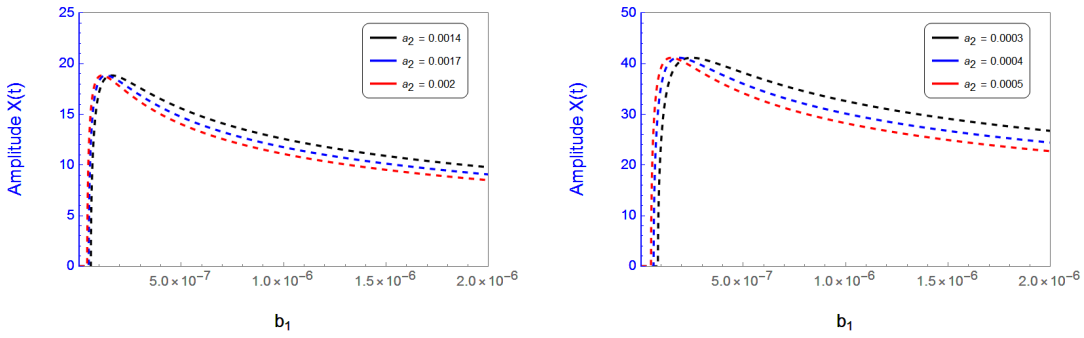

Figure 5.4: Amplitude of $X(t)$, as given by (5.1.17), vs. b_1 for Parameter Set 1 (left) and Parameter Set 2 (right).

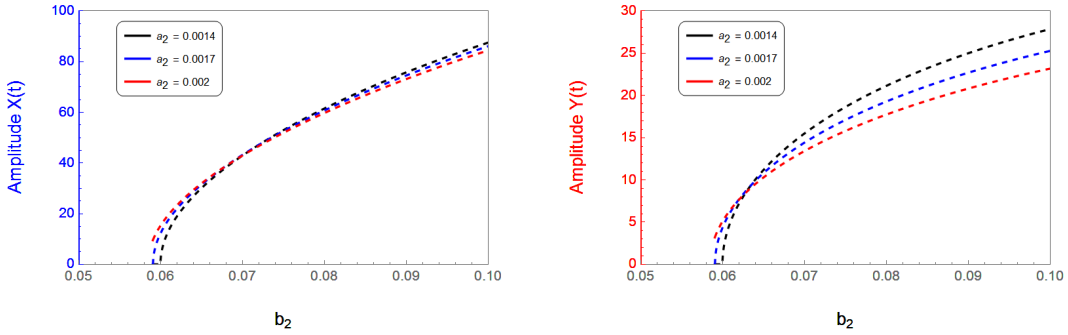

Figure 5.5: Amplitude of $X(t)$ (left) and $Y(t)$ (right), as given by (5.1.17) and (5.1.18) respectively, vs. b_2 for Parameter Set 1.

a negligible effect on the amplitude. Additionally, when $a_3 < O(10^{-2})$ changes in a_3 also have a negligible effect on the amplitudes. However, when $a_3 = 0.1$ it is observed that the amplitude of both $X(t)$ and $Y(t)$ vary with k in an oscillatory manner.

To further investigate how the closed form expressions for the amplitude and period vary with k, we now look into the variation using the parameter values given in Table. 5.2. From Fig. 5.8 we can see that k has a large influence on both the amplitude and period for Parameter Set 3. Indeed, increasing k from 1 to 7 leads to the amplitude increasing by $\approx 700\%$ and the period by $\approx 500\%$. However, it must be noted that for $k > 1$ the values of the amplitude and period are not in a physiological range. This is most likely due to the size of ϵ^2. Indeed, when $k = 7$ we note that $\epsilon^2 = 9.49476$ compared with 0.2806 when $k = 1$. Therefore, instead

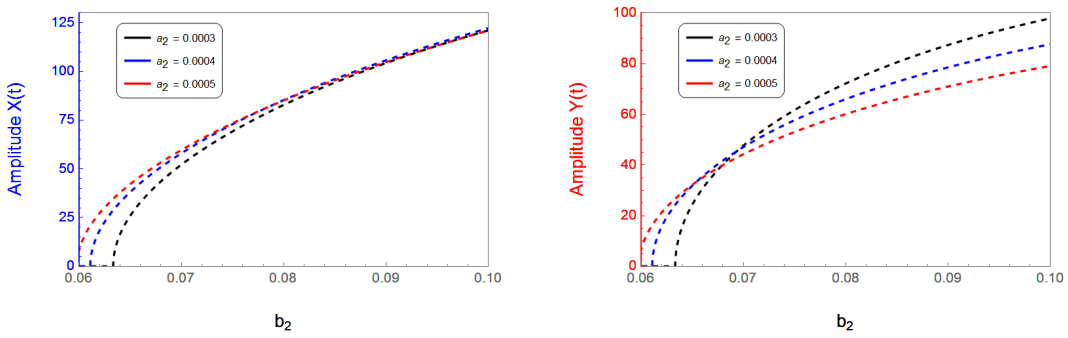

Figure 5.6: Amplitude of $X(t)$ (left) and $Y(t)$ (right), as given by (5.1.17) and (5.1.18) respectively, vs. b_2 for Parameter Set 2.

	Value	Units
a_0	285	mg min^{-1}
a_1	2.02982×10^{-4}	min^{-1}
a_2	0.00009	mU^{-1} min^{-1}
a_3	1.415	mg mU^{-1} min^{-1}
b_1	9.3×10^{-8}	mU mg^{-2} min^{-1}
b_2	0.06	min^{-1}
τ	16	min

Table 5.2: Parameter Set 3.

of setting $\tau = 16$ we shall instead we shall instead fix $\epsilon^2 = 0.16$ and compute the resulting value of $\tau = \tau_0 + \epsilon^2$, thus ensuring the perturbed solution remains close to the threshold curve. The results can be seen in Fig. 5.9. Here we observe that the amplitude remains in a physiological range for $1 \leq k \leq 7$, and that the period of the oscillations is within an acceptable physiological range for insulin levels. We also note that there is very little variation in the amplitude when k increases. This implies more accurate values of the two delays can be chosen without losing the physiological accuracy of the oscillations.

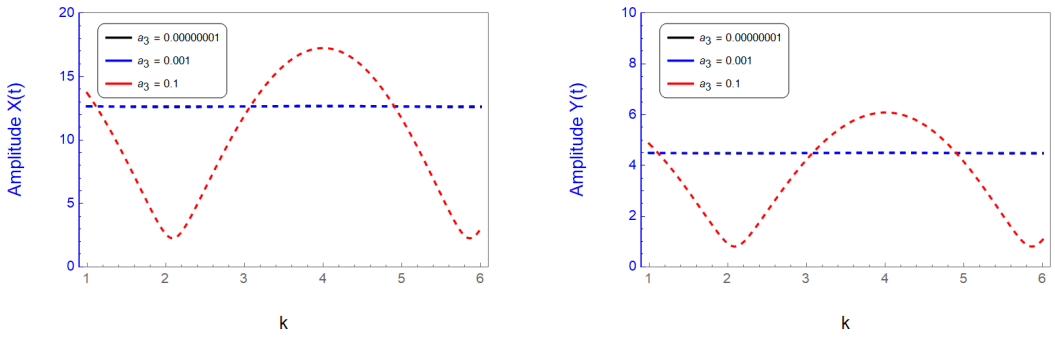

Figure 5.7: Amplitude of $X(t)$ (left) and $Y(t)$ (right), as defined by (5.1.39) and (5.1.32) respectively, as a function of k for Parameter Set 1 with $a_2 = 0.0017$.

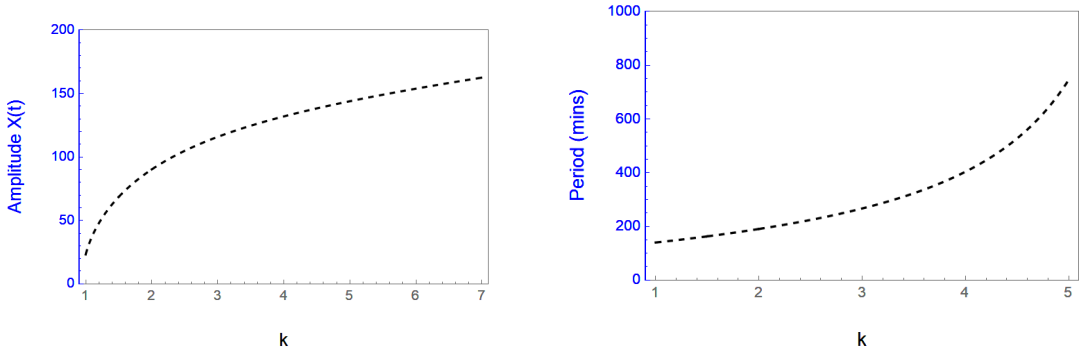

Figure 5.8: Amplitude of $X(t)$ (left) and $Y(t)$ (right), as defined by (5.1.39) and (5.1.32) respectively, vs. k for Parameter Set 3.

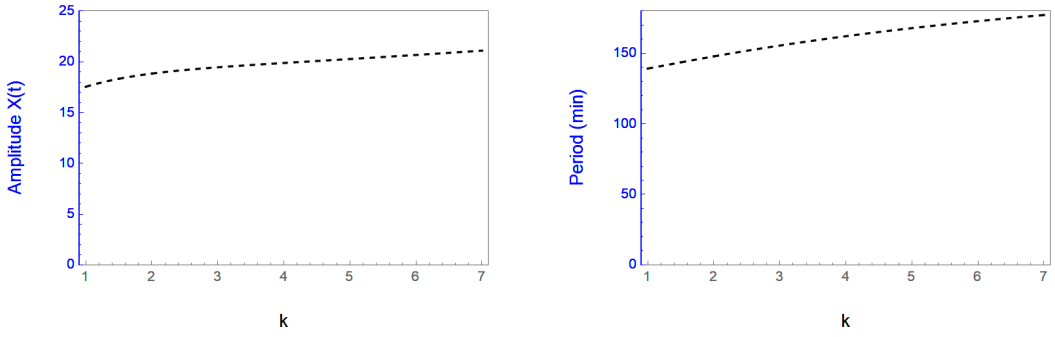

Figure 5.9: Amplitude of $X(t)$ (left) and $Y(t)$ (right), as given by (5.1.39) and (5.1.32) respectively, vs. k for fixed ϵ. All other parameters are as defined in Table (5.2).

Chapter 6

Discussion and Conclusions

The theoretical and numerical results obtained in Sections 3.1.2, 4.2 and Chapter 5 have highlighted the effect of diabetic deficiencies on the cyclic regulation of glucose and insulin in the ultradian regime. The regulatory negative feedback loop, which is modelled by taking into account production times for pancreatic insulin and hepatic glucose, provides an important mechanism for investigating this regulation. On one hand, model (3.1.1) predicts a dampening of the oscillations in the case of a reduced capacity to utilise insulin to degrade glucose. This behaviour was observed in clinical trials involving constant glucose infusions in type-2 diabetic patients (O'Meara et al. 1993). Note that a similar effect of insulin resistance was also noted on the production of fast oscillations (Lang et al. 1981) (see also e.g. Nepton (2013) for a general review of the effect of diabetes on β-cell activity). On the other hand, the usage of model (3.1.1) has permitted the recovery of healthy regulation through the original objectives: (i) the production an oscillatory regime while (ii) stabilising the average glucose levels within a physiologically acceptable range.

Here we highlighted the importance of considering variable insulin degradation rates as these have an important effect on the production of an oscillatory regime. By considering the insulin clearance term as a combination of both natural and external mechanisms for the degradation of insulin and combining its effect with other parameters such as insulin sensitivity, pancreatic secretion and hepatic glucose production, four strategies have been investigated in Section 4.2. We have shown that it is generally possible to individually alter these parameters, either positively or

negatively, to stabilise average glucose levels. These alterations take into account current therapeutical pathways, such as insulin infusions and drugs that inhibit hepatic glucose production such as Metformin, which typically only focus on reducing glucose levels. The effect of this manipulation on the generation of oscillations has been investigated. We then established regions in the space of diabetic parameters α and β where both objectives can be achieved. In several cases, it would be worth considering combinations of these strategies in order to deliver an optimal treatment which combines the benefits of having an oscillatory regime within an acceptable range. Splitting the insulin contribution into dynamically linked compartments accounting for plasma and remote insulin with individual transfer and degradation rates, as done by Wu et al. (2011), may as well lead to more precise recovery pathways. Such a study is currently under way.

However, at this stage, the qualitative contribution of the strategies described in Section 4.2 should be considered more important than specific numerical values. One reason for this is that insufficient exhaustive characterisations of the ultradian oscillatory regulation of diabetically-impaired systems are available. Additionally, it is known physiologically that both T1DM and T2DM are linked to many changes in the body, and not just variation in insulin secretion and insulin sensitivity, respectively. For example, in patients with T2DM it is observed that insulin resistance, insulin secretion and insulin degradation are altered at various stages of the disease (Kotronen et al. 2008, Pories & Dohm 2012). Hence, from a physiological point of view, the model parameters may depend on time and/or other model parameters, e.g. $\beta = \beta(t)$ and/or $\tau_1 = \tau_1(G(t))$, i.e. the delay in pancreatic insulin secretion may be state dependent. Nevertheless, the model appears to be sufficiently robust for qualitatively establishing the effect of diabetic parameters. For instance, adding a 5% white noise to the diabetic parameters does not incur very large variations in the period and amplitude of the oscillatory regime, as shown in Fig. 6.1. Two approaches could be employed in order to strengthen the current proposed pathways and provide a more quantitative framework. Firstly, appropriately designed clinical trials aiming at evaluating variations in oscillatory patterns in subjects at various diabetic states under glucose infusions would be of great value. Secondly, new mul-

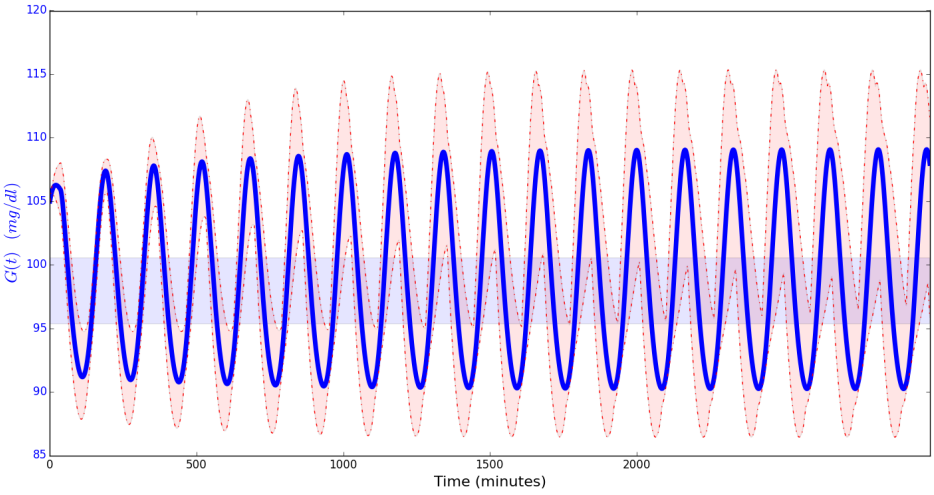

Figure 6.1: Ultradian oscillations with a 5% noise on α and β around $\alpha = \beta = 1$. The middle band represents the associated variability of $\bar{G}$. A similar effect can be observed on insulin patterns. Simulation performed with 500 repetitions.

tiscale simulations taking into account dynamics at the β-cell secretion level, as performed by De Gaetano et al. (2015) in the case of decreased insulin sensitivity, could lead to a further assessment of the current model against clinical observations. Indeed, model (3.1.1) could be adapted to incorporate these dynamics at the β-cell secretion level through the introduction of state-dependent delays, especially threshold delays. Such a model would allow for the maturation and release dynamics of insulin within the pancreas to be taken into account. The characterisation of periodic solutions in these systems is generally challenging, though theoretical results in this direction have been obtained by Smith & Kuang (1992), as well as by Gourley, Liu & Lou (2017) where a new approach was used to investigate the presence of periodic rhythms in insect larvae development.

In Chapter 5, a simplified polynomial version of model (3.1.1) is explored using a nonlinear analysis to investigate the effect of various diabetic parameters on the ultradian oscillations. The model is split into two sub-models, one with a constant hepatic glucose production (5.1.1) and one with a linear hepatic production containing a commensurate delay (5.1.20). Indeed, by performing a P-L perturbation method we have been able to obtain analytical expressions that are based on the

model parameters for the linearised amplitude and period of the two sub-models. From a Mathematical point of view, the accuracy of these expressions is of a high degree. Indeed, from Fig. 6.2 we can see that the closed form expression for the amplitude of $X(t)$ given by (5.1.17) is almost an exact match for the amplitude obtained through numerical simulations. Furthermore, Fig. 6.3 shows that the solutions for $G(t)$ and $I(t)$ of model (5.1.1) obtained using the P-L technique are a good approximation to the solutions calculated using a classical Runge-Kutta method. From a physiological perspective, it is important to note while the values of the amplitude of $X(t)$ in Figure 5.1 are within a physiologically acceptable range, the decrease in amplitude in the presence of mild insulin resistance is most notably seen experimentally in insulin levels, while the amplitude of the glucose oscillations has been observed to remain almost constant (O'Meara et al. 1993). Therefore, the expressions derived in Chapter 5 could theoretically be used to obtain estimates for insulin sensitivity through the matching of clinical insulin data to models (5.1.1) and (5.1.20). Additionally, we note that strategies aiming to restore glucose-insulin oscillations could make use of the fact the amplitude and frequency of the oscillations show very little variation in the vicinity of the Hopf threshold curve in the space of delays. These theoretical findings could therefore have an impact on optimal glycemic control.

Moreover, we have shown that taking into account an instantaneous glucose-dependent insulin production, through the introduction of an additional coefficient, enables us to characterise the existence of sinusoidal solutions by investigating roots of a cubic polynomial. This provides an additional means for investigating the curve of Hopf bifurcations, which separates asymptotically stable and oscillatory regimes in system (3.1.1), without relying on a transcendental equation. It is numerically evidenced to be part of a closed loop in the (τ_1, τ_2) domain.

Finally, in view of the recent efforts for the development of an artificial pancreas, the results in this thesis open the way for more in-depth analysis of the underlying mechanisms which are most responsible for generating the oscillations. The presence of periodic solutions in the (τ_1, τ_2) domain can be detected using Proposition 5 and these could be used for further investigation of the mechanisms involved in the

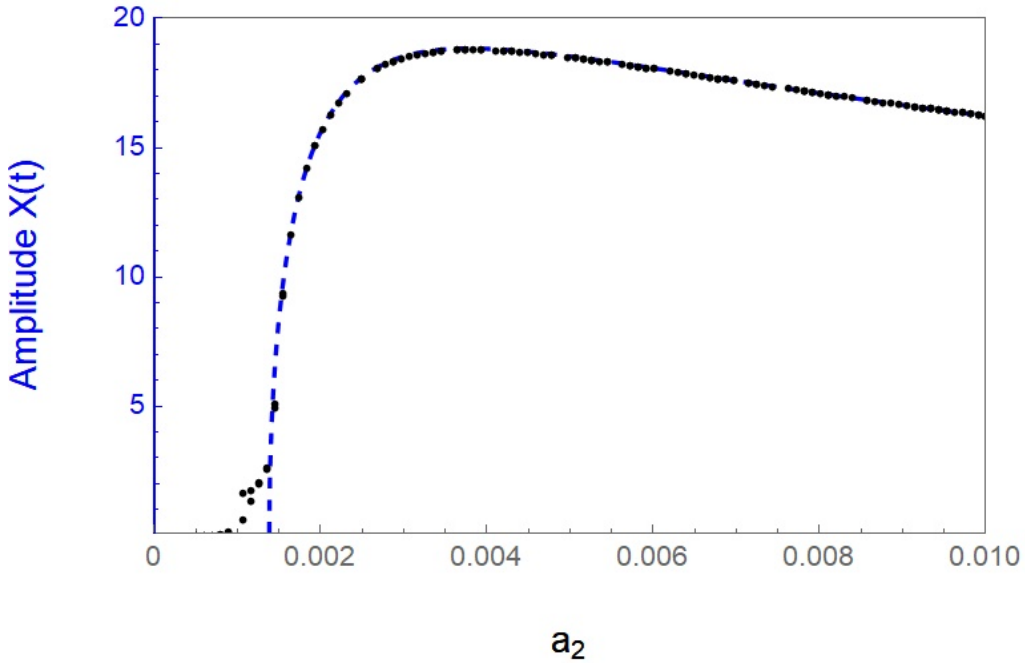

Figure 6.2: Comparison of two methods for calculating the amplitude of $X(t)$ from model (5.1.1) using Parameter Set 1. The blue line represents the P-L approximation given by (5.1.17) and the black dots represent the numerical approximations obtained using a Runge - Kutta method.

oscillatory regulation. In particular, combining strategies discussed in Section 4.2 may provide additional pathways for reintroducing a physiologically appropriate cyclic regulation and devise new regimes for personalised treatment.

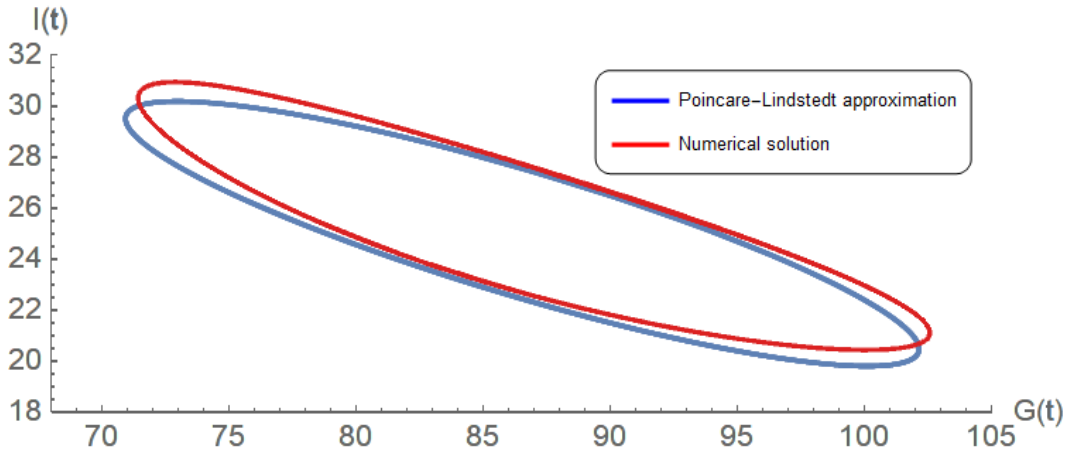

Figure 6.3: Comparison of the limit cycles corresponding to the P-L approximation, given by (5.1.17), (5.1.18) and (5.1.19), and the numerical solution of system (5.1.1). Parameter values are as defined in Parameter Set 1, with $a_2 = 0.002$.

Bibliography

Ahlqvist, E., Storm, P., Käräjämäki, A., Martinell, M., Dorkhan, M., Carlsson, A., Vikman, P., Prasad, R. B., Aly, D. M., Almgren, P. et al. (2018), 'Novel subgroups of adult-onset diabetes and their association with outcomes: a data-driven cluster analysis of six variables', *The Lancet Diabetes & Endocrinology* **6**(5), 361–369.

Ajmera, I., Swat, M., Laibe, C., Le Novere, N. & Chelliah, V. (2013), 'The impact of mathematical modeling on the understanding of diabetes and related complications', *CPT: Pharmacometrics & Systems Pharmacology* **2**(7), 1–14.

American Diabetes Association (2014), 'Diagnosis and classification of diabetes mellitus', *Diabetes care* **37**(Supplement 1), S81–S90.

American Diabetes Association (2015), 'American diabetes association - 75th anniversary timeline - diabetes complications reduced'. [Online; accessed 11-December-2015].
URL: `http://www.diabetes.org/about-us/75th-anniversary/timeline.html?referrer=https://www.google.co.uk/`

An, Q., Beretta, E., Kuang, Y., Wang, C. & Wang, H. (2019), 'Geometric stability switch criteria in delay differential equations with two delays and delay dependent parameters', *Journal of Differential Equations* **266**(11), 7073–7100.

Anderson, R. M. & May, R. M. (1992), *Infectious Diseases of Humans: Dynamics and Control*, Oxford university press.

Atkinson, M., Eisenbarth, G. & Michels, A. (2014), 'Type 1 diabetes', *The Lancet* **383**(9911), 69–82.

Barnes, D. J. & Chu, D. (2015), *Foundations of Modeling*, Springer London, London, pp. 1–14.

Bennett, D. L. & Gourley, S. A. (2004*a*), 'Asymptotic properties of a delay differential equation model for the interaction of glucose with plasma and interstitial insulin', *Applied Mathematics and Computation* **151**(1), 189–207.

Bennett, D. L. & Gourley, S. A. (2004*b*), 'Global stability in a model of the glucose-insulin interaction with time delay', *European Journal of Applied Mathematics* **15**(2), 203–221.

Beretta, E. & Kuang, Y. (2002), 'Geometric stability switch criteria in delay differential systems with delay dependent parameters', *SIAM Journal on Mathematical Analysis* **33**(5), 1144–1165.

Bergman, R. (2005), 'Minimal model: perspective from 2005', *Hormone Research in Paediatrics* **64**(Suppl. 3), 8–15.

Bergman, R., Ider, Y., Bowden, C. & Cobelli, C. (1979), 'Quantitative estimation of insulin sensitivity.', *American Journal of Physiology-Endocrinology And Metabolism* **236**(6), E667.

Bocharov, G. & Rihan, F. (2000), 'Numerical modelling in biosciences using delay differential equations', *Journal of Computational and Applied Mathematics* **125**(1), 183–199.

Bolie, V. (1961), 'Coefficients of normal blood glucose regulation', *Journal of Applied Physiology* **16**(5), 783–788.

Boutayeb, A. & Chetouani, A. (2006), 'A critical review of mathematical models and data used in diabetology', *Biomedical Engineering Online* **5**(1), 43.

Brandt, S., Pelster, A. & Wessel, R. (2006), 'Variational calculation of the limit cycle and its frequency in a two-neuron model with delay', *Physical Review E* **74**(3), 036201.

Cannon, W. (1932), *The Wisdom of the Body*, W.W. Norton & Company, inc.

Casal, A. & Freedman, M. (1980), 'A Poincaré-Lindstedt approach to bifurcation problems for differential-delay equations', *IEEE Transactions on Automatic Control* **25**(5), 967–973.

Centers for Disease Control and Prevention et al. (2011), 'National diabetes fact sheet: national estimates and general information on diabetes and prediabetes in the united states, 2011'.
URL: `http://www.diabetesincontrol.com/wp-content/uploads/PDF/ndep_diabetes_facts_2011.pdf`

Chen, C. L., Tsai, H. W. & Wong, S. (2010), 'Modeling the physiological glucose–insulin dynamic system on diabetics', *Journal of Theoretical Biology* **265**(3), 314–322.

Cobelli, C., Renard, E. & Kovatchev, B. (2011), 'Artificial pancreas: past, present, future', *Diabetes* **60**(11), 2672–2682.

Conte, R. & Musette, M. (2008), *The Painlevé Handbook*, Springer Netherlands.

Costes, S. & Butler, P. C. (2014), 'Insulin-degrading enzyme inhibition, a novel therapy for type 2 diabetes?', *Cell metabolism* **20**(2), 201–203.

De Gaetano, A. & Arino, O. (2000), 'Mathematical modelling of the intravenous glucose tolerance test', *Journal of Mathematical Biology* **40**(2), 136–168.

De Gaetano, A., Gaz, C., Palumbo, P. & Panunzi, S. (2015), 'A unifying organ model of pancreatic insulin secretion', *PloS One* **10**(11), e0142344.

Derouich, M. & Boutayeb, A. (2002), 'The effect of physical exercise on the dynamics of glucose and insulin', *Journal of Biomechanics* **35**(7), 912.

Diabetes UK (2017), 'Diabetes uk – professionals –position statements & reports – facts & figures – diabetes prevalence 2017 (november 2017)'. [Online; accessed 22-November-2018].
URL: `https://www.diabetes.org.uk/professionals/position-statements-reports/statistics/diabetes-prevalence-2017`

Diabetes UK (2018), 'Diabetes UK – preventing type 2 diabetes – prevention'. [Online; accessed 24-November-2018].
URL: `https://www.diabetes.org.uk/Preventing-Type-2-diabetes/Prevention`

Drozdov, A. & Khanina, H. (1995), 'A model for ultradian oscillations of insulin and glucose', *Mathematical and Computer Modelling* **22**(2), 23–38.

Duckworth, W. C., Bennett, R. G. & Hamel, F. G. (1998), 'Insulin degradation: progress and potential', *Endocrine Reviews* **19**(5), 608–624.

Engelborghs, K., Lemaire, V., Bélair, J. & Roose, D. (2001), 'Numerical bifurcation analysis of delay differential equations arising from physiological modeling', *Journal of Mathematical Biology* **42**, 361–385.

Farris, W., Mansourian, S., Chang, Y., Lindsley, L., Eckman, E. A., Frosch, M. P., Eckman, C. B., Tanzi, R. E., Selkoe, D. J. & Guénette, S. (2003), 'Insulin-degrading enzyme regulates the levels of insulin, amyloid β-protein, and the β-amyloid precursor protein intracellular domain in vivo', *Proceedings of the National Academy of Sciences* **100**(7), 4162–4167.

Fossion, R., Fossion, J. P. J., Rivera, A. L., Lecona, O. A., Toledo-Roy, J. C., García-Pelagio, K. P., García-Iglesias, L. & Estañol, B. (2018), Homeostasis from a time-series perspective: An intuitive interpretation of the variability of physiological variables, *in* 'Quantitative Models for Microscopic to Macroscopic Biological Macromolecules and Tissues', Springer, pp. 87–109.

Friedman, A. (2010), 'What is mathematical biology and how useful is it', *Notices of the AMS* **57**(7), 851–857.

Giannarelli, R., Aragona, M., Coppelli, A. & Del Prato, S. (2003), 'Reducing insulin resistance with metformin: the evidence today', *Diabetes & Metabolism* **29**(4), 6S28–6S35.

Goriely, A. & Hyde, C. (1998), 'Finite-time blow-up in dynamical systems', *Physics Letters A* **250**(4-6), 311–318.

Goriely, A. & Hyde, C. (2000), 'Necessary and sufficient conditions for finite time singularities in ordinary differential equations', *Journal of Differential equations* **161**(2), 422–448.

Gourley, S. A., Liu, R. & Lou, Y. (2017), 'Intra-specific competition and insect larval development: a model with time-dependent delay', *Proceedings of the Royal Society of Edinburgh Section A: Mathematics* **147**(2), 353–369.

Greenbaum, C. J. (2002), 'Insulin resistance in type 1 diabetes', *Diabetes/Metabolism Research and Reviews* **18**(3), 192–200.

Grodsky, G. M. (1972), 'A threshold distribution hypothesis for packet storage of insulin and its mathematical modeling', *The Journal of Clinical Investigation* **51**(8), 2047–2059.

Gu, K., Niculescu, S. I. & Chen, J. (2005), 'On stability crossing curves for general systems with two delays', *Journal of Mathematical Analysis and Applications* **311**(1), 231–253.

Hansen, K. (1923), 'Oscillations in the blood sugar in fasting normal persons', *Acta Med Scand Suppl* **4**, 27–58.

Hex, N., Bartlett, C., Wright, D., Taylor, M. & Varley, D. (2012), 'Estimating the current and future costs of type 1 and type 2 diabetes in the uk, including direct health costs and indirect societal and productivity costs', *Diabetic Medicine* **29**(7), 855–862.

Hogan, M. F., Meier, D. T., Zraika, S., Templin, A. T., Mellati, M., Hull, R. L., Leissring, M. A. & Kahn, S. E. (2016), 'Inhibition of insulin-degrading enzyme does not increase islet amyloid deposition in vitro', *Endocrinology* **157**(9), 3462–3468.

Hone, A. (2009), *Painlevé Tests, Singularity Structure and Integrability*, Springer Berlin Heidelberg, Berlin, Heidelberg, pp. 245–277.

Hoppensteadt, F. (1995), 'Getting started in mathematical biology', *Notices of the AMS* **42**(9), 969–975.

Huard, B., Bridgewater, A. & Angelova, M. (2017), 'Mathematical investigation of diabetically impaired ultradian oscillations in the glucose–insulin regulation', *Journal of Theoretical Biology* **418**, 66–76.

Huard, B., Easton, J. & Angelova, M. (2015), 'Investigation of stability in a two-delay model of ultradian oscillations in glucose-insulin regulation', *Communications in Nonlinear Science and Numerical Simulation* **26**(1-3), 211–222.

Hundal, R., Krssak, M., Dufour, S., Laurent, L., Lebon, V., Chandramouli, V., Inzucchi, S., Schumann, W., Petersen, K., Landau, B. & Shulman, G. (2000), 'Mechanism by which metformin reduces glucose production in type 2 diabetes', *Diabetes* **49**(12), 2063–2069.

Jaremko, J. & Rorstad, O. (1998), 'Advances toward the implantable artificial pancreas for treatment of diabetes', *Diabetes Care* **21**(3), 444–450.

Kissler, S. M., Cichowitz, C., Sankaranarayanan, S. & Bortz, D. M. (2014), 'Determination of personalized diabetes treatment plans using a two-delay model', *Journal of Theoretical Biology* **359**, 101–111.

Koschorreck, M. & Gilles, E. D. (2008), 'Mathematical modeling and analysis of insulin clearance in vivo', *BMC Systems Biology* **2**(1), 43.

Kotronen, A., Juurinen, L., Tiikkainen, M., Vehkavaara, S. & Yki-Järvinen, H. (2008), 'Increased liver fat, impaired insulin clearance, and hepatic and adipose tissue insulin resistance in type 2 diabetes', *Gastroenterology* **135**(1), 122–130.

Kraft, J. R. et al. (1975), 'Detection of diabetes mellitus in situ (occult diabetes)', *Laboratory Medicine* **6**(2), 10–22.

Lang, D. A., Matthews, D. R., Burnett, M. & Turner, R. C. (1981), 'Brief, irregular oscillations of basal plasma insulin and glucose concentrations in diabetic man', *Diabetes* **30**(5), 435–439.

Lang, S. (2013), *Complex Analysis*, Vol. 103, Springer Science & Business Media.

Li, J. & Kuang, Y. (2007), 'Analysis of a model of the glucose-insulin regulatory system with two delays', *SIAM Journal on Applied Mathematics* **63**(3), 757–776.

Li, J., Kuang, Y. & Li, B. (2001), 'Analysis of IVGTT glucose-insulin interaction models with time delay', *Discrete and Continuous Dynamical Systems Series B* **1**(1), 103–124.

Li, J., Kuang, Y. & Mason, C. (2006), 'Modeling the glucose-insulin regulatory system and ultradian insulin secretory oscillations with two explicit time delays', *Journal of Theoretical Biology* **242**(3), 722–735.

Li, J., Wang, M., De Gaetano, A., Palumbo, P. & Panunzi, S. (2012), 'The range of time delay and the global stability of the equilibrium for an IVGTT model', *Mathematical Biosciences* **235**(2), 128–137.

Lightman, S. L., Wiles, C. C., Atkinson, H. C., Henley, D. E., Russell, G. M., Leendertz, J. A., McKenna, M. A., Spiga, F., Wood, S. A. & Conway-Campbell, B. L. (2008), 'The significance of glucocorticoid pulsatility', *European Journal of Pharmacology* **583**(2-3), 255–262.

Lytton, W. W. (2008), 'Computer modelling of epilepsy', *Nature Reviews Neuroscience* **9**(8), 626.

Maianti, J. P., McFedries, A., Foda, Z. H., Kleiner, R. E., Du, X. Q., Leissring, M. A., Tang, W. J., Charron, M. J., Seeliger, M. A., Saghatelian, A. & Liu, D. R. (2014), 'Anti-diabetic activity of insulin-degrading enzyme inhibitors mediated by multiple hormones', *Nature* **511**(7507), 94–98.

Makroglou, A., Li, J. & Kuang, Y. (2006), 'Mathematical models and software tools for the glucose-insulin regulatory system and diabetes: an overview', *Applied Numerical Mathematics* **56**(3-4), 559–573.

Mathers, C. & Loncar, D. (2006), 'Projections of global mortality and burden of disease from 2002 to 2030', *PLoS Medicine* **3**(11), e442.

Mirsky, I. A. & Broh-Kahn, R. H. (1949), 'The inactivation of insulin by tissue extracts; the distribution and properties of insulin inactivating extracts.', *Archives of Biochemistry* **20**(1), 1.

National Institute for Clinical Excellence (2012), 'Type 2 diabetes: prevention in people at high risk', *NICE guideline (PH38)* .

Nepton, S. (2013), Beta-cell function and failure, *in* A. Escher & A. Li, eds, 'Type 1 Diabetes', InTech, pp. 115–126.

Nguimdo, R. M. (2018), 'Constructing hopf bifurcation lines for the stability of nonlinear systems with two time delays', *Physical Review E* **97**(3), 032211.

Nguyen, D. H. (2018), 'What if homeostasis fails?'. [Online; accessed 23-November-2018].
URL: `https://sciencing.com/homeostasis-fails-19395.html`

NHS (2014), 'NHS choices - health a-z - diabetes'. [Online; accessed 11-December-2015].
URL: `http://www.nhs.uk/Conditions/Diabetes/Pages/Diabetes.aspx`

O'Meara, N. M., Sturis, J., Van Cauter, E. & Polonsky, K. S. (1993), 'Lack of control by glucose of ultradian insulin secretory oscillations in impaired glucose tolerance and in non-insulin-dependent diabetes mellitus.', *Journal of Clinical Investigation* **92**(1), 262–271.

Palumbo, P., Ditlevsen, S., Bertuzzi, A. & De Gaetano, A. (2013), 'Mathematical modeling of the glucose–insulin system: a review', *Mathematical Biosciences* **244**(2), 69–81.

Panunzi, S., Palumbo, P. & De Gaetano, A. (2007), 'A discrete single delay model for the intra-venous glucose tolerance test', *Theoretical Biology and Medical Modelling* **4**(1), 35.

Peyser, T., Dassau, E., Breton, M. & Skyler, J. (2014), 'The artificial pancreas: current status and future prospects in the management of diabetes', *Annals of the New York Academy of Sciences* **1311**(1), 102–123.

Pories, W. & Dohm, G. (2012), 'Diabetes: have we got it all wrong? hyperinsulinism as the culprit: surgery provides the evidence', *Diabetes Care* **35**(12), 2438–2442.

Rankin, J., Walker, J. J., Windle, R., Lightman, S. L. & Terry, J. R. (2012), 'Characterizing dynamic interactions between ultradian glucocorticoid rhythmicity and acute stress using the phase response curve', *PloS one* **7**(2), e30978.

Reed, M. (2004), 'Why is mathematical biology so hard', *Notices of the AMS* **51**(3), 338–342.

Rizza, R. A., Mandarino, L. J. & Gerich, J. E. (1981), 'Dose-response characteristics for effects of insulin on production and utilization of glucose in man', *American Journal of Physiology-Endocrinology and Metabolism* **240**(6), E630–E639.

Roose, T., Chapman, S. J. & Maini, P. K. (2007), 'Mathematical models of avascular tumor growth', *SIAM review* **49**(2), 179–208.

Ruan, S. & Wei, J. (1999), 'Periodic solutions of planar systems with two delays', *Proceedings of the Royal Society of Edinburgh: Section A Mathematics* **129**(05), 1017–1032.

Satin, L. S., Butler, P. C., Ha, J. & Sherman, A. S. (2015), 'Pulsatile insulin secretion, impaired glucose tolerance and type 2 diabetes', *Molecular Aspects of Medicine* **42**, 61–77.

Scheen, A. J., Sturis, J., Polonsky, K. S. & Van Cauter, E. (1996), 'Alterations in the ultradian oscillations of insulin secretion and plasma glucose in aging', *Diabetologia* **39**(5), 564–572.

Shi, X., Kuang, Y., Makroglou, A., Mokshagundam, S. & Li, J. (2017), 'Oscillatory dynamics of an intravenous glucose tolerance test model with delay interval', *Chaos: An Interdisciplinary Journal of Nonlinear Science* **27**(11), 114324.

Simmendinger, C., Wunderlin, A. & Pelster, A. (1999), 'Analytical approach for the floquet theory of delay differential equations', *Physical Review E* **59**(5), 5344.

Simon, C. & Brandenberger, G. (2002), 'Ultradian oscillations of insulin secretion in humans', *Diabetes* **51**(Suppl1), S258–261.

Sipahi, R. & Olgac, N. (2004), A novel stability study on multiple time-delay systems (MTDS) using the root clustering paradigm, *in* 'American Control Conference, 2004. Proceedings of the 2004', Vol. 6, pp. 5422–5427 vol.6.

Smith, H. & Kuang, Y. (1992), 'Periodic solutions of differential delay', *Oscillation and Dynamics in Delay Equations: Proceedings of an AMS Special Session Held January 16-19, 1991* **129**, 153.

Smith, H. L. (2011), *An introduction to delay differential equations with applications to the life sciences*, Vol. 57, Springer New York.

Song, X., Huang, M. & Li, J. (2014), 'Modeling impulsive insulin delivery in insulin pump with time delays', *SIAM Journal on Applied Mathematics* **74**(6), 1763–1785.

Steil, G. & Reifman, J. (2009), 'Mathematical modeling research to support the development of automated insulin-delivery systems', *Journal of Diabetes Science and Technology* **3**(2), 388–395.

Sturis, J., Polonsky, K., Mosekilde, E. & Van Cauter, E. (1991), 'Computer model for mechanisms underlying ultradian oscillations of insulin and glucose', *American Journal of Physiology* **260**(5), E801–E809.

Sturis, J., Scheen, A. J., Leproult, R., Polonsky, K. S. & Van Cauter, E. (1995), '24-hour glucose profiles during continuous or oscillatory insulin infusion. demonstration of the functional significance of ultradian insulin oscillations', *Journal of Clinical Investigation* **95**(4), 1464.

Tang, W. J. (2016), 'Targeting insulin-degrading enzyme to treat type 2 diabetes mellitus', *Trends in Endocrinology & Metabolism* **27**(1), 24–34.

Thomas, R., Thieffry, D. & Kaufman, M. (1995), 'Dynamical behaviour of biological regulatory networks—i. biological role of feedback loops and practical use of

the concept of the loop-characteristic state', *Bulletin of Mathematical Biology* **57**(2), 247–276.

Tolic, I., Mosekilde, E. & Sturis, J. (2000), 'Modeling the insulin-glucose feedback system: The significance of pulsatile insulin secretion', *Journal of Theoretical Biology* **207**(3), 361 – 375.

Topp, B., Promislow, K., DeVries, G., Miura, R. & Finegood, D. (2000), 'A model of β-cell mass, insulin, and glucose kinetics: Pathways to diabetes', *Journal of Theoretical Biology* **206**, 605 – 619.

Tuominen, J. A., Ebeling, P. & Koivisto, V. A. (1997), 'Exercise increases insulin clearance in healthy man and insulin-dependent diabetes mellitus patients', *Clinical Physiology* **17**(1), 19–30.

Turksoy, K. & Cinar, A. (2015), 'Real-time insulin bolusing for unannounced meals using CGM measurements', *IFAC-PapersOnLine* **48**(20), 219–224.

Turner, R. C., Holman, R. R., Matthews, D., Hockaday, T. D. R. & Peto, J. (1979), 'Insulin deficiency and insulin resistance interaction in diabetes: estimation of their relative contribution by feedback analysis from basal plasma insulin and glucose concentrations', *Metabolism-Clinical and Experimental* **28**(11), 1086–1096.

Verdugo, A. & Rand, R. (2008), 'Hopf bifurcation in a DDE model of gene expression', *Communications in Nonlinear Science and Numerical Simulation* **13**(2), 235–242.

Verhulst, F. (2006), *Nonlinear differential equations and dynamical systems*, Springer Science & Business Media.

Walker, J. J., Terry, J. R. & Lightman, S. L. (2010), 'Origin of ultradian pulsatility in the hypothalamic–pituitary–adrenal axis', *Proceedings of the Royal Society B: Biological Sciences* **277**(1688), 1627.

Wang, H., Li, J. & Kuang, Y. (2007), 'Mathematical modeling and qualitative analysis of insulin therapies', *Mathematical Biosciences* **210**(1), 17–33.

Woods, S. C. & Ramsay, D. S. (2007), 'Homeostasis: beyond curt richter', *Appetite* **49**(2), 388–398.

World Health Organization (2016), 'Global Health Estimates 2016 Summary Tables: Global deaths by cause, age and sex, 2000-2016'. [Online; accessed 24-November-2018].

World Health Organization et al. (1999), Definition, diagnosis and classification of diabetes mellitus and its complications: report of a who consultation. part 1, diagnosis and classification of diabetes mellitus, Technical report, Geneva: World Health Organization.

Wu, Z., Chui, C.-K., Hong, G.-S. & Chang, S. (2011), 'Physiological analysis on oscillatory behavior of glucose–insulin regulation by model with delays', *Journal of Theoretical Biology* **280**(1), 1–9.